

CHALMERS



Modelling and Verification of Doubly Fed Induction Generator (DFIG) using Real Time Digital Simulator (RTDS)

Master Thesis in the Master Degree Program, Electrical Engineering Power

FARHAD SHAFIEI

Department of Energy and Environment
Division of Electric Power Engineers
CHALMERS UNIVERSITY OF TECHNOLOGY
Göteborg, Sweden, 2012

Modelling and Verification of Doubly Fed Induction Generator (DFIG) using Real Time Digital(RTDS)

FARHAD SHAFIEI

Department of Energy and Environment
Division of Electric Power Engineers
CHALMERS UNIVERSITY OF TECHNOLOGY
Göteborg, Sweden, 2012

Modelling and Verification of Doubly Fed Induction Generator (DFIG) using Real Time Digital Simulator (RTDS)

FARHAD SHAFIEI

©FARHAD SHAFIEI

ABB/HVDC/TSM

**In collaborating with ABB -Ludvika.
HVDC /TSM Department.**

Department of Energy and Environment
Division of Electric Power Engineering
Chalmers University of Technology
SE-412 96 Göteborg
Sweden
Telephone + 46 (0)31-772 1000

Department of Energy and Environment
Division of Electric Power Engineers
CHALMERS UNIVERSITY OF TECHNOLOGY

FARHAD SHAFIEI

Department of Energy and Environment
Division of Electric Power Engineering
Chalmers University of Technology

Project Objective:

First objective of this study is to verify a 200 MW Doubly fed Induction Generator (DFIG) in RSCAD against the base model in PSCAD .The RSCAD model is built based on the available PSCAD model, and consequently the results in both models should be close enough and compatible to each other. This project was defined as the previous RSCAD model results were different from the PSCAD model, and they couldn't be verified against each other. The reason for this difference is due to the continuous changing and updating the PSCAD model, which was not followed by updating of the RSCAD model ,and consequently after a while the models became quite different and as a result not showing same behavior, and as mentioned one aim of this project is to update the RSCAD model and it's control parameters according to the new PSCAD model and make them more compatible in a way they can be verified and this verification is highly demanded and is observed by customers in wind farm projects.

In practice for modeling wind farms the total power can be around 600 MW or 800 MW or even higher, the built model in RSCAD is rated for 200 MW, due to the require total wind farm power it is required to increase this power up to for example 800 MW to be able to represent a real wind farm, at the moment this is done by making parallel connection of 4 wind farm in Real time Digital Simulator (RTDS), which is using more processors and needs more hardware. Another way which is more convenient is to implement a scaling transformer in RSCAD for a 200 MW DFIG and aggregate the power to the desired level to reduce the number of required processors and hardware in projects. It will be shown that the scaled RSCAD model will become totally unstable by adding the scaling transformer for reaching to 800 MW, which is not the case for PSCAD model. Therefore it is needed to find why this instability is happening in RSCAD.

Abstract

This master thesis deals with Doubly Fed Induction Generator (DFIG) controller in RSCAD model. The controller in RSCAD is built and designed according to the available PSCAD model and differences between two models are highlighted. Also an investigation is made to increase power in RSCAD by using a scaling transformer; finally scaled models in both models are verified against each other.

The work starts with a brief introduction of different wind turbine generators and their specifications, and describing the theory of variable wind turbines and their advantages over the fixed wind turbines. In this project doubly fed Induction generator (DFIG) wind turbines are considered and studied, DFIG and different parts of its controller are discussed, and required equations for DFIG are derived. Real Time Digital Simulator (RTDS) hardware and RSCAD software, which are used as the simulator tools at this project are introduced for readers and then a sample DFIG is modeled in RSCAD.

For verification purposes in first part of the project a 5 MW DFIG model with complete controllers and scaling transformer in PSCAD are used, by sending scaling level to 40 in PSCAD the model will represent 200 MW. The base model in RSCAD is a single 200 MW DFIG; both models in PSCAD and RSCAD are connected to an infinite 154 kV network with known R, L and C values. Different fault cases are applied to both models to compare behavior of models during transients and also in normal operation. System studies show that current RSCAD model behavior is completely different from the PSCAD model. The controllers in both models in RSCAD and PSCAD, with all possible reasons for having different results were investigated and it was tried to make the RSCAD model similar to the PSCAD model as much as it was possible.

The second task of this work is about adding scaling feature to the model in RSCAD, as in most cases 800 MW wind farm or even higher power ratings should be implemented in RSCAD for a typical wind farm project. As the base model in PSCAD is 5 MW to model an 800 MW DFIG in PSCAD scaling factor of 160 should be used, and for RSCAD model scaling should be 4 as the RSCAD base model is 200 MW. It was shown that the scaled model in RSCAD would be unstable after scaling, and the second task at this project was to study the scaling system concept in both RSCAD and PSCAD, and find any possible differences between the two models .

Index terms: Wind turbine, Doubly Fed Induction Generator (DFIG), Rotor side controller, Grid side controller, Phase-locked Loop (PLL), Crowbar logic, Fault sequencer, Speed controller, Scaling transformer, Real Time Digital Simulator (RTDS), RSCAD.

Acknowledgements:

This thesis would not have been possible unless with my wife support, who was always beside me and encouraging me from the beginning to the end of this work at all the moments. My dear **SEPIDEH**, I will never forget your selflessness for standing all of my busy days and my absences. Also I am heartily thankful to my supervisor at Chalmers university Massimo Bongiorno, who I learned a lot from him during this project, and also It is a pleasure to thank those who made this thesis possible at ABB company specially TSM department; my supervisor Tahir Awan and my manager David shearer.

FARHAD SHAFIEI
2012-12-12

FARHAD SHAFIEI

Department of Energy and Environment
Division of Electric Power Engineering
Chalmers University of Technology

Göteborg, Sweden 2012

Contents

Chapter 1

Project Objective:.....	5
Abstract.....	6
Acknowledgements:.....	7
1 Sustainable Energy.....	11
1.1 Wind Power Plants.....	11
1.2 Different Types of Wind Turbines.....	12
1.2.1 Fixed Speed.....	12
1.2.2 Variable Speed Wind Turbines.....	13

Chapter 2

2 Power Converter.....	18
2.1 Rotor-Side Converter.....	18
2.2 Grid-Side Converter.....	20
2.3 Fault Ride-Through Procedures.....	20
2.3.1 DC Crowbar (DC-Chopper).....	21
2.3.2 AC Crowbar.....	21

Chapter 3

3 Aerodynamic Model and Pitch Controller.....	23
3.1 Operation Modes.....	23
3.2 Operating Regions.....	26
3.2.1 Minimum Speed Operation Region.....	26
3.2.2 Optimum Speed Operation Region.....	26
3.2.3 Maximum Speed Operation Region.....	27
3.2.4 Power Limitation Operation Region.....	27
3.3 Optimum Power Tracking of a Variable-Speed Wind Turbine.....	27
3.3.1 Current-Mode Control.....	28
3.3.2 Speed-Mode Control.....	29
3.3.3 Stall regulation:.....	29

Chapter 4

4	Modeling of DFIG	30
4.1	Control of Supply-Side PWM Converter	30
4.1.1	D and Q Axis Current Regulator.....	31
4.2	Control of Rotor Side Converter	36
4.2.1	Current Reference Pulse Width Modulation:.....	39

Chapter 5

5	Real Time Digital Simulator (RTDS)	41
5.1	Small Time Step Approach	47
5.1.1	Fundamentals of Small Time-Step Simulation	48
5.1.2	The Challenge	49
5.1.3	Solution	49
5.1.4	Open Circuit.....	50
5.1.5	Short Circuit.....	50
5.1.6	Small Time Constraints:.....	51
5.1.7	Modeling Approach Issues.....	51
5.2	Simulation Software.....	52

Chapter 6

6	Overview of System in RSCAD	55
6.1	Small Time Step Box.....	56
6.2	Scherbius Drive	58
6.3	Three Winding 3 Phase Transformer	59
6.4	Doubly Fed Induction Generator (DFIG)	60
6.5	Three Phase-Two Level Converters.....	61
6.6	Grids Side VSC Control	62
6.7	Phase Compensation Calculation.....	64
6.8	Phase Locked Loop (PLL)	65
6.9	Rotor Side VSC.....	66
6.10	Crowbar Logic	66
6.11	Fault Control	67

Chapter 7

7	PART I-Verification of DFIG model in RSCAD against PSCAD	68
7.1	CASE I: 10% Remaining Voltage 3ph – G.....	69
7.2	200 MW DFIG, RSCAD Model Verification against PSCAD:.....	81
7.2.1	Modifying PLL in RSCAD	81

Chapter 8

8	Output from TS plot (AFTER MODIFICATION):.....	83
8.1	CASE II: 80% Remaining Voltage 3ph – G.....	95

Chapter 9

9	PART II- Scaling of DFIG in RSCAD and modifying the model against PSCAD	105
9.1	PART A: Investigations in Scaling transformer settings, Small time step blocks, and Infinite voltage source model.....	105
9.2	Model with GIS and Ramp Function -Without RC Values.....	107
9.3	Model with GIS and Ramp Function-With RC Values	108
9.4	No GIS-Ramp Function-No RC Values	108
9.5	No GIS-Ramp Function- RC Values.....	109
9.6	No GIS –No Ramp Function - No RC Values	110
9.7	No GIS-No Ramp Function - RC Values	110
9.8	PART B: Investigations in interfacing of Scaling Transformer	111
9.9	Possible Causes for Instability.....	113
9.9.1	Stiffness of Network	113
9.9.2	Time Delays in Interfacing Loop	113
9.10	Plots for 800 MW DFIG Verified against PSCAD.....	118
9.10.1	Normal Operation	118
9.10.2	CASE I: 10% Remaining Voltage 3ph-G	119

Chapter 10

10	Conclusion and future work.....	120
10.1	Conclusion.....	120
10.2	Future Work.....	120

Chapter 1

1 Sustainable Energy

Due to limited fossil fuel resources and considerable environmental problems caused by them, renewable energies like wind power are developing quickly in the world, fossil sources of energy are running out and the main part of our world energy, which was taken from these sources should find a good replace for them, however human will face fuel crises in a close future. Over the last two decades by increasing the demand for the energy, environmental and climate problems are more considered. Currently more countries around the world started to support and develop renewable energies, and politicians support and confirm more budgets about sustainable energy projects.

1.1 Wind Power Plants

The production of energy sources like wind, and photovoltaic are becoming more popular around the world. During the last decade use of wind energy has raised substantially, and its share in total energy production has increased to a great extent (figure 1.1). There are many countries around the world that are investing on wind projects from the research to installation .Wind energy is a very clean and convenient solution to be one the answers for increasing energy demand. According to wind energy prospection wind power can contribute to 12% of total world energy demand by 2020, and it is also possible to increase this amount up to 22% by 2030. This pattern is agreed in Kyoto protocol, and is backed up by the governments in some countries like Germany, Denmark, and Spain. For instance in European Union it is predicted to increase the wind power capacity from 2.1% to 21% of overall energy capacity. [5]

Worldwide installed wind power/year (MW)

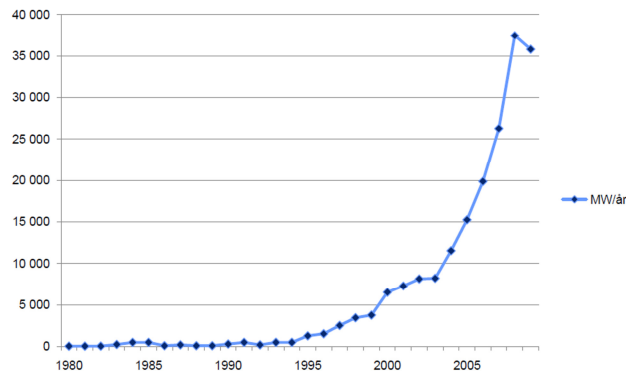


Figure 1.1- Wind Power Developments

For example ABB has delivered more than 30000 wind power generators during the past 30 years, which can give an idea about available demand in market; this volume of wind generation is equal to 30 GW and is still increasing rapidly. [7]

1.2 Different Types of Wind Turbines

There are different methods for wind power conversion, which are introduced during the last decades; these methods mainly use asynchronous and synchronous generators. By utilizing the multi pole synchronous generators there is no need for gear box, on the other hand the squirrel cage asynchronous machines use two gear boxes with different turn ratio. [1]

1.2.1 Fixed Speed

Fixed speed wind turbines are typically using induction generators, which are connected to the grid directly. Due to the fixed frequency of grid, speed of the machine should be changed using gear box, and also by changing the number of poles in the generator. To enhance the range of power production fixed speed wind turbines can be supplied with a pole change generator, which enables the generator to operate at two different speeds. Because of the large currents during the start sequence, while the rotor speed is lower than a certain level soft starters should be used with induction machines to avoid high currents as it is shown in figure 1.2.1.

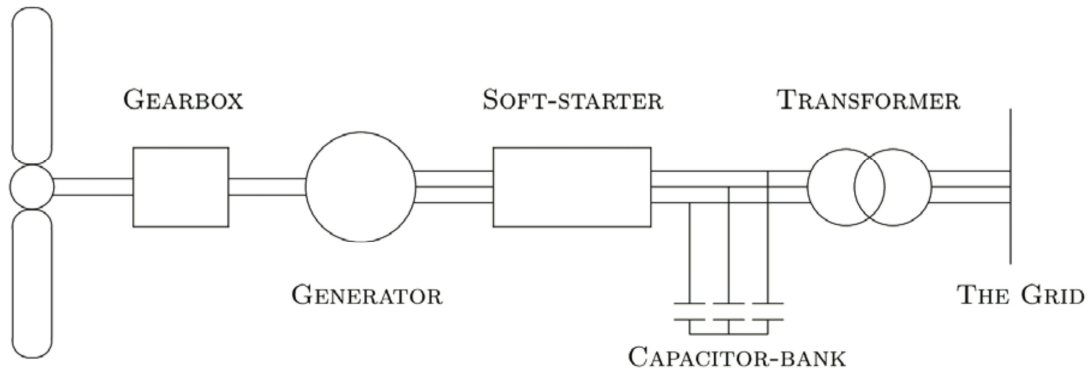


Figure 1.2.1- Fixed Speed Wind Turbine

1.2.2 Variable Speed Wind Turbines

One advantage of using variable wind turbines is reducing mechanical stresses in turbines, and also removing gust of wind. Also the torque and power disturbances will be decreased incredibly. [2]

These advantages are increasing the application of variable wind turbines, as they introduce lower power fluctuation, and higher power quality compared the fixed speed generators. The produced electricity with wind turbines has low power quality characteristic due to the wind speed variations, which will lead to disturbances, fluctuations, voltage variations and flicker in delivered power to the networks. [2] Using the induction machines in wind turbines will cause another problem due to the absorption of high reactive power from network which can be variable with generator speed and time. [3]

Due to all these draw backs of fixed wind turbines, different types of variable speed wind generators are introduced in the market.

1.2.2.1 Limited Variable Speed

As it is shown in figure 1.2.2, wind turbines can have limited speed variation if they have a variable rotor resistance, this way the slip of the generator, and consequently the output power can be controlled. The range for speed variation normally is within 0 to 10% of the rated speed. Induction generators are usually used for this type, and they can be connected to grid directly. The amount of speed change depends on the range of resistance variation in rotor. Induction machines need reactive power for operation, and this is drawn from the network, therefore this type of generator still needs capacitor bank to compensate reactive power, and also a soft starter should be used for a smooth connection to the grid. [4]

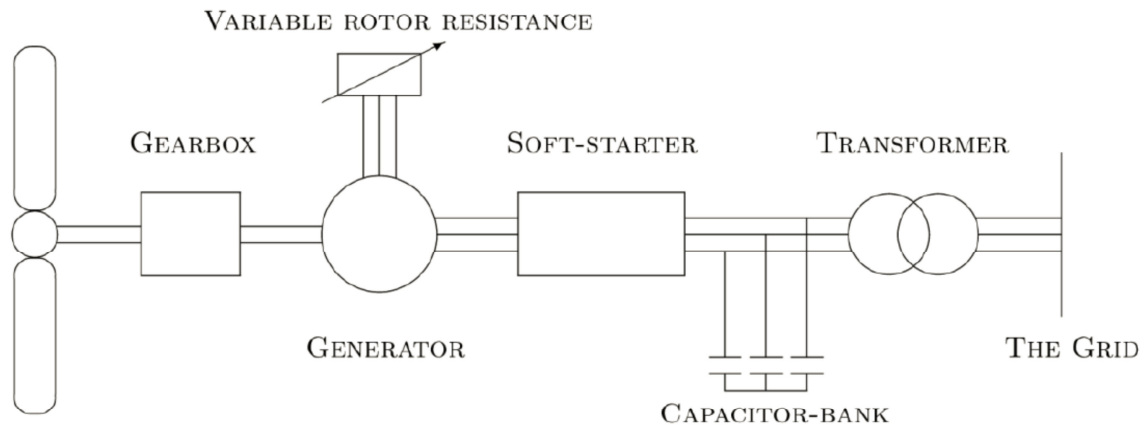


Figure 1.2.2- Limited Variable Speed Wind Turbines

1.2.2.2 Full Scale Frequency Converter Synchronous Generator (FCWT)

This type of variable wind turbine uses synchronous generator (SG). Magnetic field is created by poles inside the rotor or it can be produced by regular field windings. By using permanent magnet type SG the needed reactive power for the generator will not be provided by the converter any longer.

If an appropriate number of poles are used in rotor then they can be used without gearbox.

Wind turbines with fully scaled converters have different advantages that make them suitable for power applications. First they can decouple the grid and generator completely, which minimizes the effect of faults in the grid on the generator side, also having a full scaled converter provides a wider range of speed variation compared to the limited variable speed wind turbines. Due to the higher rating of converter, which should be designed for 100% of generator power, they also are capable of supporting grids with more reactive power which is especially very useful for supporting of network voltage especially if the grid is weak.

Permanent magnet synchronous generators (PMSG) are excellent solutions for FCWT as they are self magnetized and they can have high efficiency keeping high power factor in grid. Their efficiency is higher than wound rotor synchronous generators, and induction generators as they do not need any external source for excitation, and also capacitor banks. But still building materials that can be used as permanent magnets are expensive, and the production line is still complicated. PMSG reduces excitation losses, and enhances torque density in the generator. By removing field windings it is possible to remove slip rings, which normally need regular maintenance, and this is not desired in remote offshore wind turbine applications. Using the fully scaled power converter it is possible to change the frequency and voltage of the wind power

easily and the capability of producing the power at any speed is an advantage. Rotor in PMSG may have salient poles or may be cylindrical. Salient poles are more convenient to be used with the slow speed applications, and wind applications.

As it is shown in figure 1.2.3 full converter wind generator may consist of a turbine, generator, rectifier and inverter. Using six pulse converters with thyristors will create odd harmonics of 5th, 7th, 13th, 17th, 19th ... and because these are low order harmonics they need a large grid filter to remove the harmonics, which is bulky and expensive. On the other hand this filter also can produce reactive power, and enhance the power factor of the grid, which is an advantage. If instead of thyristor IGBT with pulse width modulation frequency (PWM) is used this method of modulation will create high order harmonics around the switching frequency of converter, which needs smaller and less expensive filter.

Using full scale frequency converter results in smoother grid connection therefore it will not be necessary to install soft starter. If the system is designed with the PMSG then gear box is not required. This technology is being more preferred to the other systems especially for wind power application due to several advantages, and its capability of producing the power with higher quality especially during transients in network, which can fulfill more restrictive grid codes forcing wind turbine producers to help the network during the fault conditions. With FCSG it would be possible to decouple the grid, and generator which will improve performance of wind turbine, and can inject reactive power during the faults into network keeping the voltage, and also make it possible for the generator to operate in a large speed range without introducing power fluctuation into grid. This converter will add to cost although this cost is decreasing using new technologies as this technology is matured. The size of converter in FCSG is rated for 100% of rated power, which leads to a higher converter size rather than the DFIG converter, which usually is rated for 30% of generator rated power, it should be noticed that p.u values of switching losses are still the same for DFIG and FCSG. Synchronous generator with or without gear box and induction generators with gear box can be used in FCWT. Switches in the converter are usually IGBTs with the voltage level of 690 V.

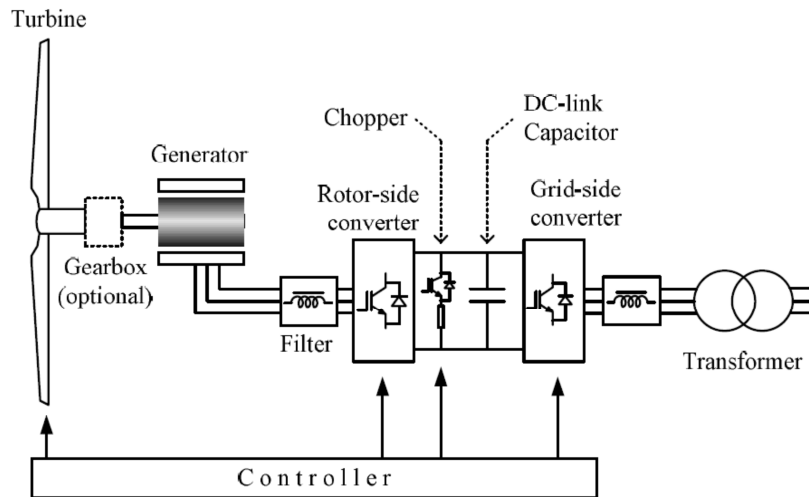


Figure 1.2.3- Schematic Diagram of Full Converter Wind Turbine

1.2.2.3 Doubly Fed Induction Generator (DFIG)

Doubly fed induction generator (DFIG) is a choice for many utilities, and introducing an efficient solutions in wind turbine applications due its ability to provide reactive power during grid faults, which can support power system in low voltage conditions. DFIG is capable of extracting optimum wind energy over a wide range of wind speeds, which is not possible with fixed speed induction generators, this characteristic will be explained later. DFIG is based on a slip-ring wound rotor for working in a partial speed variable mode, which is suitable for wind applications with limited speed range [1], and this it is enough to rate converter for a part of nominal power, which decreases converter price.

Characteristics of DFIG is as follows: [3]

1. Operation below, above and through synchronous speed with the speed range restricted only by the rotor voltage ratings of the DFIG
2. Operation at synchronous speed, with DC currents injected into the rotor with the inverter working in chopping mode
3. Low distortion stator, rotor and supply currents independent control of the generator torque and rotor excitation
4. Control of the displacement factor between the voltage and current in supply side converter, and controlling system power factor

Among wind turbine conversion technologies DFIG wind turbine is one of the most attractive concepts in market.

Table 1.2.1 shows some known DFIG manufacturers. [4]

Wind turbine products with DFIG concept					
Manufacturer/type	Power(MW)	Rotor(m)	$\left(\frac{m}{s}\right)$	Rpm	Gear ratio
Nodex N100/2500kW	2.5	99.8	12.5	9.6-14.9	1:77.4
Nodex N80/2500kW	2.5	80	15	10.9-19.1	1:68
Vestas V80-2.0,50Hz	2	80	15	9-20.7	1:92.6
GE 1.5sle,60Hz	1.5	77	14	12.1-22.2	1:72

DFIG includes different Components as shown in Fig1.2.4. Stator of DFIG is working synchronously with network frequency. Rotor converter controls rotor current to adjust electromagnetic torque and machine excitation. Power converter size is a percentage of the generator rating, usually in the range between 15 to 30 percent. Since power converter operates in both current directions DFIG can generate power either in sub-synchronous or in super-synchronous operation modes, these operation modes are discussed in section 3.1. DFIG is capable of providing reactive power, which supports network during voltage collapse and faults. When wind speed varies in a limited range DFIG is able to extract optimum wind energy and maximize power tracking, which is not possible with the fixed speed induction generators. By using DFIG power factor can be adjusted by the stator side converter even if the machine is operating in speeds different from synchronous speed. With DFIG there is no need to use shunt compensation and soft starters. [4]

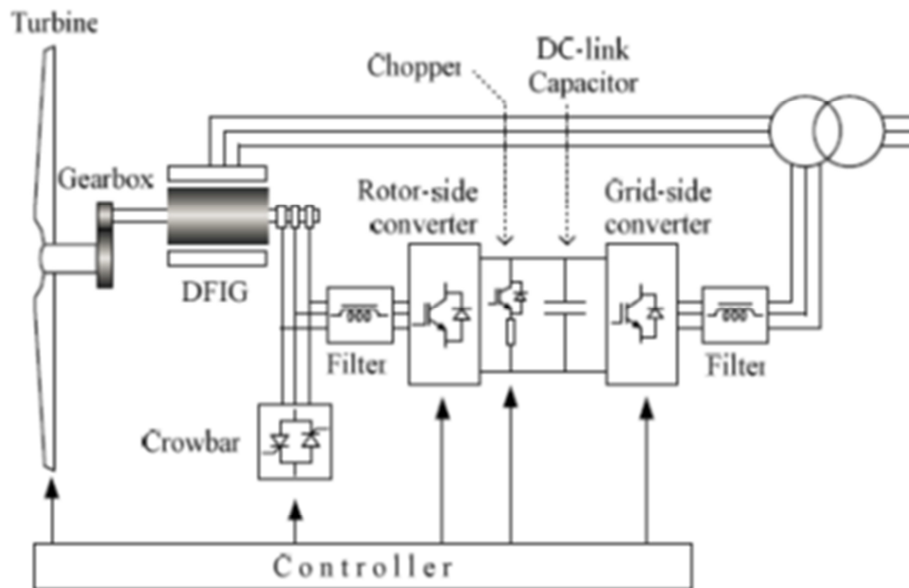


Figure 1.2.4- DFIG System Overview

Chapter 2

2 Power Converter

The Converter that is used in DFIG is a back to back voltage source converter. Grid side converter uses Pulse Width Modulation method (PWM) to create desired voltage in the stator side, and rotor side converter is injecting current keeping reference active and reactive current variations in a certain band, and for this uses the hysteresis band control method, which will be explained in section 4.2.1 and 2.1. DFIG is made up of a back-to-back converter connecting rotor circuit and the grid, which is known as Scherbius scheme. These converters usually are made by IGBT, which enable them to have two directional current and power flow. Inverter valves make use of IGBTs provided with freewheeling diodes (see Fig2.1). Filters are used in both sides to minimize the effect of harmonics due to switching frequency. [4]

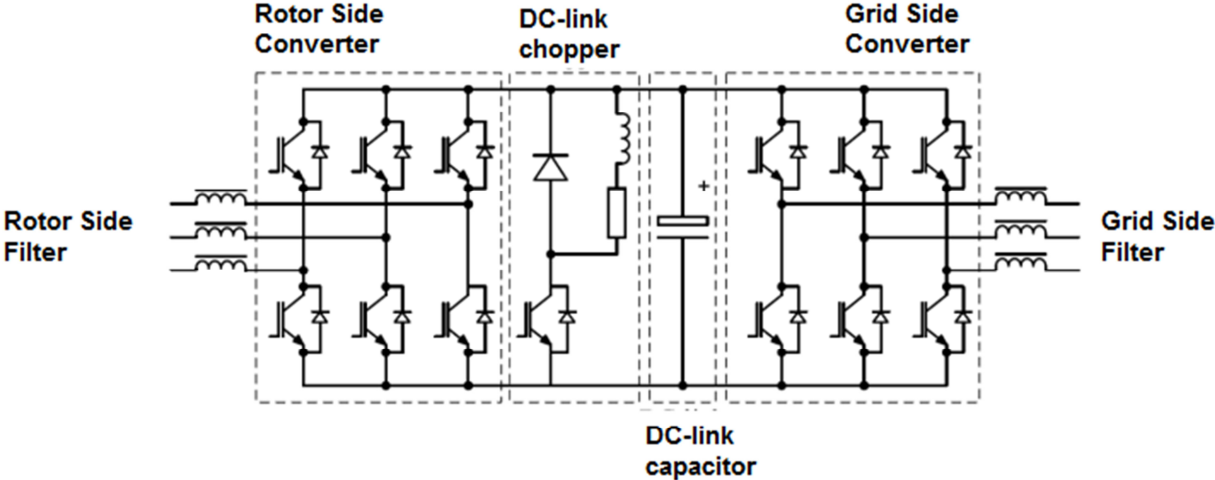


Figure 2.1- Voltage Source Converter

2.1 Rotor-Side Converter

In normal mode operation, rotor side converter provides reactive power to the rotor, and this way controlling grid power factor, this reactive power should be provided by the stator connected to the grid in conventional induction generators, rotor side controller also adjusts the developed electric power (P_{elec}), and as a result controls rotor speed for having optimum power extraction from wind.

Rotor frequency can be shown by:

$$\omega_{mech} = \omega_{syn} - \omega_{slip} = \omega_{syn} - 2\pi f_r$$

$$\omega_{mech} = \text{Rotor rotational speed} \left(\frac{\text{rad}}{\text{s}} \right)$$

$$\omega_{syn} = \text{Synchronous Speed} \left(\frac{\text{rad}}{\text{s}} \right)$$

$$f_r = \text{Electrical Frequency in Rotor}$$

Synchronous speed is constant, and by adjusting the electrical frequency in the rotor windings rotor speed can be controlled. As it was mentioned before the rotational speed is imposed by the real power flow controlled by the rotor side converter that is used to provide a suitable torque control loop resulting in forcing rotor frequency to the desired frequency and slip. Rotor side converter power is limited by 2 parameters as maximum slip power and maximum reactive power control ability. The active power flowing through the rotor circuit to voltage source converter is named slip power, which is proportional with slip value. Slip is a percent of the rated speed, and consequently the converter needs to be rated only for a limited speed range, which is not the case for the full converter wind turbines, which has equal rating for either SG and the converter. This range starts from the lowest wind speed that is called cut-in speed, and if the speed is lower than this speed it is not practical to extract power from wind. Generator speed at rated wind speed can be adjusted to any point by using the gearbox, and as the slip increases efficiency of the system drops due to higher power losses in the power converter, rotor iron and frictional losses.

Rotor side controller is a current controlled voltage source converter, and rotor current can be controlled by different methods. One method is utilizing pulse width modulation method (PWM) and the other one is using the hysteresis band control method (see fig.2.2), which also is called current regulated modulation using a tolerance band control or either adaptive current control. Current controller at this method is using reference current, and hysteresis band and trying to keep actual rotor current within the defined band. The controller always tracks phase current to be in the hysteresis band limits, when phase current is exceeding the upper limits the lower valve of the related phases are turned on, and the upper valves are turned off, and when the current is beyond the lower hysteresis band limit the upper valves of the corresponding phase will be turned on, and the lower valves are turned off. This method doesn't use the firing pulse, and this way tries to keep the actual current to follow the reference current. The hysteresis band width is defined by considering the switching frequency limitations, and switching losses in IGBTs. [4], [8]

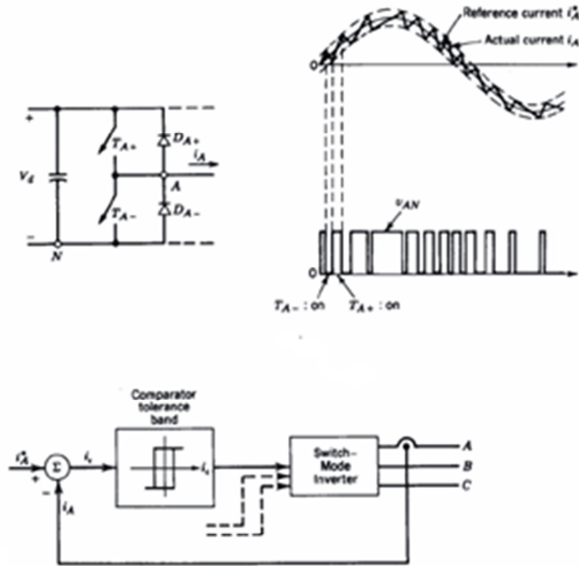


Figure 2.2- Hysteresis Band Control Method

2.2 Grid-Side Converter

Rating of grid side converter is also determined by the maximum slip power. There are different voltage levels for grid side converter such as 480 V, 690 V. Grid side converter is current regulated with the real component used to adjust the DC-link voltage and the quadrature component used to regulate injected reactive power to the Grid. During normal operation grid side converter is controlling DC-link voltage between the two converters by keeping active power in both converter sides in balance, grid side converter is also capable of reactive power injection to the grid, and this way controlling network voltage, this is considerable advantage specially during faults and for network voltage stability. Converter is modeled as a current-controlled voltage source and uses the PWM method to produce the desired voltage at the grid side. [4]

2.3 Fault Ride-Through Procedures

When a fault occurs consequently a voltage dip will happen on wind turbine terminals. This will create high transient current in rotor, which can damage rotor or possibly create overvoltage on dc link capacitor. Before the regulations allowed wind turbines to be disconnected from grid during network faults, but this is not allowed with the new regulations any more, and operators want to keep wind turbines connected to grid during grid faults, for this purpose and to prevent DC link over-voltages during grid faults, DFIG can be equipped by two types of protection circuits DC-chopper (DC-crowbar), and AC-crowbar, which make it possible for DFIG to stay

connected to the network. DC crowbar in DFIG is an optional choice ,which helps by smoothing DFIG operation,and reducing DC-link voltage imbalances during heavy faults,but using AC-crowbar is a must for DFIG operation.[17]

2.3.1 DC Crowbar (DC-Chopper)

DC link braking resistor is known as DC-link chopper, and can be proposed in the dc link to dissipate additional energy in the dc link during grid faults,and this way prevent from over voltages in DC-link during grid disturbances.This protection includes a resistor and an electronic switch, which is normally IGBT.To increase the amount of energy dissipation units of dc-link braking resistor can be placed in parallel.[4]

2.3.2 AC Crowbar

The AC crowbar can short-circuit the rotor windings ,when excessive currents are created in rotor during voltage dips in network. The crowbar that is used here at this project is an active crowbar, which uses IGBT switches. The active crowbar can be disconnected very quickly, and this way rotor side converter performance can be started again only after 20-60 ms from the start of the grid disturbance, consequently it is possible to generate reactive power to the grid during the left of the voltage dip ,and this way helping the network to be recovered from the fault. Crowbar can be activated either by dc link overvoltage protection or by rotor side converter over current protection. Typically crowbar should be activated, when dc link voltage reaches to 12% above nominal value. [4] IGBT's can withstand peak currents twice the nominal current for 1ms; as a result the converter over current protection normally is adjusted at 1.8 pu. If the thyristors are used it will take tens of ms for crowbar to remove the short circuit from rotor, because thyristors cannot be forced to be turned off immediately as they need to wait until the zero crossing of the current. This should be considered also that during fault there may be a dc component in current ,which will make it more difficult to turn off thyristors,to remove this limitation active crowbars are proposed, by this design the rotor current, can be forced to turn off and this will propose faster fault current clearing. [4]

DFIG with both AC and DC crowbar protections is depicted in figure 2.3

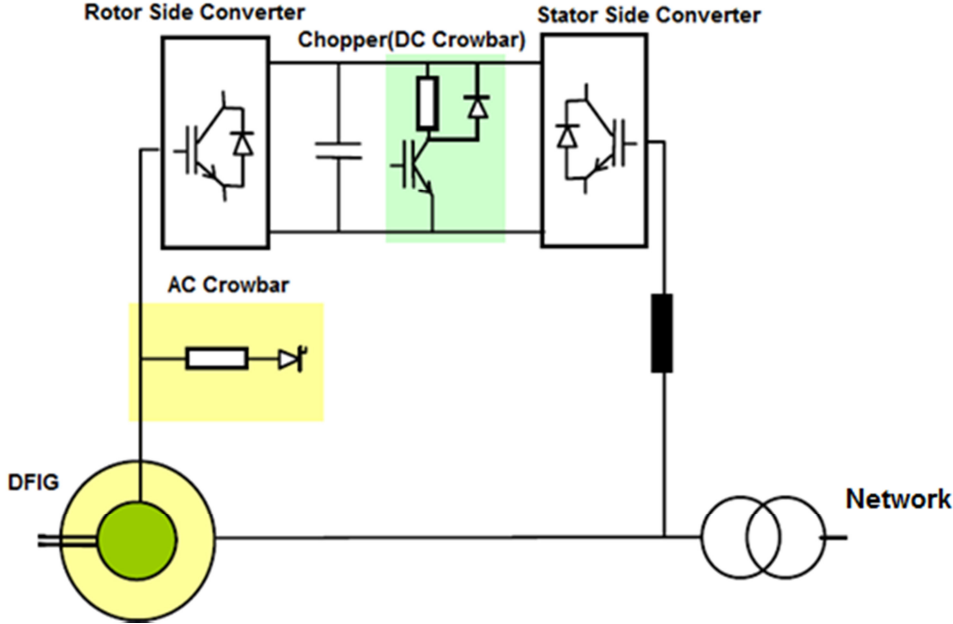


Figure 2.3- AC and DC Crowbars in DFIG

Chapter 3

3 Aerodynamic Model and Pitch Controller

The kinetic energy from the wind flow is converted into rotational energy in the form of mechanical torque and speed in aerodynamic system. Mechanical torque of a wind turbine is expressed as [4]

$$T_t = \frac{1}{2\omega_t S_b} \rho \pi R^2 v_w^3 C_p(\lambda, \beta)$$

Equation 3-1

Where ρ is air density in $\frac{kg}{m^3}$, and v_w is the wind speed in $\frac{m}{s}$, R is blade Length in m, C_p is the power coefficient, S_b is the generator power base value, β is Pitch angle, and λ is tip-speed ratio obtained from following equation: [4]

$$\lambda = \frac{\omega_t R}{v_w}$$

Equation 3-2

When wind speed exceeds rated value electromagnetic torque is not enough to control the rotor speed since this will lead to an overload on the generator and converter. To keep the rotor speed from becoming too high the absorbed power from the incoming wind should be limited. This power limitation can be done by reducing the power coefficient of turbine or the C_p value.

C_p Value also depends to the pitch angle. Rotating the turbine blades by hydraulic or electric drives along the axis can change this pitch angle.

3.1 Operation Modes

DFIG can operate in two operation modes with different power directions in the converter, super-synchronous and sub-synchronous operation. If the speed of the rotor is lower than synchronous speed DFIG is operating in sub-synchronous mode and if the rotor speed is higher than synchronous speed, then generator is operating in super-synchronous mode. Figure 3.1.1 indicates direction of power flow in sub-synchronous operation mode. In this situation rotor speed is lower than synchronous speed, which leads to a positive slip. In order to enable DFIG to operate as a generator even during sub-synchronous mode this positive slip power should be transmitted and injected from grid to rotor through the power converter. In super synchronous mode, which is shown in figure 3.1.2 the slip power flow is in the opposite direction, and

mechanical power from shaft is splitted into two parts, the largest part of the power goes to the stator ,and a fraction of the power ,which is slip power passes through the rotor causing a negative slip.

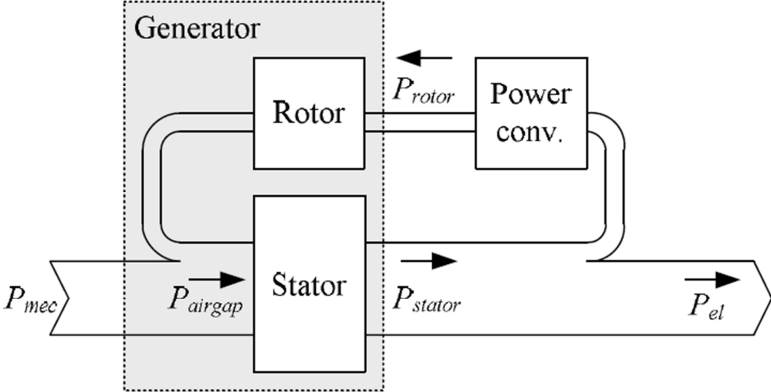


Figure 3.1.1 Sub-Synchronous Operation

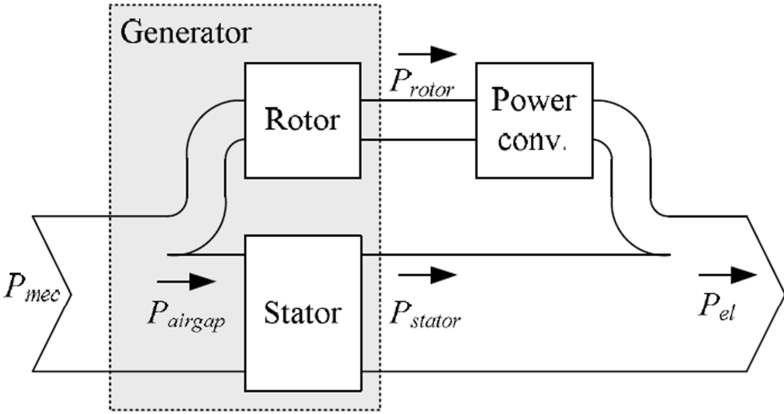


Figure 3.1.2 Super-Synchronous Operation

In the studied model n_p , was not given in the model ,but according to figure 8.8 ,and following calculations, it could be concluded that rotor speed is higher than synchronous speed for this generator ,which means the generator is in super synchronous operation mode,and slip power is injected from rotor to network.

$$f_s = 20f_r \rightarrow f_r = 0.05f_s$$

$$\omega_s = \frac{60 \times 50}{n_p} = \frac{3000}{3} = 1000 \left(\frac{rad}{s} \right)$$

$$\omega_{sl} = \omega_s - \omega_m = 1000 - 1050 = 50 \left(\frac{rad}{s} \right) \rightarrow s = \frac{\omega_{sl}}{\omega_s} = 0.05$$

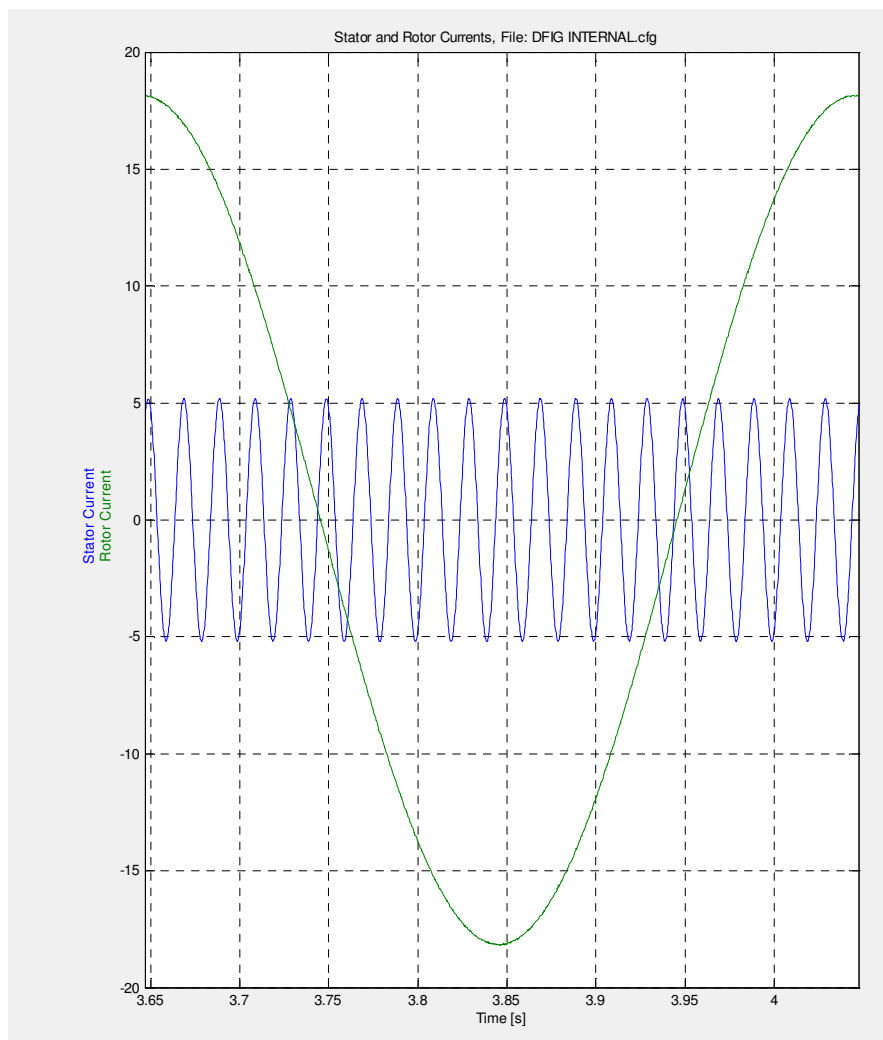


Figure 3.1.3-Stator and Rotor Current frequencies

3.2 Operating Regions

Depending on the available wind speed DFIG will operate in different operating regions, which are illustrated in figure 3.2.

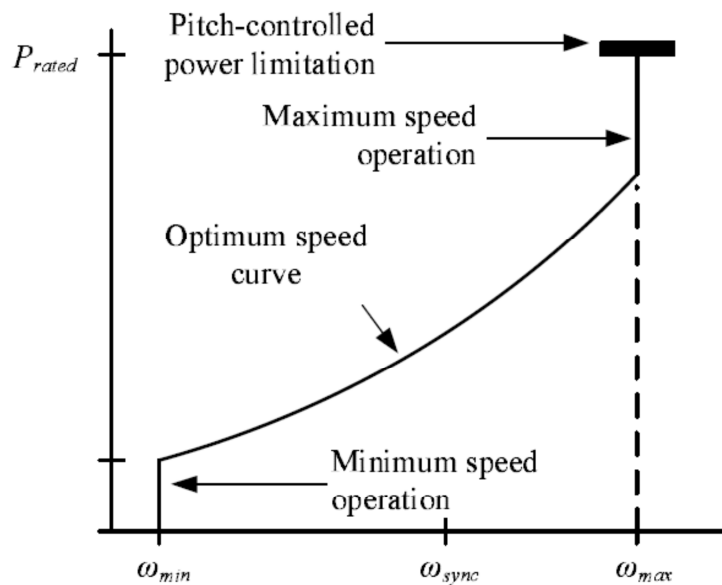


Figure 3.2 Operating Regions

3.2.1 Minimum Speed Operation Region

There is a lowest amount of wind speed that the generator can operate, and produce power, at this operating point generator speed is kept at its lowest possible speed, is typically around 30% below of synchronous speed.

3.2.2 Optimum Speed Operation Region

In optimum speed operation region speed of turbine is increased with wind speed, and rotor speed is adjusted by rotor side controller to provide a maximum output power from generator, and keeping the efficiency at its maximum level. This is the most efficient operation mode of DFIG until generator reaches its rated speed.

3.2.3 Maximum Speed Operation Region

By increasing wind velocity, generator speed reaches to its rated speed, and it is not allowed to increase generator speed any more, as a result the generator will not operate at the optimum operation mode. At this point the rotor side controller task is to maintain the maximum generator speed and prevent the generator from exceeding the rated speed value. Normally this maximum speed will be about 15-20 percent above the synchronous speed.

3.2.4 Power Limitation Operation Region

If wind speed exceeds even more, the produced power increases until it reaches to the rated power and limiting controllers try to decrease the mechanical input torque, and consequently produced power by using pitch controller, which changes blade angle.

3.3 Optimum Power Tracking of a Variable-Speed Wind Turbine

By using DFIG in wind turbine applications controller will be capable of controlling rotor speed, and forcing the machine to produce optimum power similar to figure 3.3. The extracted mechanical power from wind can be expressed as [4]:

$$P = \frac{1}{2} c_p \rho A v^3$$

Equation 3-3

P = Wind power (W)

ρ = Density of air [$\frac{kg}{m^3}$]

A = swept rotor area [m^2]

v = wind speed [$\frac{m}{s}$]

$c_p(\lambda, \beta)$ = Power coefficient, which is a function of λ tip speed ratio and β pitch angle. Tip speed ratio is an important parameter that is considered, when the wind turbine is designed and determine how quickly the blades of the wind turbine can rotate in comparison with wind speed.

$$\lambda = \frac{v_{blade}}{v_{wind}} = \frac{\omega r}{v_{wind}}$$

Equation 3-4

λ = Tip speed ratio v_{blade} = speed of the blades $\frac{m}{s}$ v_{wind} = Wind speed $\frac{m}{s}$

r = Radius of the rotor [m] ω = angular velocity $\frac{rad}{s}$

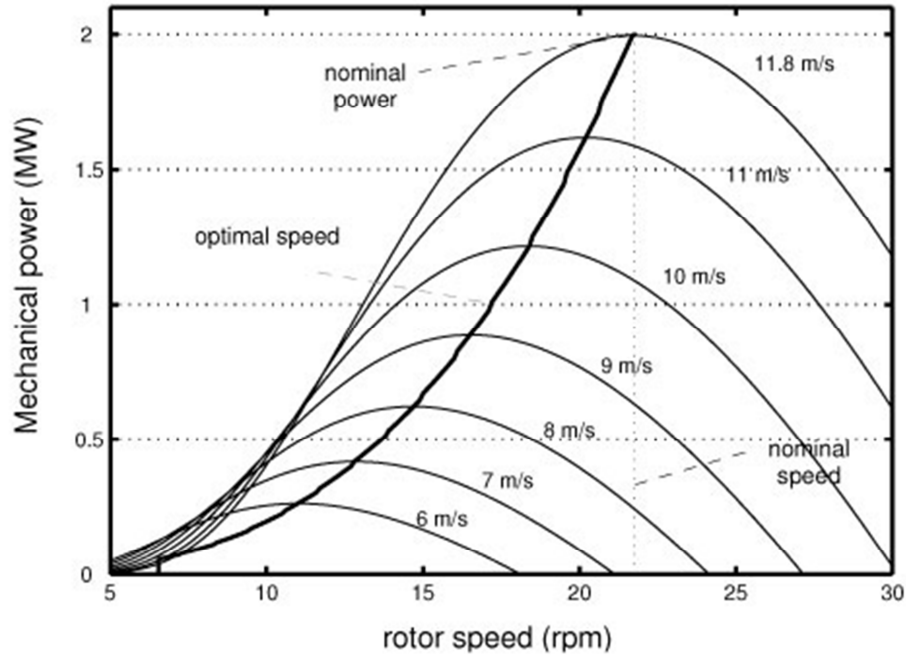


Figure 3.3 Optimal Power Tracking

As it is shown in figure 3.3 by tracking optimal power coefficient, and controlling speed of wind turbine it is possible to track maximum power production in power characteristic curve. For each wind speed there is a rotor speed that gives highest amount of produced power. This curve can be called P_{opt} curve. The purpose of the controller in variable speed wind turbine is to keep operating point on this curve. If wind velocity is more than rated value power produced should be limited to be equal to rated power by applying pitch control. There are two common methods to achieve this control concept:

3.3.1 Current-Mode Control

In this method which is standard tracking mode shaft speed is measured and considering the value of K_{opt} certain electrical torque is applied to generator, required electrical torque will be adjusted by controlling i_{dr} in rotor side controller. As a result this is a current control that creates optimal power tracking proportional to shaft speed. Assuming equation 3-3 following relations are derived:

$$P_{opt} = K_{opt} \omega_r^3 \qquad T = K_{opt} \omega_r^2 \qquad T_e^* = K_{opt} \omega_r^2 - \beta \omega_r$$

Equation 3-5

$$i_{dr}^* = \frac{-2T_e^*}{3pL_m i_{ms}}$$

Equation 3-6

$\beta \omega_r$ = fraction loss ω_r = shaft speed

Rotating reference in the rotor side model used in simulations is aligned with the stator voltage, as a result in the studied model Q will be determined with by i_{qr} and P will be controlled by i_{dr} in the controller.

3.3.2 Speed-Mode Control

Using a torque observer and measuring T_m turbine will follow optimized reference speed derived from equation 3-9.

$$\omega_r^* = \sqrt{\frac{T_m}{K_{opt}}}$$

Equation 3-7

ω_r = reference speed for speed controller.

Studying optimal power tracking feature of DFIG was not this project objective, and the behavior of the models in PSCAD and RSCAD are investigated considering a constant speed for wind, which means above controllers for optimizing are not deployed here in this work.

3.3.3 Stall regulation:

If speed control mode is used the torque can be observed and stall regulation can directly be implemented to the system, which is a type of over speed protection. The controller takes into account instantaneous power $P_m = T_m \omega_r$, and consequently determines the speed demand according to following equations:

$$\text{if } P_m < P_{\max} \text{ then } \omega_r = \sqrt{\frac{\hat{T}_m}{K_{opt}}}$$

Equation 3-8

$$\text{if } P_m \geq P_{\max} \text{ then } \omega_r = \frac{P_{\max}}{\hat{T}_m}$$

Equation 3-9

Power limitation reduces energy capture, and DFIG will track stall curve. Stall protection has simpler blade mechanism rather than pitch control method, which uses adjustable pitch blade angle and has more complicated construction; on the other hand stall regulation needs accurate torque observer.

Chapter 4

4 Modeling of DFIG

4.1 Control of Supply-Side PWM Converter

Grid side converter objective is to adjust the dc link by controlling input and output active power in balance, and also the terminal voltage by controlling reactive power injection to the grid during network fault in either sub synchronous or super synchronous mode independent of magnitude and direction of the rotor power. By aligning the reference frame with the stator (grid) voltage vector position it possible to control active and reactive power flow between stator and grid side converter independently. The method which is used for controlling supply side converter at this study is current regulated PWM method, enabling the control of dc link voltage by direct axis current and controlling reactive power flow to grid by quadrature axis current component. Modeling of DFIG follows the same principal either in PSCAD and RSCAD. Simulation in RSCAD is based on small time step (approximately 2-3 μ seconds) ,which in PSCAD is in large time step .Using equations 4-1 and 4-2 it can be shown that Dc-link voltage is a funciotn of net power flow into the capacitor.The amount of energy stored in the dc-link capacitor can be written as:[16]

$$E_c = \int P dt = \frac{1}{2} C v_{dc}^2$$

Equation 4-1

where C is capacitsance of the dc-link capacitor ,P is net power into the capacitor, and value of v_{dc} is capacitor voltage. P is equal to $P_r - P_c$, where P_r is the rotor power inflow and P_c is the grid power outflow:

$$\frac{dv_{dc}}{dt} = \frac{P}{v_{dc0} C} = \frac{P_r - P_c}{v_{dc0} C}$$

Equation 4-2

v_{dc0} = Initial value for dc-link voltage

4.1.1 D and Q Axis Current Regulator

The voltage over the series inductors can be obtained from the single line diagram in figure 4.1:

$$\begin{bmatrix} v_a \\ v_b \\ v_c \end{bmatrix} = R \begin{bmatrix} i_a \\ i_b \\ i_c \end{bmatrix} + L \frac{d}{dt} \begin{bmatrix} i_a \\ i_b \\ i_c \end{bmatrix} + \begin{bmatrix} v_{a1} \\ v_{b1} \\ v_{c1} \end{bmatrix}$$

Equation 4-3

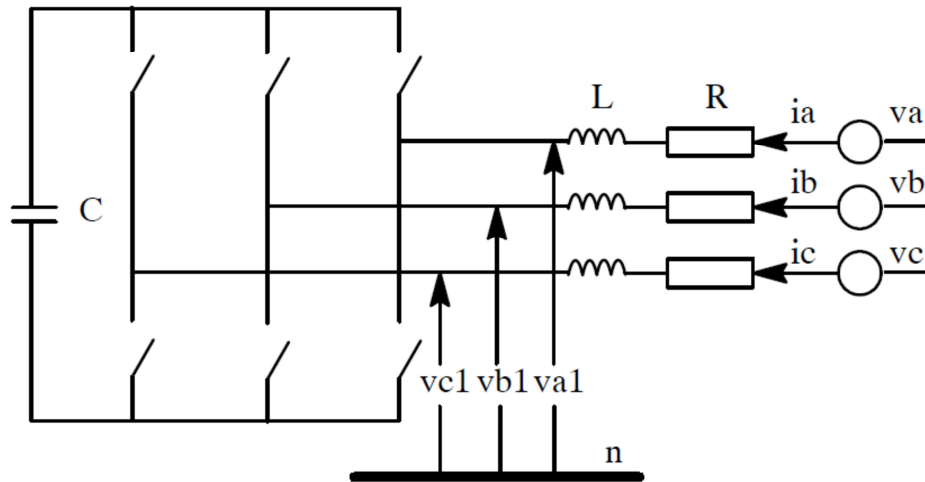


Figure 4.1- Network and supply side converter

$$e = \frac{Nd\phi}{dt} \quad e = \frac{d\psi}{dt} \quad U_s - R_g i_g = \frac{d\psi_s}{dt}$$

$$U_c + R_g i_g + L_g \frac{di_g}{dt} = U_g$$

Equation 4-4

U_c = Converter voltage vector

U_g = Grid voltage vector

R_g & L_g = Grid resistance and inductance

steady state equation of grid voltage vector in reference frame rotating at ω_e :

$$\underline{U}_g = U e^{j(\omega_e t + \varphi_u)} = U e^{j\varphi_u} e^{j\omega_e t} = \underline{U}_g e^{j\omega_e t}$$

$$\underline{U}_g e^{j\omega_e t} = \underline{U}_c e^{j\omega_e t} + R_g \underline{i}_g e^{j\omega_e t} + L_g \frac{d\underline{i}_g}{dt} e^{j\omega_e t}$$

$$\underline{U}_g e^{j\omega_e t} = \underline{U}_c e^{j\omega_e t} + R_g \underline{i}_g e^{j\omega_e t} + L_g e^{j\omega_e t} \frac{d\underline{i}_g}{dt} + j\omega_e e^{j\omega_e t} L_g \underline{i}_g$$

By removing $e^{j\omega_e t}$ from two sides of equation: [10]

$$\underline{U}_g = \underline{U}_c + R_g \underline{i}_g + L_g \frac{d\underline{i}_g}{dt} + j\omega_e L_g \underline{i}_g$$

Equation 4-5

To implement the controller in the grid side voltage source converter (VSC) it is very helpful to express the equations in d and q axis. Different reference frames can be selected for designing the controller and making different selections doesn't influence the accuracy of the controller, but, it is more convenient to use the stator voltage reference frame since the quantity can be directly defined. In this thesis, therefore, the reference frame is aligned to the stator voltage according to figure 4.2 [10], [4].

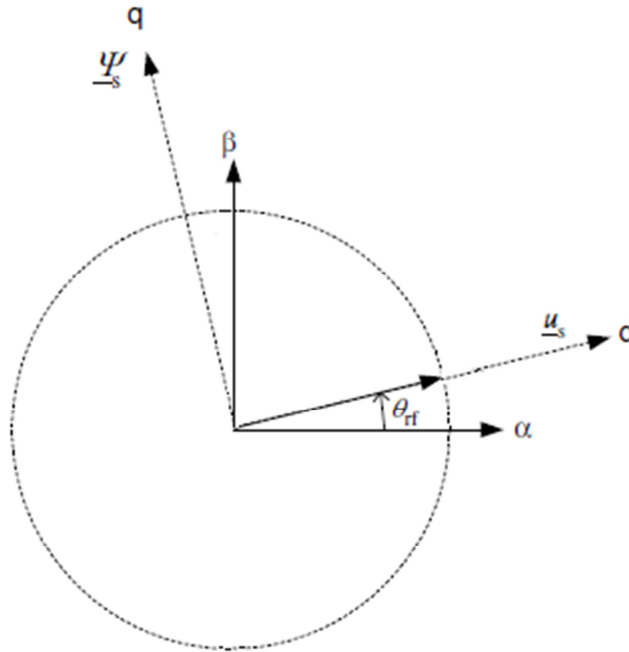


Figure 4.2- Reference Selection for Grid Side Converter

$$\underline{U}_{gd} = \underline{U}_{cd} + R_g \underline{i}_{gd} + L_g \frac{d\underline{i}_{gd}}{dt} + \omega_e L_g \underline{i}_{gq}$$

Equation 4-6

$$\underline{U}_{gq} = \underline{U}_{cq} + R_g \underline{i}_{gq} + L_g \frac{d\underline{i}_{gq}}{dt} - \omega_e L_g \underline{i}_{gd}$$

Equation 4-7

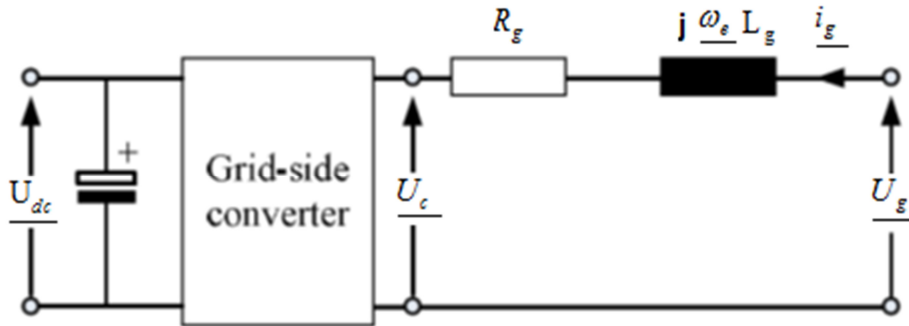


Figure 4.3- Grid Side Converter-Network Connection

$$\underline{U}_{gd} = \text{constant} \quad \underline{U}_{gq} = 0$$

R_g and L_g = Line inductance and resistance

\underline{i}_{gd} and \underline{i}_{gq} = Grid current vectors in dq axis

\underline{U}_{gd} and \underline{U}_{gq} = Grid voltage expressed in dq axis

\underline{U}_{cd} and \underline{U}_{cq} = Converter voltage in dq axis

ω_e = Grid frequency

There are cross coupling terms in d and q components between \underline{U}_{gd} and \underline{U}_{gq} equations, which means any change in \underline{U}_{gd} to change \underline{i}_{gd} will lead to a transient in \underline{i}_{gq} and all changes in \underline{U}_{gq} influence \underline{i}_{gd} which is not desired in controller performance, consequently modifications should be made to decouple the response. These terms should be removed for controlling d and q components independent from each other and better performance of controller. [10],[11]

$$\text{If } \underline{U}_{gd} = v_d \quad \text{and} \quad \underline{U}_{gq} = v_q = 0$$

If instead, define new quantities x_1 and x_2 to control the currents, the resulting equations are decoupled: [10]

$$\underline{U}_{gd} = \underline{U}_{cd} + R_g i_{gd} + L_g \frac{di_{gd}}{dt} - \omega_e L_g i_{gq}$$

Equation 4-8

$$\underline{U}_{gq} = \underline{U}_{cq} + R_g i_{gq} + L_g \frac{di_{gq}}{dt} + \omega_e L_g i_{gd}$$

Equation 4-9

[10],[11]:

$$\frac{d}{dt} \begin{bmatrix} i_{gd} \\ i_{gq} \end{bmatrix} = \begin{bmatrix} -\frac{R_g}{L_g} & \omega_e \\ -\omega_e & -\frac{R_g}{L_g} \end{bmatrix} \begin{bmatrix} i_{gd} \\ i_{gq} \end{bmatrix} + \frac{1}{L} \begin{bmatrix} U_{gd} - U_{cd} \\ -U_{cq} \end{bmatrix} = \begin{bmatrix} -\frac{R_g}{L_g} & 0 \\ 0 & -\frac{R_g}{L_g} \end{bmatrix} \begin{bmatrix} x_1 \\ x_2 \end{bmatrix}$$

$$x_1 = \frac{U_{gd} - U_{cd}}{L_g} + \omega_e i_{gd}$$

$$x_2 = \frac{-U_{cq}}{L_g} - \omega_e i_{gq}$$

$$U_{cd} = -L_g x_1 + U_{gd} + \omega_e L_g i_{gq}$$

$$U_{cq} = -L_g x_2 - \omega_e L_g i_{gd}$$

Current control loops for deriving v'_d and v'_q is given by:

$$F(s) = \frac{i_d(s)}{v'_d(s)} = \frac{i_q(s)}{v'_q(s)} = \frac{1}{Ls + R}$$

$$R_g i_{gd} + L_g \frac{di_{gd}}{dt} = v'_d$$

$$R_g i_{gq} + L_g \frac{di_{gq}}{dt} = v'_q$$

$$R_g i_{gd} + L_g \frac{di_{gq}}{dt} = v'_q = L_g x_1 \quad R_g i_{gq} + L_g \frac{di_{gd}}{dt} = v'_d = L_g x_2$$

$$U_{cd}^* = -v'_d + (\omega_e Li_q + v_d)$$

Equation 4-10

$$U_{cq}^* = -v'_q - (\omega_e Li_d)$$

Equation 4-11

Where starred values are calculated references, and primed values are output of PI controller, the terms in bracket are the voltage compensation or decoupling terms. Compensation terms which would exist without internal VSC voltage are eliminated from control loop when calculating voltage references. Control scheme of dc-link voltage and grid power factor by means of grid-side converter is illustrated in figure 4.4.[10]

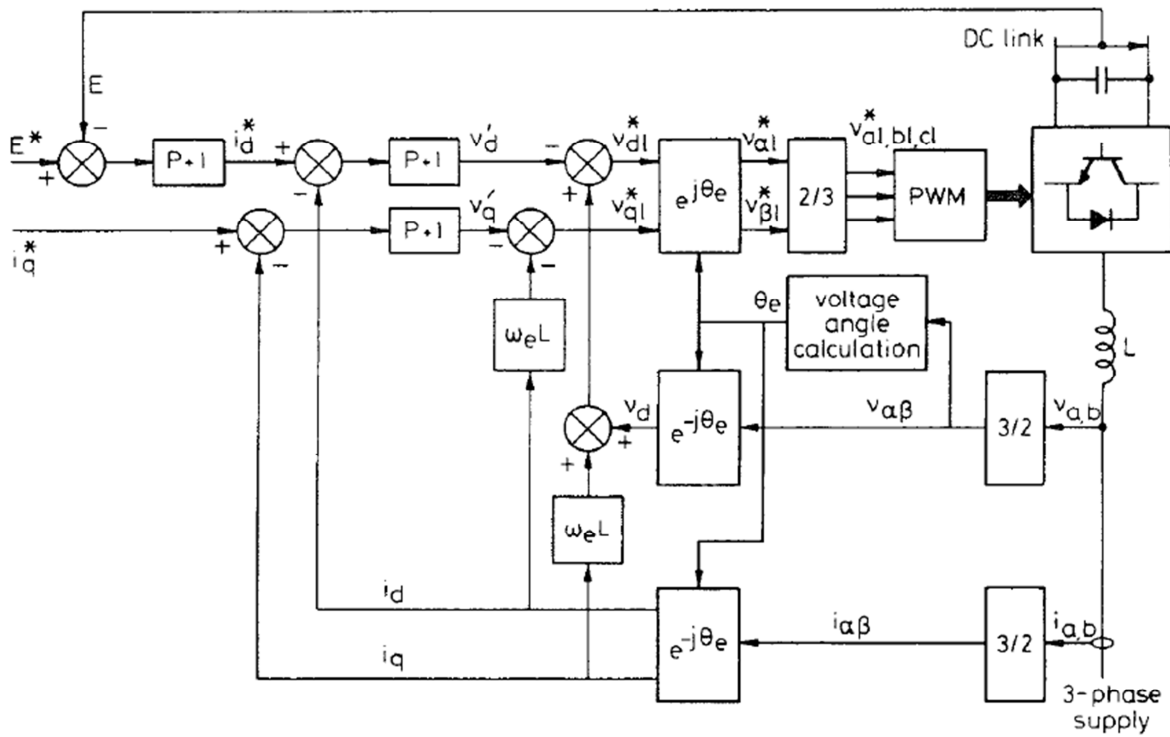


Figure 4.4 -Typical Grid Side Controller in DFIG

Active and reactive power flow calculation in power invariant scaling ($K = \sqrt{\frac{3}{2}}$) can be written as : [10]

$$P_s = \frac{3}{2K^2} (\vec{v}_{sd} \vec{i}_{sd} + \vec{v}_{sq} \vec{i}_{sq}) = (\vec{v}_{sd} \vec{i}_{sd})$$

Equation 4-12

as $v_q = 0$

i_q demand reactive power on supply side of inductors;

$$Q_s = \frac{3}{2K^2} (\vec{v}_{sd} \vec{i}_{sq} + \vec{v}_{sq} \vec{i}_{sd}) = (\vec{v}_{sd} \vec{i}_{sq})$$

Equation 4-13

Neglecting switching losses and losses in inductor and resistor, i_d^* demand in figure 4.4 can be calculated from dc link voltage error, as a result using figure 4.5 it is shown that dc link voltage can be adjusted by controlling i_d .

$$E i_{os} = 3 v_d i_{gd} = P$$

Equation 4-14

$$v_d = \frac{m_1}{2\sqrt{2}} E \quad C \frac{dE}{dt} = i_{os} - i_{or} \quad i_{os} = \frac{3}{2\sqrt{2}} m_1 i_{gd}$$

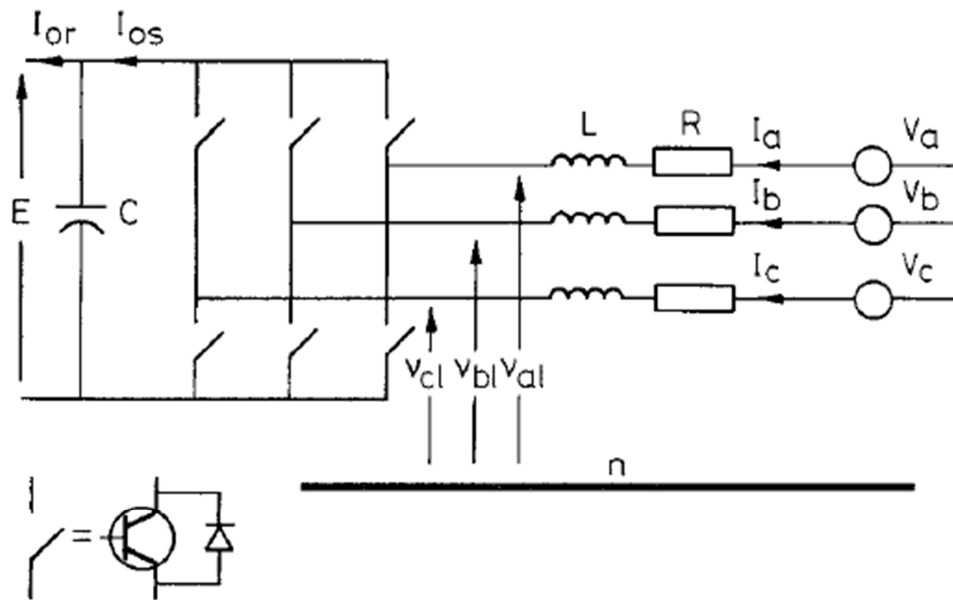


Figure 4.5 Control of DC Link Voltage

4.2 Control of Rotor Side Converter

For rotor-control derivation, the direct-axis of rotating reference frame is aligned with stator voltage. The principle of rotor VSC is very similar to the Grid VSC. By using the stator voltage as reference frame it would be possible to relate active power and reactive power to i_{rd} and i_{rq} respectively. Rotor currents are transformed to dq components and are regulated using regular PI current controllers. In this way decoupled control between active and reactive power is obtained.

As a result active power can be adjusted by changing i_{rd} and reactive power can be controlled by i_{rq} . Rotor controller is providing excitation for rotor. Stator magnetizing current can be assumed constant as stator resistance is small and stator terminal is directly connected to the grid. Stator voltage vector can be expressed as:

$$\underline{U}_{gd} = \text{constant}$$

$$\underline{U}_{gq} = 0$$

$$\Psi_{sd}^s = 0$$

$$\Psi_{sq}^s = |\bar{\Psi}_s|$$

These vectors correspond to stator frame. Magnetizing current i_{ms} is aligned with the stator flux vector, and is expressed as:

$$\bar{\Psi}_s = L_m \vec{i}_{ms}$$

4-15

$$\bar{\Psi}_s = L_s \vec{i}_s + L_m \vec{i}_r$$

4-16

Combining equations 4-15 and 4-16:

$$\vec{i}_{ms} = \frac{L_s}{L_m} \vec{i}_s + \vec{i}_r$$

4-17

Knowing $\Psi_{sd}^s = 0$ related d component of i_{ms} is zero and $\bar{\Psi}_{sq} = L_m \vec{i}_{msq}$ therefore:

$$\vec{i}_{msq} = \frac{L_s}{L_m} \vec{i}_{sq} + \vec{i}_{rq}$$

4-18

$$\vec{i}_{msd} = \frac{L_s}{L_m} \vec{i}_{sd} + \vec{i}_{rd} = 0$$

4-19

Above equations can be written as;

$$\Psi_{sq}^s = L_m \vec{i}_{msq}^s$$

4-20

$$i_{sq}^s = \frac{L_m}{L_s} (i_{msq}^s - i_{rq}^s)$$

Equation 4-21

$$i_{sd}^s = -\frac{L_m}{L_s} i_{rd}^s$$

Equation 4-22

The stator voltage vector can be expressed as:

$$\vec{v}_s = \vec{i}_s R_s + j\omega_e \vec{\Psi}_s + \frac{d\vec{\Psi}_s}{dt}$$

$$\vec{v}_s = \vec{i}_s R_s + j\omega_e L_m i_{ms}^s + L_m \frac{di_{ms}^s}{dt}$$

$$\vec{v}_s = \vec{i}_{sd} R_s - \omega_e L_m i_{msq}^s + L_m \frac{di_{msq}^s}{dt}$$

4-23

It can be assumed that the influence of stator resistance R_s is very small, and the stator flux is relatively constant, i.e. the stator flux rate of change is close to zero as a result the equation can be written as:

$$\vec{v}_s = -\omega_e L_m i_{msq}^s$$

4-24

Equation 4-24 indicates that stator voltage vector is perpendicular to the stator flux vector. Considering that $\omega_e = 1$ p.u and $v_{sq} = 0$, equation can be written as

$$\vec{v}_{sd} = -L_m i_{msq}^s$$

4-25

Stator active and reactive power for power invariant scaling ($K = \sqrt{\frac{3}{2}}$) can be written as;

$$P_s = \frac{3}{2K^2} (\vec{v}_{sd} \vec{i}_{sd} + \vec{v}_{sq} \vec{i}_{sq}) = (\vec{v}_{sd} \vec{i}_{sd})$$

Equation 4-26

$$Q_s = \frac{3}{2K^2} (\vec{v}_{sd} \vec{i}_{sq} + \vec{v}_{sq} \vec{i}_{sd}) = (\vec{v}_{sd} \vec{i}_{sq})$$

Equation 4-27

Substitution of 4-21 and 4-21 into equations 4-26 and 4-27 produces the following expressions

$$i_{sd}^s = -\frac{L_m}{L_s} i_{rd}^s$$

Equation 4-28

$$P_s = -\frac{v_{sd}^s L_m}{L_s} i_{rd}^s$$

Equation 4-29

Electrical torque can be expressed:

$$T_e = \frac{3n_p}{2K^2} (\psi_{sd} i_{sq} - \psi_{sq} i_{sd}) = n_p (\psi_{sd} i_{sq} - \psi_{sq} i_{sd})$$

$$T_e = -n_p P L_m i_{ms} i_{dr}$$

Equation 4-30

$$i_{sq}^s = \frac{L_m}{L_s} (i_{msq}^s - i_{rq}^s)$$

Equation 4-31

$$Q_s = \frac{v_{sd}^s L_m}{L_s} (i_{msq}^s - i_{rq}^s) = \left[\frac{-(v_{sd}^s)^2}{L_s} - \frac{v_{sd}^s L_m}{L_s} i_{rq}^s \right]$$

Equation 4-32

It is shown that the reactive power and active power are controlled by i_{rq}^s and i_{rd}^s respectively. If value of i_{rq}^s is set to zero all the required reactive power for the machine will be supplied by the stator and the grid which is not desirable. The reference values of active and reactive powers will create references for i_{rq}^s and i_{rd}^s by using the relevant PI controllers.

4.2.1 Current Reference Pulse Width Modulation:

At this study produced i_{rq}^s and i_{rd}^s are transformed to three phase, the produced three phase current produced is considered as the reference value and should be regulated by means of hysteresis band control and the current regulator keeps the difference between the actual current and the reference current in the desired hysteresis band by switching on and off the IGBTs in the rotor side controller. This method also is called current reference pulse width modulation. This method which is used in this study can generate any desired current wave form in R-L circuit. As shown in figure 4.6 the upper and lower tolerance band is defined around the chosen reference value. If the error of actual current is lower than the threshold the upper switch is turned applying

a positive voltage ($E/2$) to the load and the current start to increase. When this error is higher than the defined hysteresis band the upper switch is turned off and the lower switch is turned on to decrease the current applying a negative voltage ($E/2$) to the load and the current start to drops. Thus the difference between the desired and actual currents is kept to within the tolerance band. By creating a smaller hysteresis band the degree of the accuracy can be higher but with the expense of higher switching expenses. With using the method any type of current can be made and injected to the rotor of the machine. The problem with this technique is that the switching frequency is not fixed and can vary [11].

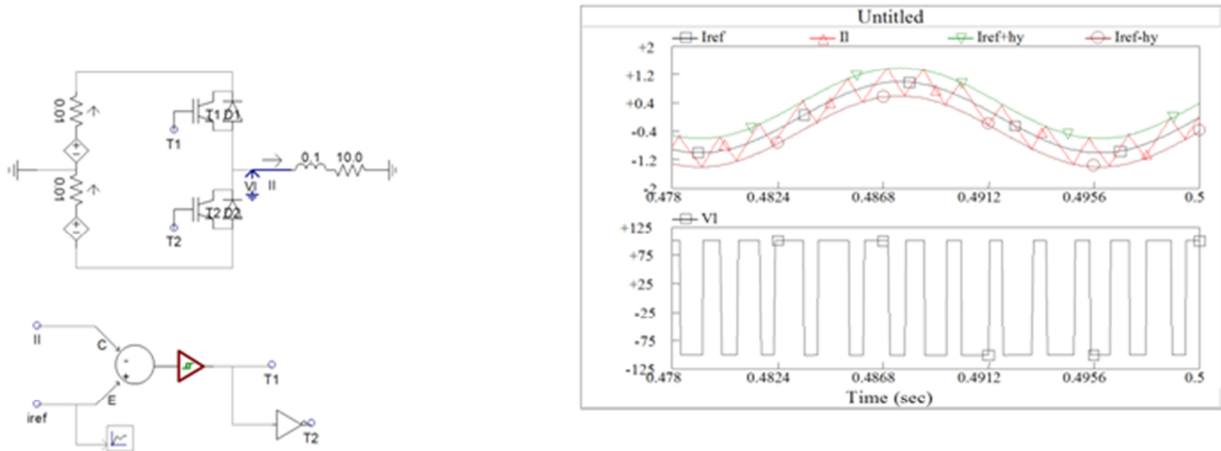


Figure 4.6- Hysteresis control Method

There are also some papers that use pulse width modulation(PWM) method for rotor side controller exactly same as grid side controller .In that method i_{rq}^s and i_{rd}^s are changed to voltages using another PI controller and pulse width modulation is implemented with the help of triangular wave and firing pulses. [10]

Chapter 5

5 Real Time Digital Simulator (RTDS)

RTDS simulation uses Electromagnetic transient solution (EMTP simulation type) .This method is based on Dommel algorithm and Trapezoidal rule of integration which produces new solution in each time step. If physical control and protection equipment are used in simulation studies then continuous hard real time response must be provided and sustained. Special high speed processing and signal communication is needed to reach real time execution.

Applying Kirchoff's current and voltage rules for solving the circuit in figure 5.1 would lead to differential equations which can be complicated to solve. It would be greatly desired to have a more straight forward approach which can be solved without much difficulty. [15]

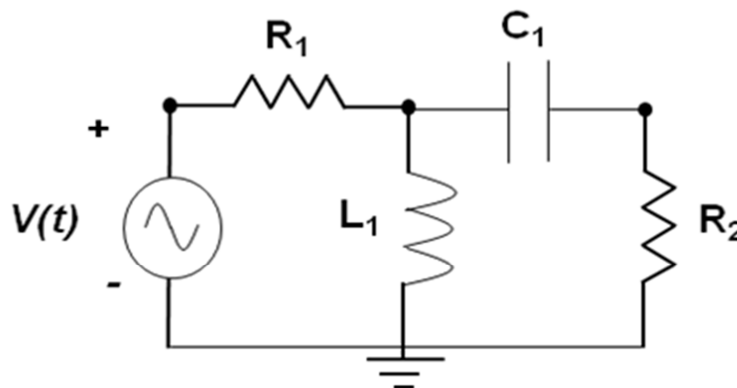


Figure 5.1 RL Circuits

Fig.5.2 shows a simple inductor circuit

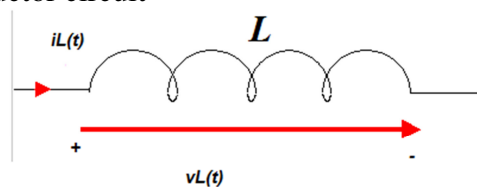


Figure 5.2- Inductor Voltage - Current

The voltage equation can be expressed

$$v_L(t) = L \frac{di_L(t)}{dt}$$

Equation 5-1

Integration of two sides of equation results;

$$i_L(t) = \frac{1}{L} \int_{t-\Delta t}^t v_L(\tau) d\tau + i_L(t - \Delta t)$$

Equation 5-2

Applying n of trapezoidal integration leads to;

$$i_L(t) = \frac{1}{L} v_L(t) + \underbrace{\left[\frac{\Delta t}{2L} v_L(t - \Delta t) + i_L(t - \Delta t) \right]}_{I_H(t)} \rightarrow i_L(t) = g_L v_L(t) + I_H(t)$$

Equation 5-3

Above equation can be expressed as the circuit shown in fig5.3:

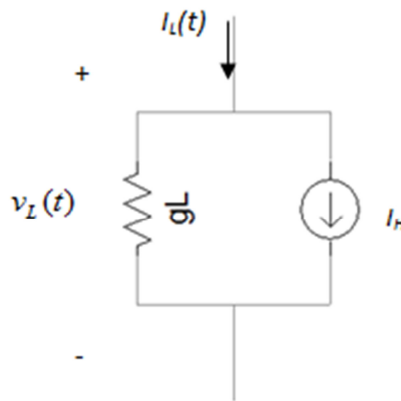


Figure 5.3-Inductor representation in RTDS

Same approach can be used for capacitor circuits in figure 5.4:

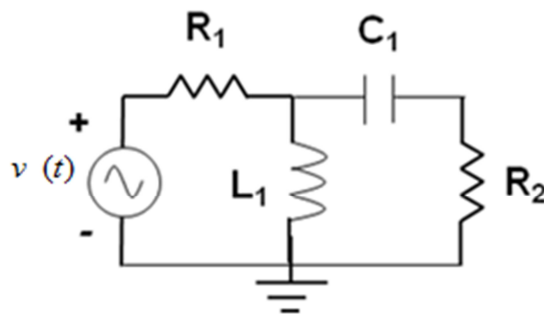


Figure 5.4- Simple RC Circuit

By changing voltage sources to their equivalent Norton circuit in figure 5.5;

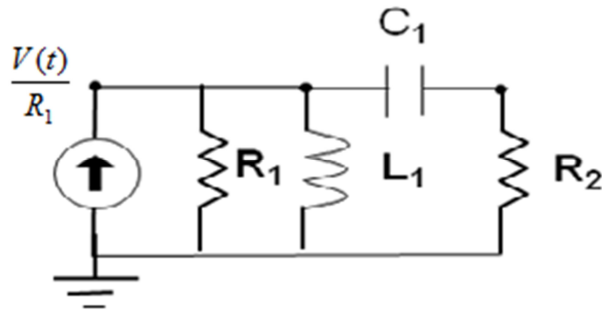


Figure 5.5-Norton Equivalent Circuit

The passive elements in the circuit also can be expressed to their equivalent elements. This is shown in figure 5.6:

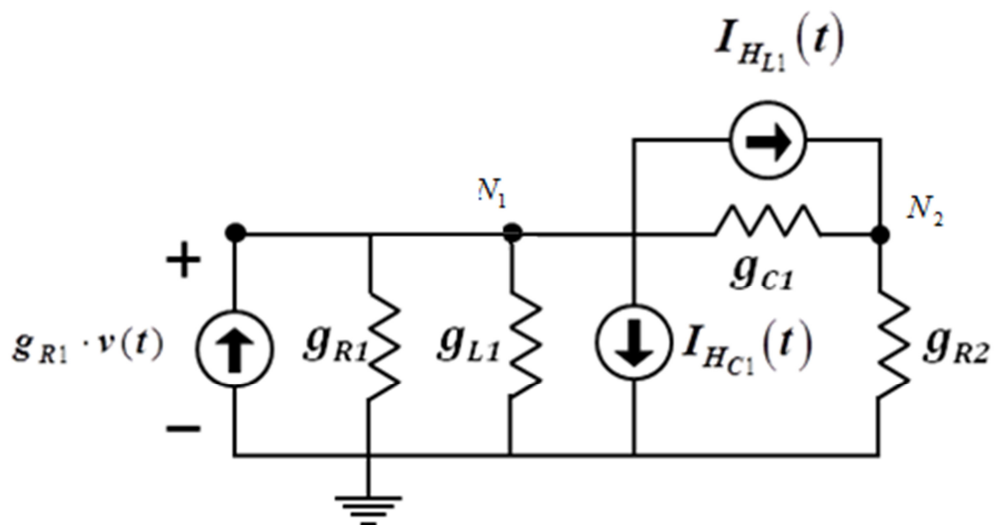


Figure 5.6- Network Equivalent Circuit in RTDS

Writing node equations:

$$\begin{bmatrix} V_{N1} \\ V_{N2} \end{bmatrix} = \begin{bmatrix} g_{R1} + g_{L1} + g_{C1} & -g_{C1} \\ -g_{C1} & g_{R2} + g_{C1} \end{bmatrix}^{-1} \begin{bmatrix} g_{R1} \cdot v(t) - I_{HL1} - I_{HC1} \\ I_{HL1} \end{bmatrix}$$

Equation 5-4

$$V = G^{-1} \cdot I$$

Equation 5-5

By these matrixes it is possible to calculate voltage at nodes N1 and N2 at any time provided the input voltage $V(t)$ and the history terms I_{HL1} and I_{HC1} are known. Using the node voltages and history terms then it is easy to find branch currents. The simulation of the circuit's responses will take one time step at a time.

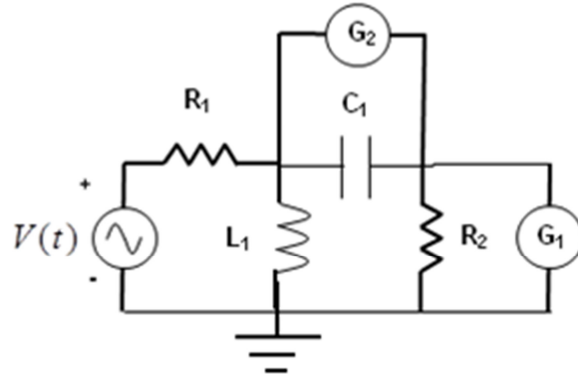


Figure 5.7-Network with Different Components

All complicated components can be modeled using a current source in parallel with a conductance (see figure 5.7 and 5.8). Difficult part is to find accurate representation that can exactly model the behaviour of real component. System components such as travelling wave, transmission lines, transformers, synchronous generators etc can be modeled using this approach.

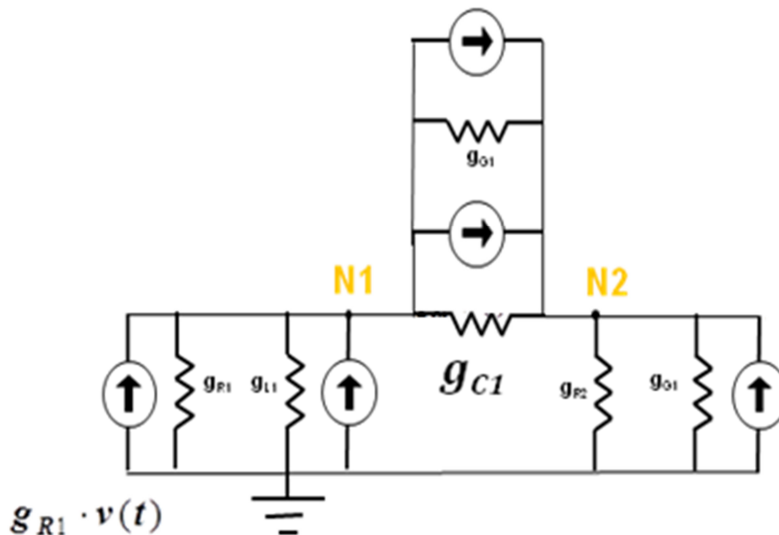


Figure 5.8-Network and Components in equivalent circuit in RTDS

This algorithm can be admitted for modeling of breakers and faults. For example in figure 5.9, switch can be represented by conductance g_3 which has a small values, when the switch S1 is open, and accordingly has a large value, when switch is closed. (see figure 5.10)

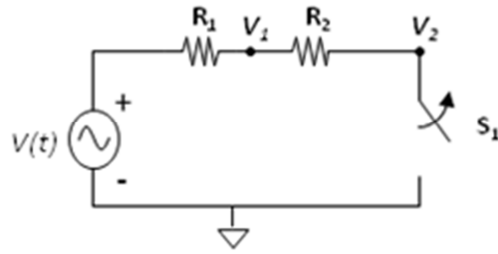


Figure 5.9-Modeling a Breaker or a Fault in a Circuit

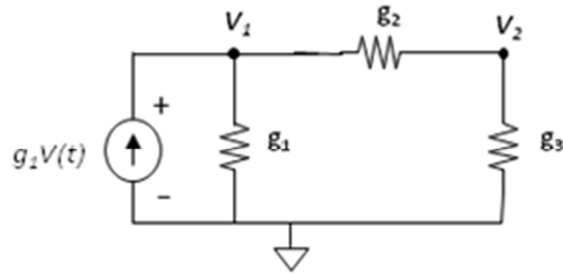


Figure 5.10-Modeling a Breaker operation or Fault in RTDS

Writing nodal equations for this circuit the in figure 5.10 will give:

$$\begin{bmatrix} v_1 \\ v_2 \end{bmatrix} = \begin{bmatrix} g_1 + g_2 & -g_2 \\ -g_2 & g_2 + g_3 \end{bmatrix}^{-1} \begin{bmatrix} g_1 V(t) \\ 0 \end{bmatrix}$$

Equation 5-6

This models switching by modifying g_3 and re inverting the conductance matrix every time a switching event occurs.

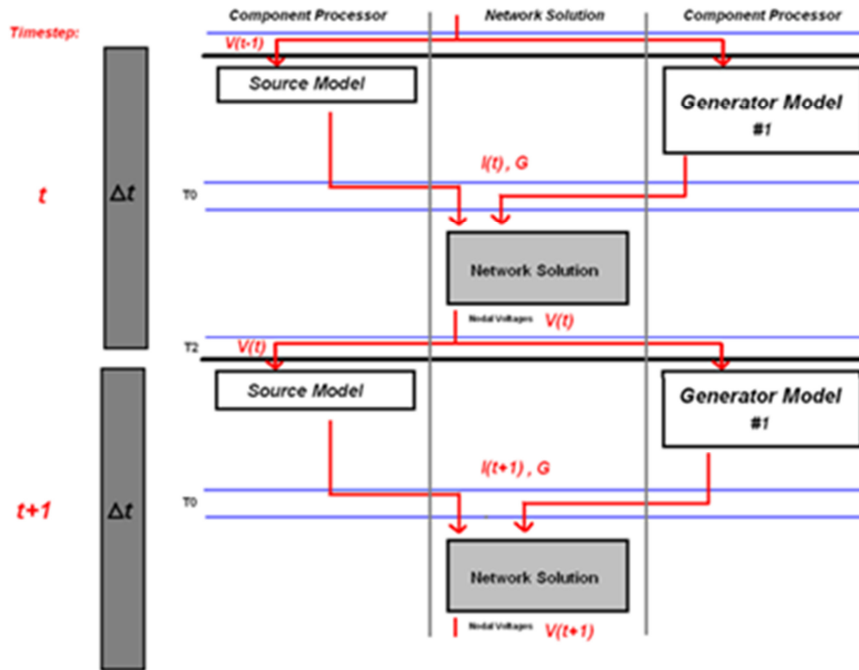


Figure 5.11- Time Steps in RTDS

Whatever number of nodes increases consequently the size of conductance matrix increases. For simulating fault and breakers in our model it is required to decompose and invert G matrix at each time step. But there are always limited numbers of calculations that can be performed during one time step (50μs). Consider a system in figure 5.12 with one hundred nodes if calculation time τ becomes bigger than one time step then it is needed to split the larger network into some smaller sub networks, which in RTDS should be separated by long t lines in model. This way sub systems don't influence the other sub systems calculations during a single time step, and therefore can be solved independently as it is shown in figure5.13.

$$G = \begin{bmatrix} Y_{11} & Y_{12} & \dots & Y_{1N} \\ Y_{21} & \dots & \dots & \dots \\ \dots & \dots & \dots & \dots \\ Y_{N1} & \dots & \dots & Y_{NN} \end{bmatrix}$$

Equation 5-7

N*N matrix

N=Number of nodes in network

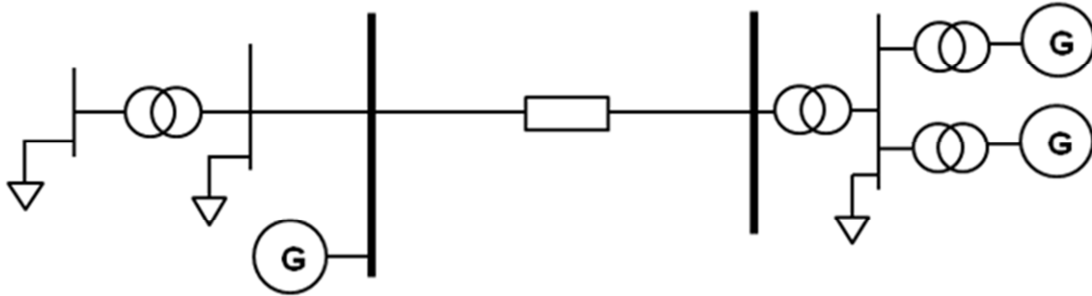


Figure 5.12- Illustration for a large Network

$$G = \begin{bmatrix} \begin{bmatrix} Y_{1,1} & \cdots & Y_{1,50} \\ \vdots & & \vdots \\ Y_{50,1} & \cdots & Y_{50,50} \end{bmatrix} & 0 \\ 0 & \begin{bmatrix} Y_{51,51} & \cdots & Y_{51,100} \\ \vdots & & \vdots \\ Y_{100,51} & \cdots & Y_{100,100} \end{bmatrix} \end{bmatrix}$$

Two 50 x 50 matrix

Figure 5.13- Conductance matrix for two subsystems

5.1 Small Time Step Approach

Normally Electro-magnetic Transient Program (EMTP) simulation type uses a typical time step of 50 μ s. Such simulation type is permitting to have simulation of events occurring in the range of 0 to ~3 kHz. There is a need for an approach with smaller time steps to model modern high frequency switching circuits because the phenomena of interest take place at higher frequencies. That is used in today's power electronic industries. RTDS perform simulations for these purposes using high speed processors and special calculation method to reduce the time step to lower values between 1 and 3 μ s, which should be reached for high frequency applications. This field of simulation is the biggest application for the RTDS simulator. This small time step simulations are available on both GPC and PB5 processors and RTDS is continuously increasing the new components in the related library ,which now includes: Induction Machine, Permanent Magnet Synchronous Machine, Two Level Converter Bridges, Three Level Converter Legs, Discrete switching elements, Transformers, Transmission lines Modular Multi-Level Converters, and etc. [15].

5.1.1 Fundamentals of Small Time-Step Simulation

As it was discussed Dommel algorithm and Trapezoidal integration are used to perform a new solution in each time-step to solve the following equation:

$$V = G^{-1}I$$

In order to keep the real time simulation performance the conductance matrix inversion should be executed in every time step because the controller is changing the switching states of the network at any time leading to changes in G matrix. According to figure 5.14 as the network size increases sustaining real time situation becomes more problematic because the processors need more time for G matrix inversion, and this increases the calculation time.

$$G = \begin{bmatrix} Y_{11} & Y_{12} & \dots & Y_{1N} \\ Y_{21} & \dots & \dots & \dots \\ \dots & \dots & \dots & \dots \\ Y_{N1} & \dots & \dots & Y_{NN} \end{bmatrix}$$

Equation 5-8

N*N matrix

N=Number of nodes in the network

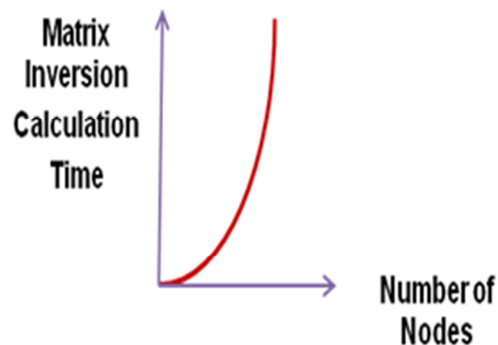


Figure 5.14-Calculation Time in RTDS

5.1.2 The Challenge

Even by using the most advanced processors, it will take about 50 μsec to invert and decompose a 72×72 conductance matrix. In the other hand using the previous defined modeling of switches if the purpose is to perform real time simulation for high frequency equipment then all these calculations for the same 72×72 matrix should be finished within 1 μsec , which consequently will require a processor with 50 times more powerful. Due to these limitations in high frequencies another approach for modeling the switches should be proposed.

5.1.3 Solution

In this approach instead of using a large conductance an inductor is used to represent a short circuit using and rather than a small conductance for open circuit a series RC circuit will be utilized. Both inductor and capacitor can be replaced by their equivalent circuits as before in figures 5.15 and 5.16:

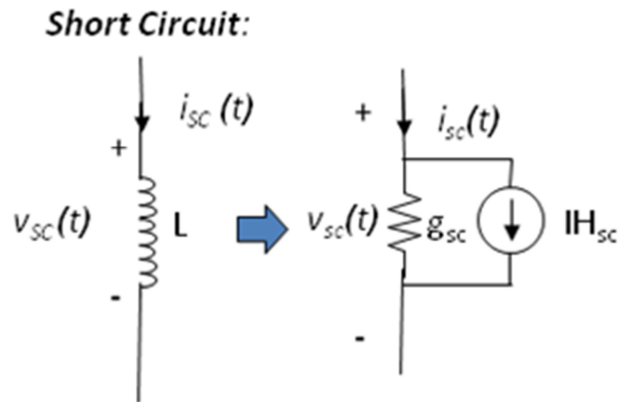


Figure 5.15-Short Circuit Representation in RTDS

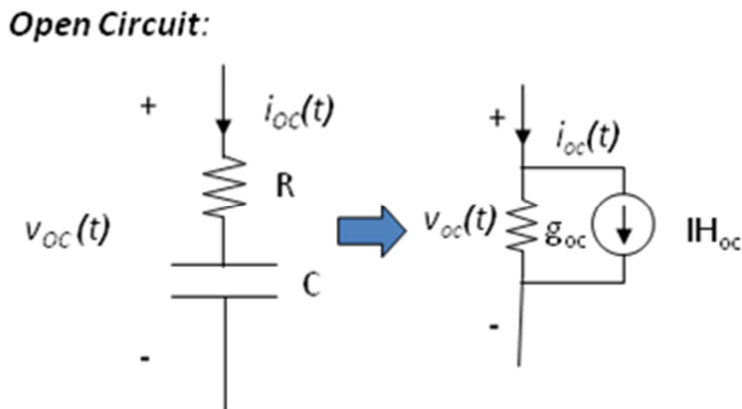
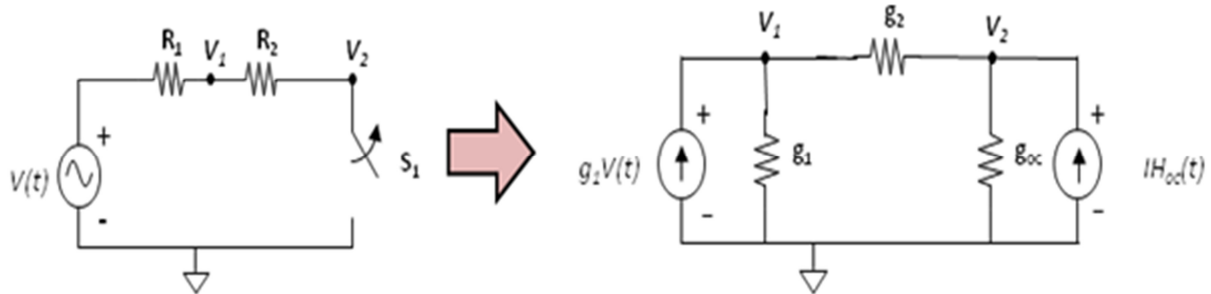


Figure 5.16-Open Circuit Representation in RTDS

It is shown in figures 5.17 and 5.18 that changing switching states involves changing g_{sc} to g_{oc} and $I_{H_{sc}}$ to $I_{H_{oc}}$ or vice-versa.

5.1.4 Open Circuit

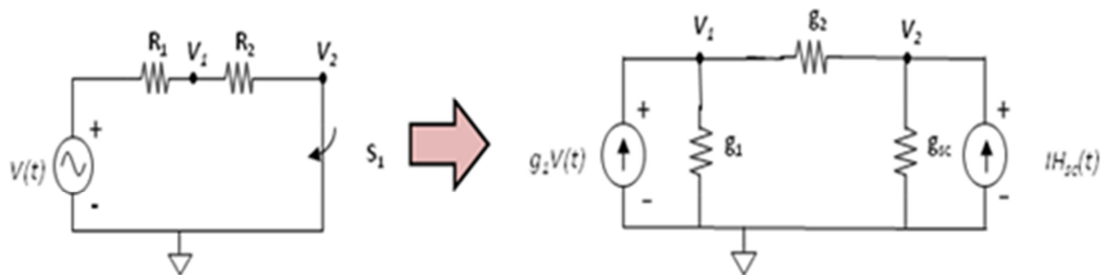


$$\begin{bmatrix} V_1 \\ V_2 \end{bmatrix} = \begin{bmatrix} g_1 + g_2 & -g_2 \\ -g_2 & g_2 + g_{oc} \end{bmatrix}^{-1} \begin{bmatrix} g_1 \cdot V(t) \\ I_{H_{oc}} \end{bmatrix}$$

Equation 5-9

Figure 5.17-Open Circuit Conductance Matrix in RTDS

5.1.5 Short Circuit



$$\begin{bmatrix} V_1 \\ V_2 \end{bmatrix} = \begin{bmatrix} g_1 + g_2 & -g_2 \\ -g_2 & g_2 + g_{sc} \end{bmatrix}^{-1} \begin{bmatrix} g_1 \cdot V(t) \\ I_{H_{sc}} \end{bmatrix}$$

Equation 5-10

Figure 5.18-Open Circuit Conductance Matrix in RTDS

If the values of g_{sc} to g_{oc} are chosen in a way that they become equal then it is not required to change the G-matrix each time a switching happens, therefore the conductance matrix inversion can be completed once before the simulation starts to run, which will result in considerable time saving, and all the changes in switching states can be represented by a varying the history currents. [14]

5.1.6 Small Time Constraints:

It should be considered that selecting g_{sc} to g_{oc} in this method will impose some constraint on selection of R, L, and C as it is depicted in figure 5.19.

$$g_{sc} = g_{oc} \Rightarrow r_{sc} = r_{oc} \Rightarrow R + \frac{\Delta t}{2C} = \frac{2L}{\Delta t}$$

Equation 5-11

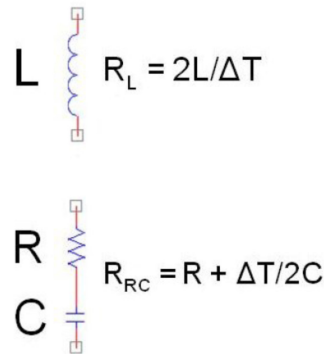


Figure 5.19 R and L selection in Small Time Step

5.1.7 Modeling Approach Issues

Using this method it should be noticed that the modeled impedance of open and short circuit using this approach should be large and small enough over the complete bandwidth of simulation. There is a small amount of energy that can be stored in the capacitance and inductance in each switching state, and when the switching event happens each time simply the model is changed from one state to another one and this energy is lost. This loss is not real and can increase by switching frequency. Consequently here is a limitation for the maximum switching frequency of about 3 kHz. When modeling switched by capacitors and inductors there is a possibility that the model transient response is not well damped. Proper selection of R, L and C can keep the transient response well damped.

The ratio between the off impedance and on impedance can be defined at frequency of f, this ratio is greater than $\frac{1}{(2\pi f \Delta t)^2}$. According to this relation by decreasing the time step this ratio

becomes larger which is desirable and similarly by having larger time steps the open circuit and short circuit impedances become closer which should be prevented. In RTDS simulation the minimum limit for small time step size is 1.4 μsec. usually but not always it is suggested to keep the small time step lower than 2.5 μsec. If there are different VSC subsystems in the model each sub system in small time step should be linked to the other small time sub systems via a cable or transmission line.

5.2 Simulation Software

RSCAD is a Java based GUI program for RTDS, which runs under Windows and Linux. This software creates the circuits that can be simulated using RTDS simulator. As shown in figure 5.20 file manager in RSCAD helps to organize the projects, launch modules and access manual.

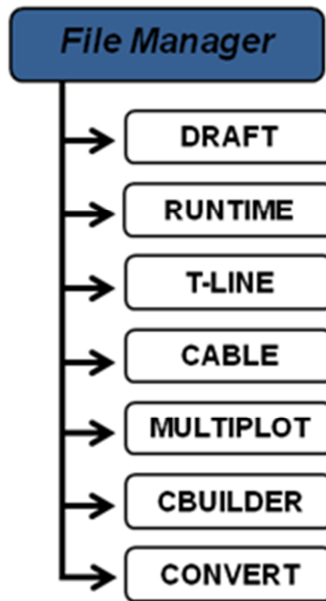


Figure 5.20-File Manager View

First of all a draft icon on the task bar shown in figure 5.21 should be clicked to create page.

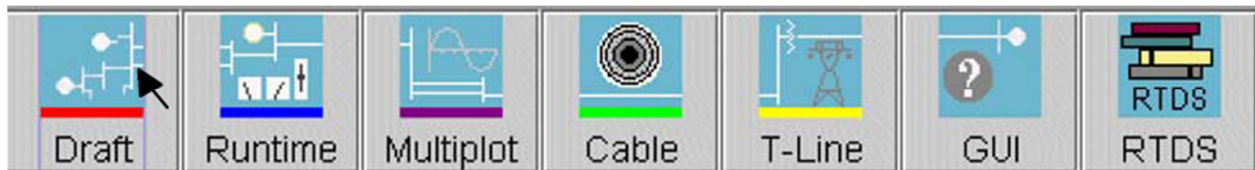


Figure 5.21-RSCAD Toolbar

Draft page is depicted in figure 5.22 and has a drawing space on the left and the library on the right side. In Draft the layout of circuit, entering the data, 3phase or single phase view and load flow tolls are places.

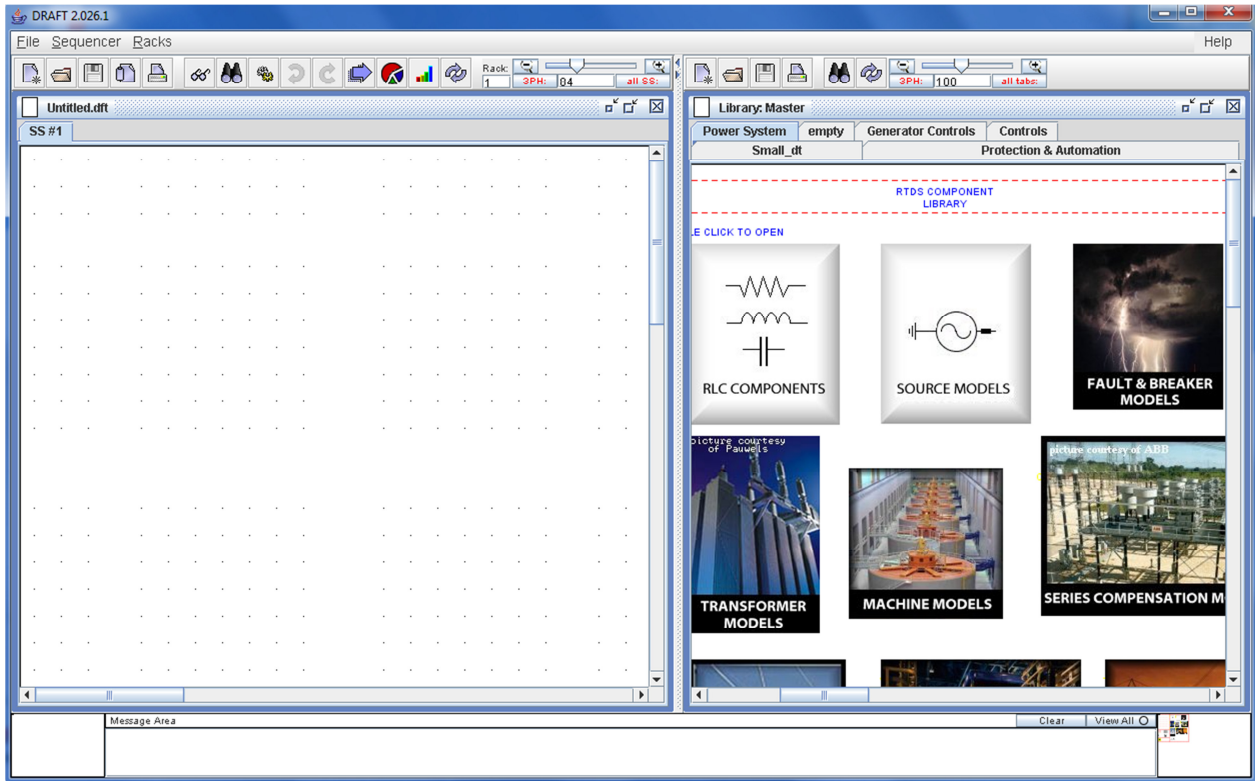


Figure 5.22-Drawing Page in DRAFT

All components can be copied from library and dragged to the draft window, after drawing the desired circuit and entering the parameters draft is ready for compiling, because each model need to be compiled in RTDS before running to create an executable code which is used by RTDS for running the simulation. Rack numbers on RTDS should be also selected before compiling as it is illustrated in figure 5.23.

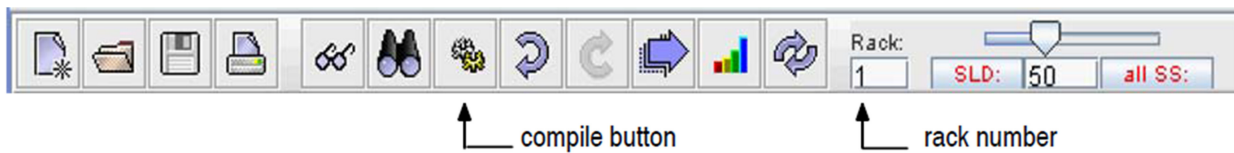


Figure 5.23-DRAFT Toolbar

RTDS simulations can be started from Runtime icon shown in figure 5.24.

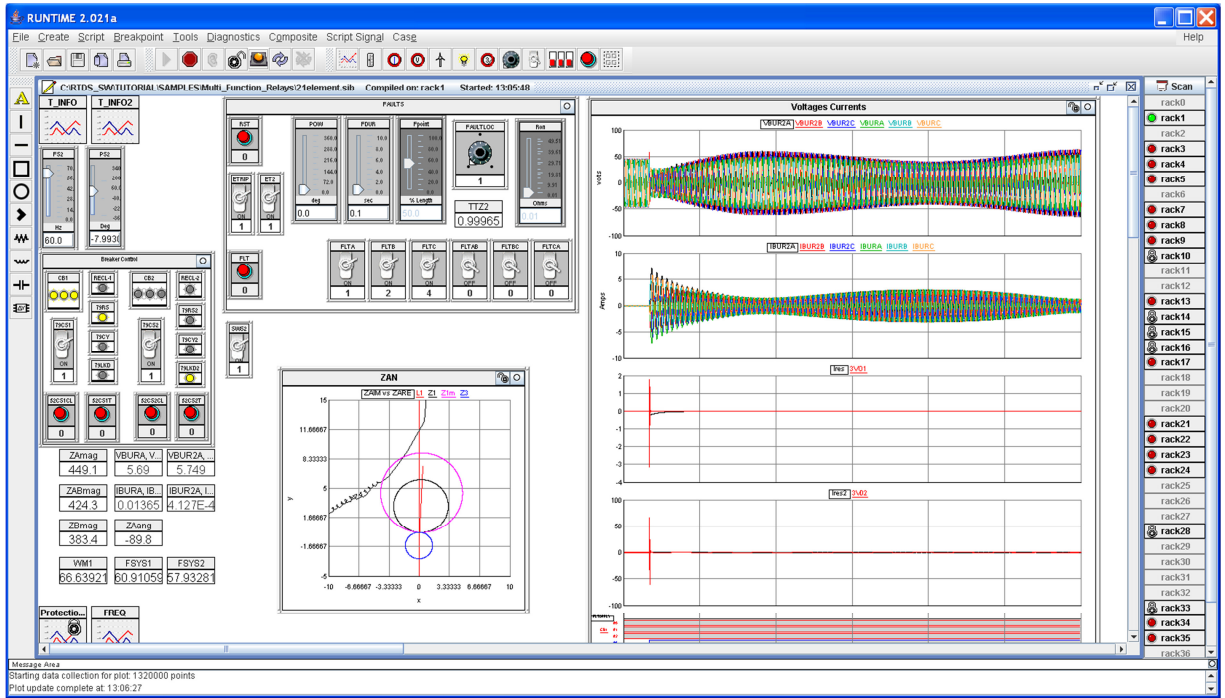


Figure 5.24-Simulation Page in RTDS

Figure 5.24 shows run time window, where signals can be monitored, different plot tools are available, and events can be triggered.

Chapter 6

6 Overview of System in RSCAD

The implemented model in DRAFT is shown in figure 6.1:

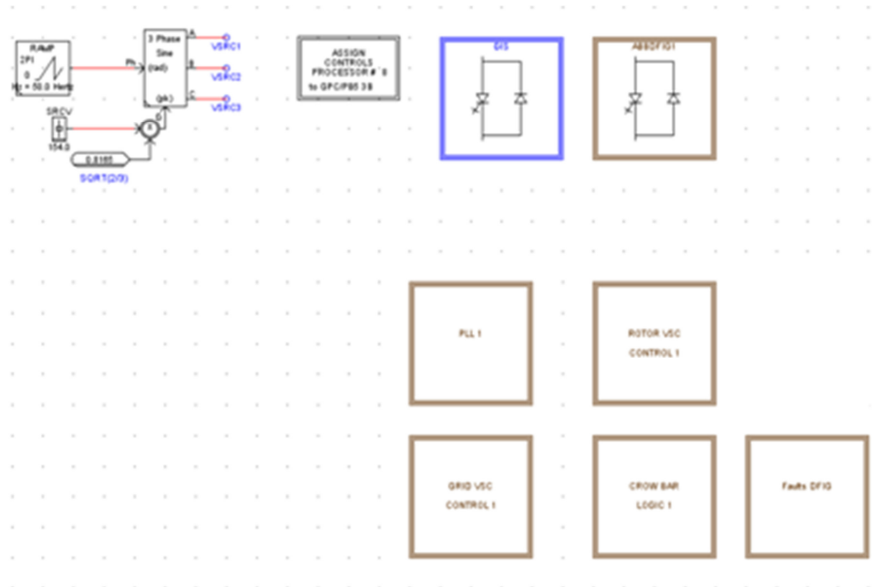


Figure 6.1-DFIG Controller Overview in RSCAD

The case is representing an infinite voltage source connected to two small time step BRIDGE_BOX labeled GIS and ABBDFIG1 and four brown hierarchy boxes containing the grid side and rotor side controllers, crowbar logic, phase locked loop (PLL). There is also a block which controls fault sequences. Except of GIS and ABBDFIG1 all the control components in this figure 6.1 are solved in large time step. The main network is solved with normal time step size of about 53 μ sec whereas the VSC circuit is solved with a time step of about 3.117647 μ sec.

6.1 Small Time Step Box

The figure displays two instances of the 'rtds_vsc_BRIDGE_BOX' dialog box, showing the 'BRIDGE PARAMETERS' tab. The dialog box contains a table of parameters and their values, along with buttons for 'Update', 'Cancel', and 'Cancel All'.

Top Screenshot (Bridge: GIS):

Name	Description	Value	Unit	Min	Max
Name	Bridge Name	GIS			
Desc	Description	GIS			
rqnmp	Requested Number of Processors:	One			
vscmrg	Calculation Margin in each small DT	360	nanoSec	360	1500
autocc	Order of Execution of VSC blocks is:	DEFAULT		0	1
stpmon	Enable Small-Step Step No. Monitor:	NO			
enabdi	Enable Digital Input 1 from GTDI:	NO			
enbdi2	Enable Digital Input 2 from GTDI:	NO			
clkmon	Enable Performance Counter:	NO			
mntyp	-- If YES: Code Zone to be Monitored is:	SML_DT		0	8
pmonu1	-- If YES: PMC1 Quantity Selection Mode:	BY_TOGGLE		0	2
pmonu2	-- If YES: PMC2 Quantity Selection Mode:	OFF		0	2
pmonu3	-- If YES: PMC3 Quantity Selection Mode:	OFF		0	2
pmonu4	-- If YES: PMC4 Quantity Selection Mode:	OFF		0	2
pmonu5	-- If YES: PMC5 Quantity Selection Mode:	OFF		0	2
pmonu6	-- If YES: PMC6 Quantity Selection Mode:	OFF		0	2
AorM	Assignment of Model to Processor	Manual			
CARD	-if Manual: Begin on Processor Card	1	1 to 6	1	6
Rprc	-if Manual: Begin on Processor	A			

Bottom Screenshot (Bridge: ABBDFIG1):

Name	Description	Value	Unit	Min	Max
Name	Bridge Name	ABBDFIG1			
Desc	Description	DFIG1			
rqnmp	Requested Number of Processors:	Two			
vscmrg	Calculation Margin in each small DT	360	nanoSec	360	1500
autocc	Order of Execution of VSC blocks is:	DEFAULT		0	1
stpmon	Enable Small-Step Step No. Monitor:	NO			
enabdi	Enable Digital Input 1 from GTDI:	NO			
enbdi2	Enable Digital Input 2 from GTDI:	NO			
clkmon	Enable Performance Counter:	NO			
mntyp	-- If YES: Code Zone to be Monitored is:	SML_DT		0	8
pmonu1	-- If YES: PMC1 Quantity Selection Mode:	BY_TOGGLE		0	2
pmonu2	-- If YES: PMC2 Quantity Selection Mode:	OFF		0	2
pmonu3	-- If YES: PMC3 Quantity Selection Mode:	OFF		0	2
pmonu4	-- If YES: PMC4 Quantity Selection Mode:	OFF		0	2
pmonu5	-- If YES: PMC5 Quantity Selection Mode:	OFF		0	2
pmonu6	-- If YES: PMC6 Quantity Selection Mode:	OFF		0	2
AorM	Assignment of Model to Processor	Manual			
CARD	-if Manual: Begin on Processor Card	2	1 to 6	1	6
Rprc	-if Manual: Begin on Processor	A			

Figure 6.2-Small Time Step Setting Window

The small time steps parameters can be changed by right click on each small time step box and selecting **Edit** → **Parameters**. These parameters in small time steps will not appear by double clicking on the components as is the case for almost all the components in RSCAD. The name and description of the bridge name can be edited here. Digital input and analogue outputs are not used in our model and the assignment. On each GPC card there are two processors that can be

used for solving the simulation which are called A, and B and the latter option is possible if more than one processor in GPC card is used. This selection can be made automatically or manually, but automatic option is suitable if I/O cards are not used otherwise it is recommended to use the manual selection. In our case GIS block is solved in card one processor one, and as it is shown in MAP file in figure 6.3, DFIG block is using processors A and B on card 2. on processor A the voltage source converter, firing pulse generator and triangle blocks are located and on processor B, DFIG, transformer and the t-line are placed. All the controls required for VSC box like PLL, rotor side controller, stator side controller, crowbar logic, fault and speed controllers are solved by card 3 processor B. It is possible to assign the control components to the desired processor manually and also automatically. It is recommended to minimize the number of node voltages that should be solved on one processor to reduce the computational time and communication time. Each processor calculated the node voltages that are required for its model, consequently grouping the models that use same voltages nodes save the calculation time. Also the load on the processors should be balanced on each processor, and this will affect time step. This can be checked by looking into MAP file after compiling the case. If the load on each processor is too high this will increase the small time step which is not desirable.

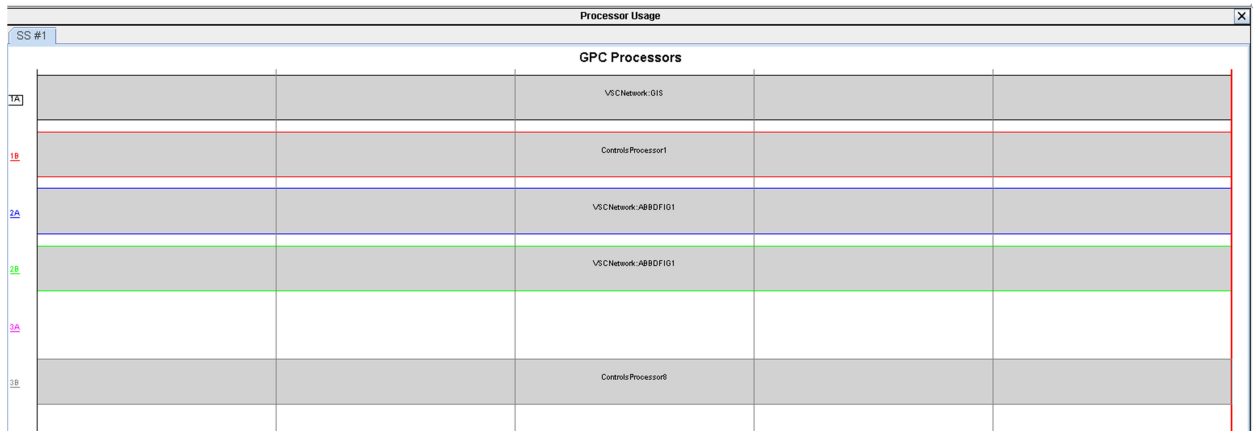


Figure 6.3-Small Time Step Processor Usage

In this project a 200 MW DFIG model is going to be implemented in RSCAD, the purpose is to have a model in RSCD that represents the equivalent model in PSCAD .

6.3 Three Winding 3 Phase Transformer

Parameters of transformer in RSCAD can be adjusted by changing values in figure 6.3.1 and 6.3.2:

rtds_vsc_T3PH3W					
GTAO D/A CHANNEL ASSIGNMENTS		SIGNAL NAMES FOR RUNTIME AND D/A			
ENABLE GTAO D/A OUTPUT		FACEPLATE D/A CHANNEL ASSIGNMENTS			
SIGNAL MONITORING IN RT AND CC		ENABLE FACEPLATE D/A OUTPUT			
CONFIGURATION	ENABLE POWER CALCULATIONS	TRANSFORMER PARAMETERS			
Name	Description	Value	Unit	Min	Max
Name	Transformer name:	T1			
prc12	If BRIDGE uses 2 proc, place on #:	2		1	2
YD1	Winding #1 Type	Delta			
YD2	Winding #2 Type	Y			
YD3	Winding #3 Type	Y			
tapch	Include Winding #1 Tap Changer:	No		0	0
vsrw2	Include Winding #2 Voltage Sources:	No		0	0
vsrw3	Include Winding #3 Voltage Sources:	No		0	0
enpdm	Damper Branches on TRF Primary ?	None		0	2

Figure 6.3.1-Three Winding 3 Phase Transformer Configuration

rtds_vsc_T3PH3W					
GTAO D/A CHANNEL ASSIGNMENTS		SIGNAL NAMES FOR RUNTIME AND D/A			
ENABLE GTAO D/A OUTPUT		FACEPLATE D/A CHANNEL ASSIGNMENTS			
SIGNAL MONITORING IN RT AND CC		ENABLE FACEPLATE D/A OUTPUT			
CONFIGURATION	ENABLE POWER CALCULATIONS	TRANSFORMER PARAMETERS			
Name	Description	Value	Unit	Min	Max
TMVA	Rated Transformer MVA	210.0	MVA	0.001	
freqb	Base frequency	50.0	Hertz	0.001	
W1VLL	Rated Winding #1 L-L RMS Voltage	154.0	kV	0.001	
W2VLL	Rated Winding #2 L-L RMS Voltage	33.0	kV	0.001	
W3VLL	Rated Winding #3 L-L RMS Voltage	3.795	kV	0.001	
W1lag	Winding #1 Lags Y (degrees):	Lag330		0	3
W2lag	Winding #2 Lags Y (degrees):	Lag30		0	3
W3lag	Winding #3 Lags Y (degrees):	Lag30		0	3
XI12	Leakage reactance (#1 + #2)	0.08	P.U.	0.0001	2.0
XI13	Leakage reactance (#1 + #3)	0.0725	P.U.	0.0001	2.0
XI23	Leakage reactance (#2 + #3)	0.0077	P.U.	0.0001	2.0
W1R	Winding #1 resistance	0.003	P.U.	0.0	
W2R	Winding #2 resistance	0.003	P.U.	0.0	
W3R	Winding #3 resistance	0.003	P.U.	0.0	

Figure 6.3.2-Three Winding 3 Phase Transformer Parameters

6.4 Doubly Fed Induction Generator (DFIG)

rtds_vsc_INDM

ENABLE GTAO D/A OUTPUT	SIGNAL NAMES FOR RUNTIME AND D/A
ENABLE MONITORING IN RUNTIME	ENABLE FACEPLATE D/A OUTPUT
MOTOR ELECTRICAL PARAMETERS	MECHANICAL PARAMETERS
INITIAL CONDITIONS	CONTROLS COMPILER INPUT
VSC INDUCTION MACHINE CONFIGURATION	ENABLE POWER CALCULATIONS

Name	Description	Value	Unit	Min	Max
vbsll	Rated Stator Voltage (L-L RMS)	33	kV	0.01	
trato	Turns Ratio, Rotor over Stator	0.2967	p.u.	0.01	
pbase	Rated MVA	264.6875	MVA	0.0001	
hrtz	Rated Frequency	50.0	Hertz	5.0	150.0
ra	Stator Resistance	0.02413	p.u.	0.002	
xa	Stator Leakage Reactance	0.4513	p.u.	0.03	
xmnd0	Unsaturated Magnetizing Reactance	15.2778	p.u.	0.75	
rfd	First Cage Rotor Resistance	0.02326	p.u.	0.003	
xfd	First Cage Rotor Leakage Reactance	0.6163	p.u.	0.03	
rkd	Second Cage Rotor Resistance	0.2	p.u.	0.003	1.0e6
xkd	Second Cage Rotor Leakage Reactance	0.07	p.u.	0.0	1.0e6

Figure 6.4.1-DFIG Parameters Setting Window

Parameters of DFIG in figure 6.4.1 are taken from p.u values for 5MW DFIG in PSCAD model.

6.5 Three Phase-Two Level Converters

rtds_vsc_LEV2BB					
GTAO D/A CHANNEL ASSIGNMENTS, GENERAL			SIGNAL NAMES FOR RUNTIME AND D/A		
GTAO D/A CHANNEL ASSIGNMENTS, SIDE 1			GTAO D/A CHANNEL ASSIGNMENTS, SIDE 2		
FACEPLATE D/A CHANNEL ASSIGNMENTS, GENERAL					
FACEPLATE D/A CHANNEL ASSIGNMENTS, SIDE 2					
ENABLE GTA0 D/A OUTPUT			FACEPLATE D/A CHANNEL ASSIGNMENTS, SIDE 1		
ENABLE MONITORING IN RUNTIME			ENABLE FACEPLATE D/A OUTPUT		
SIDE #1, LEG FIRING PULSE INPUTS			SIDE #2, CURRENT ORDER INPUTS		
INTERNAL CAPACITOR CONNECTIONS			ENABLE POWER CALCULATIONS		
SIDE #2 GENERAL PARAMETERS			EXTERNAL RAIL CONNECTIONS		
VSC 2 LEVEL BB CONFIGURATION			SIDE #1 GENERAL PARAMETERS		
Name	Description	Value	Unit	Min	Max
Name	BRIDGE NAME	BRDG1			
prc12	If BRIDGE uses 2 proc, place on #:	1		1	2
pogrd	Connect Positive Rail to Ground:	No		0	1
negrd	Connect Negative Rail to Ground:	No		0	1
addg	Add Controllable Crowbar Conductance:	No		0	1

Figure 6.5.1-VSC Configuration Window

rtds_vsc_LEV2BB					
GTAO D/A CHANNEL ASSIGNMENTS, GENERAL			SIGNAL NAMES FOR RUNTIME AND D/A		
GTAO D/A CHANNEL ASSIGNMENTS, SIDE 1			GTAO D/A CHANNEL ASSIGNMENTS, SIDE 2		
FACEPLATE D/A CHANNEL ASSIGNMENTS, GENERAL					
FACEPLATE D/A CHANNEL ASSIGNMENTS, SIDE 2					
FACEPLATE D/A CHANNEL ASSIGNMENTS, SIDE 1					
ENABLE FACEPLATE D/A OUTPUT			ENABLE GTA0 D/A OUTPUT		
SIDE #2, LEG FIRING PULSE INPUTS			ENABLE MONITORING IN RUNTIME		
DC BUS CROWBAR CONTROL INPUT			SIDE #1, LEG FIRING PULSE INPUTS		
INTERNAL CAPACITOR CONNECTIONS			ENABLE POWER CALCULATIONS		
SIDE #2 GENERAL PARAMETERS			EXTERNAL RAIL CONNECTIONS		
VSC 2 LEVEL BB CONFIGURATION			SIDE #1 GENERAL PARAMETERS		
Name	Description	Value	Unit	Min	Max
nmlg1	Side #1, Number of Legs:	3		1	3
firt1	Side #1, Type of Firing Control Orders:	Pulses		0	1
ract1	Side #1, Resistance of Reactors:	0.0015	Ohms	0.0	
racth1	Side #1, Inductance of Reactors:	120.0e-6	Henries	0.000005	
rvalon1	Side #1, Valve ON Resistance:	0.001	Ohms	0.0001	
rvalof1	Side #1, Valve OFF Resistance:	5000	Ohms	1.0	
snbc1	Side #1, Snubber Series Capacitance:	0.2	MicroF	0.001	
snbr1	Side #1, Snubber Series Resistance:	30.0	Ohms	1.0	
ackv1	Side #1, AC RMS L-N Voltage (re: errors):	0.5	kV	0.001	
acka1	Side #1, AC RMS Line Current (re: errors):	1.0	kA	0.001	
acfq1	Side #1, AC Rated Frequency (re: errors):	50.0	Hz	5.0	

Figure 6.5.2-VSC General Parameters Window

Input and output of this model are calculated within one time step (around 3μsec).

6.6 Grids Side VSC Control

Design and function of a typical grid side controller in DFIG is discussed earlier and RSCAD model is also following the same principles. The models that are shown in figures 6.6.1, to 6.6.4 are taken from a sample model in RSCAD, which is similar to our studied model and follows same principal that is applied at this work. All the parameters for the controls are in p.u to create the possibility of using this controller for different ratings of DFIG models.

Figure 6.6.1 is showing the outer loop of grid side controller which produces I_{dref} (G1IDGPU0).

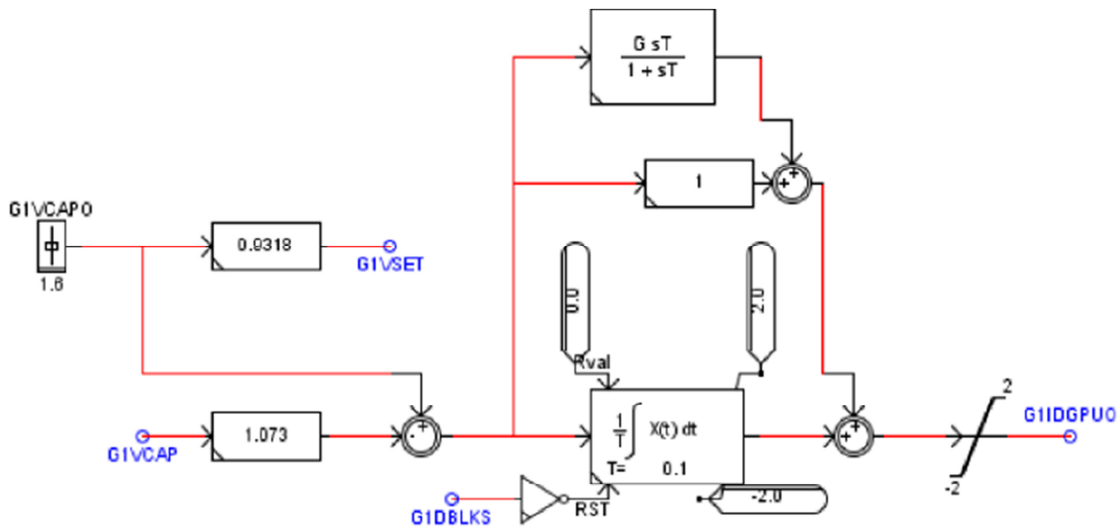


Figure 6.6.1-Capacitor voltage regulator outer loop

In figure 6.6.2 inner part of the controller is shown. Error values of I_{derr} and I_{qerr} are calculated from reference and measured values of I_d and I_q and later applied to input of PI controllers to create reference dq values for voltages V_{dref} and V_{qref} . Compensation terms are calculated and added to the PI controller to decouple d and q components by removing cross coupling terms.

$$(\omega_e L i_d = 0.2 \text{ and } \omega_e L i_q = 0.2)$$

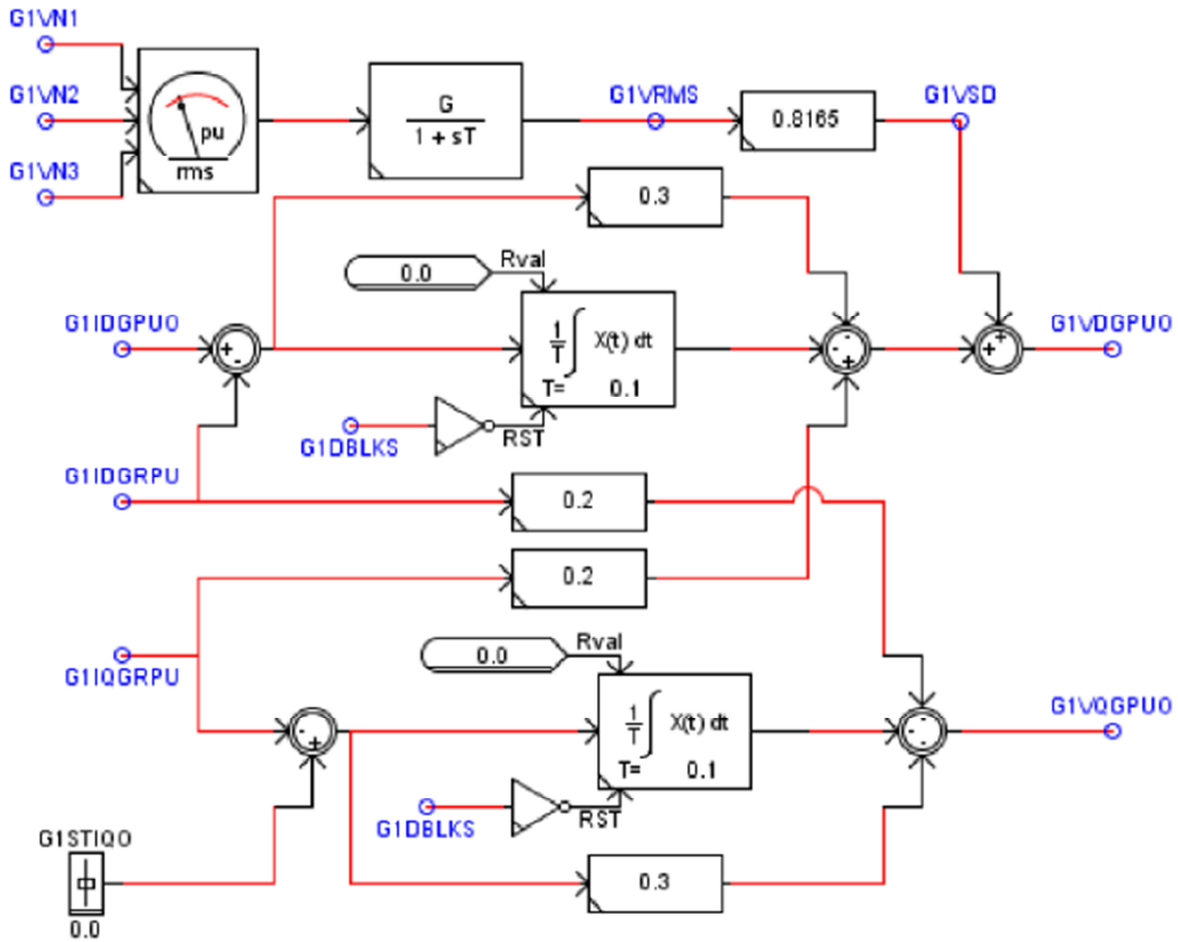


Figure 6.6.3-PI controllers in Grid side controller

The output in figure 6.6.3 is a voltage vector that is needed to create the required currents. As it is depicted in figure 6.6.4 this signal should first be transformed to its magnitude and angle and then to the stationary ac reference frame. The output of figure 6.6.4 are reference voltages used in modulation in the controller.

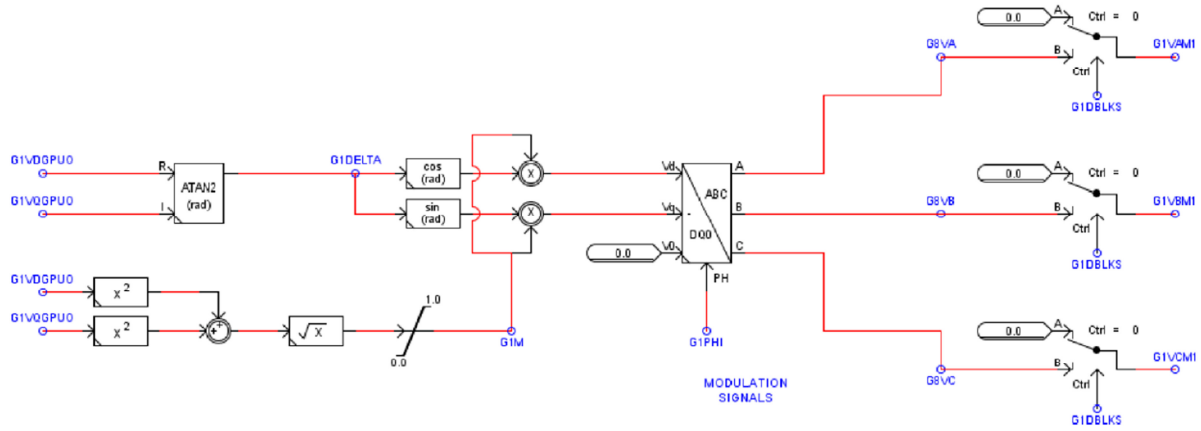


Figure 6.6.4-PWM Modulation

It is needed to perform transformation from 3 phases to dq in the controller, and for this purpose the angle from Phase Locked Loop (PLL) is used at these transformations. In RSCAD model the stator voltage and grid side converter currents in DQ axis which are needed in grid side controller are calculated in PLL block. Measured voltage and current therefore are too noisy and should be passes through low pass filters to remove the noises form it. [14]

6.7 Phase Compensation Calculation

In steady state low pass filters effects can be represented by,

$$G(j\omega_0) = \frac{1}{(1 + j\omega_0\tau)} = Me^{j\phi}$$

Equation 6-1

Where M and ϕ are the magnitude and the phase shift caused by low pass filter. Consequently phase compensation should be considered in 3 phase to dq blocks. This value can be calculated and is different for different models. In figure 6.7 filter time constant is 0.002 which after inversion gives $M \sin \phi$ value of 0.628 at 50 Hz.

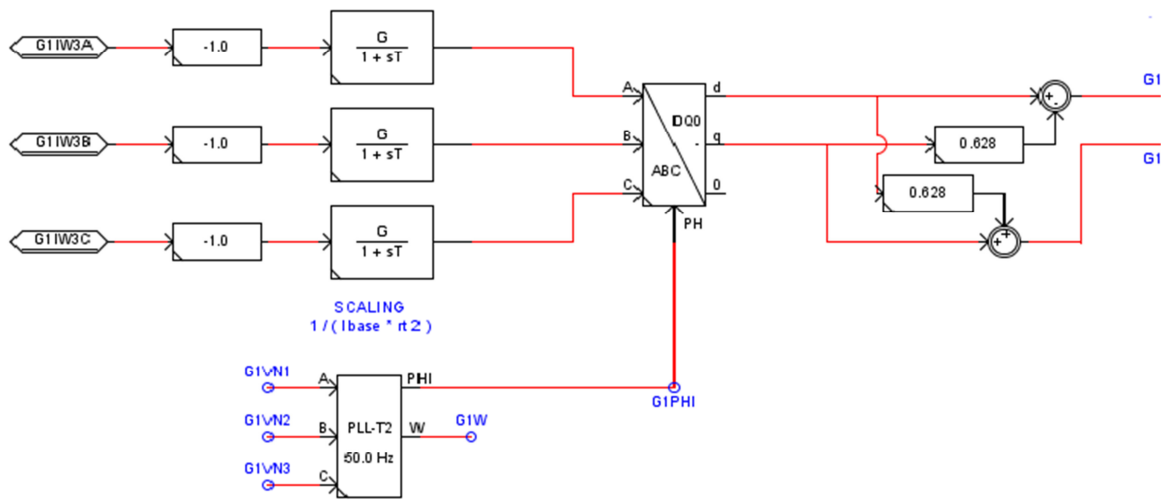


Figure 6.7-Phase Compensation for ABC-DQ Block

6.8 Phase Locked Loop (PLL)

Typical method to make a PLL block is shown in figure 6.8.1. AC voltages (V_{sys}) from the DFIG stator are transformed from ABC reference to DQ rotating reference frame, and is used as input for this PLL, the PI controller then tries to keep the Q component of the voltage, which is regarded as an error $e(t)$ to zero using a PI controller, and by this align D axis with the voltage vector. The output of PLL (θ_{PLL}) will be a ramp function, which increases from 0 to 2π representing the AC system phase, by using (θ_{PLL}) which is locked with the voltage vector the error $e(t)$ becomes zero. (θ_{PLL}) will be used in ABC to DQ transformation blocks for producing d and q axis currents, and also for creating the modulation signals using DQ to 3phase blocks. The comparator in RSCAD controls a switch which creates this ramp function. Compensation for the phase lag in the synchronous reference dq-frame controller improves the controller performance [12], [13].

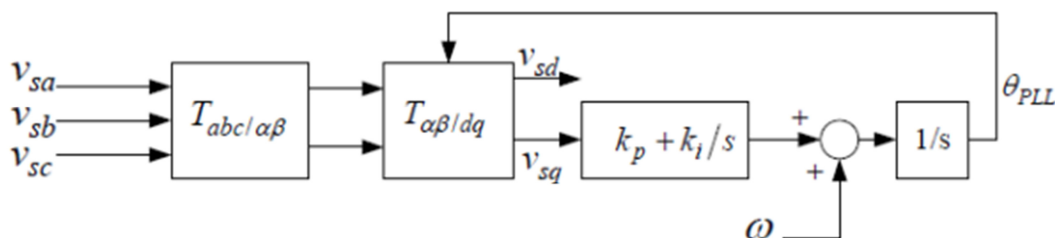


Figure 6.8.1-Typical PLL Block

6.9 Rotor Side VSC

The way that rotor controller is designed in RSCAD in figure 6.9.1 is following almost the same principal mentioned before and used in this project, the main difference is that the modulation technique, which is used in this sample is PWM, which is hysteresis band in our studied model. All the parameters for the controls are in p.u to create the possibility of using this controller for other DFIG models with different ratings.

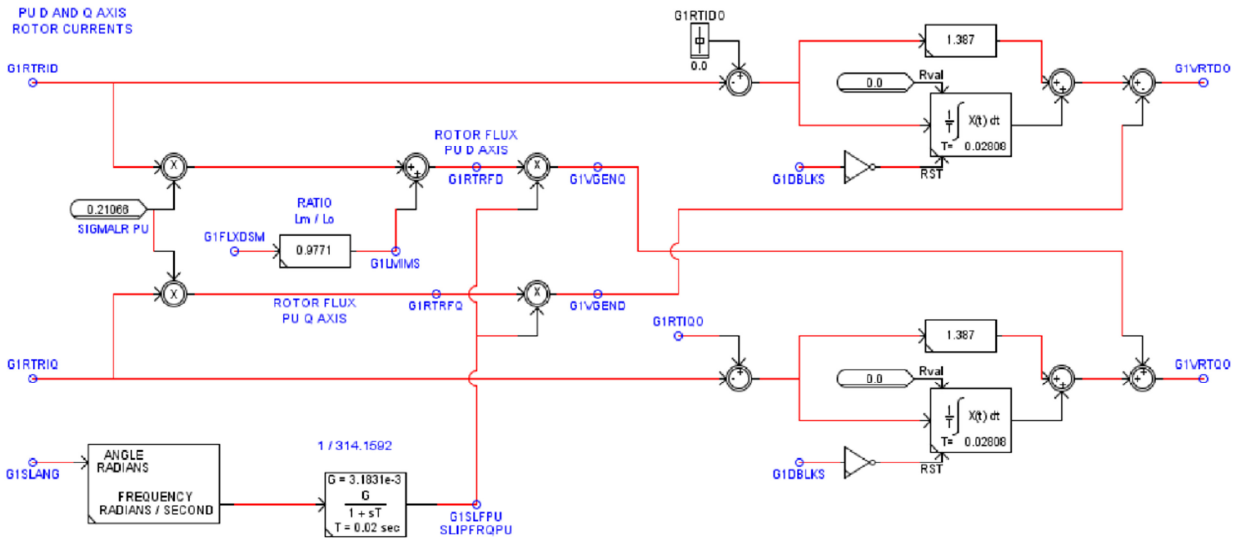


Figure 6.9.1-Rotor Side Converter PI Controllers

6.10 Crowbar Logic

As explained before in section 2.3 the crowbar is a shunt resistor which is in series with a switch. When due to the faults in network capacitor voltage exceeds a certain amount, the crowbar switch will be closed and consequently will reduce capacitor voltage. At this sample model in figure 6.15 the voltage is compared with 2 pu, and if capacitor voltage is higher than 2 p.u then latches the flip flop and activate the crowbar, and if the voltage goes lower than 1.7p.u then the flip flop will be reset and the crowbar switch will be off.

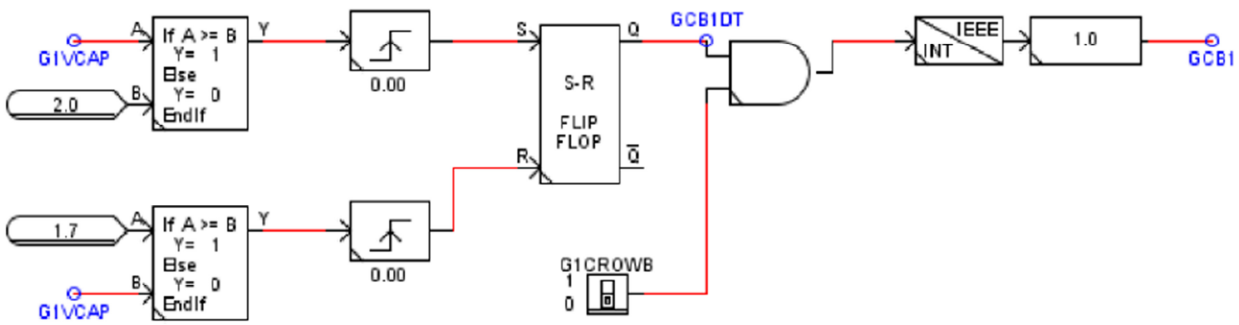


Figure 6.15-Sample Crowbar Model

6.11 Fault Control

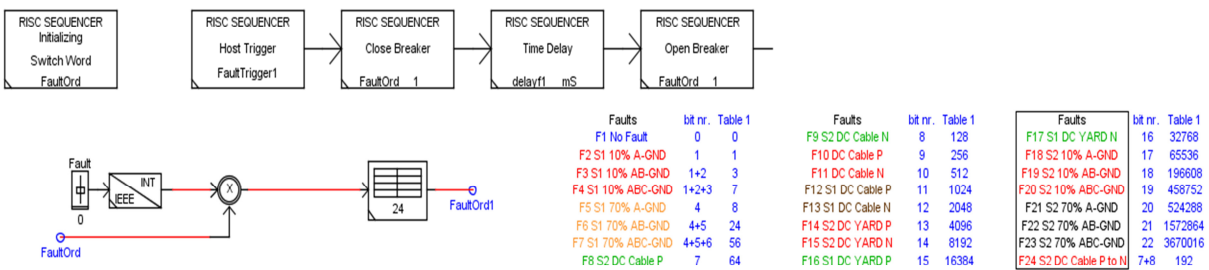


Figure 6.11.1-Fault Control

The fault can be initiated by pushing a button in run time. Using a fault sequence block it is possible to create following different fault cases in RSCAD in figure 6.11.1.

The percent of the remaining fault voltage can be adjusted by R, L values in fault branch.

F1=No fault

F2=10% A-GND (10% remaining voltage 3-phase to ground)

F3=10% AB-GND (10% remaining voltage 2-phase to ground)

F4=10% ABC-GND (10% remaining voltage 3-phase to ground)

F5=78% A-GND (78% remaining voltage 1-phase to ground)

F6=78% AB-GND (78% remaining voltage 2-phase to ground)

F7=78% ABC-GND (78% remaining voltage 3-phase to ground)

Delayf1 in this block is determining duration of fault.

Fault cases I and II in RSCAD are compared with equivalent PSCAD results:

CASEI: 10% remaining voltage 3ph to Ground- Fault duration 1000 msec

CASEII: 78% remaining voltage 3ph to Ground- Fault duration 1000 msec

Chapter 7

7 PART I-Verification of DFIG model in RSCAD against PSCAD (Before modification)

At this section models in PSCAD and RSCAD are being compared before doing any modification on the available RSCAD model. The plots will be studied during a disturbance with duration of 1 sec and 10% remaining voltage, and differences between two models are shown and discussed.

7.1 CASE I: 10% Remaining Voltage 3ph – G

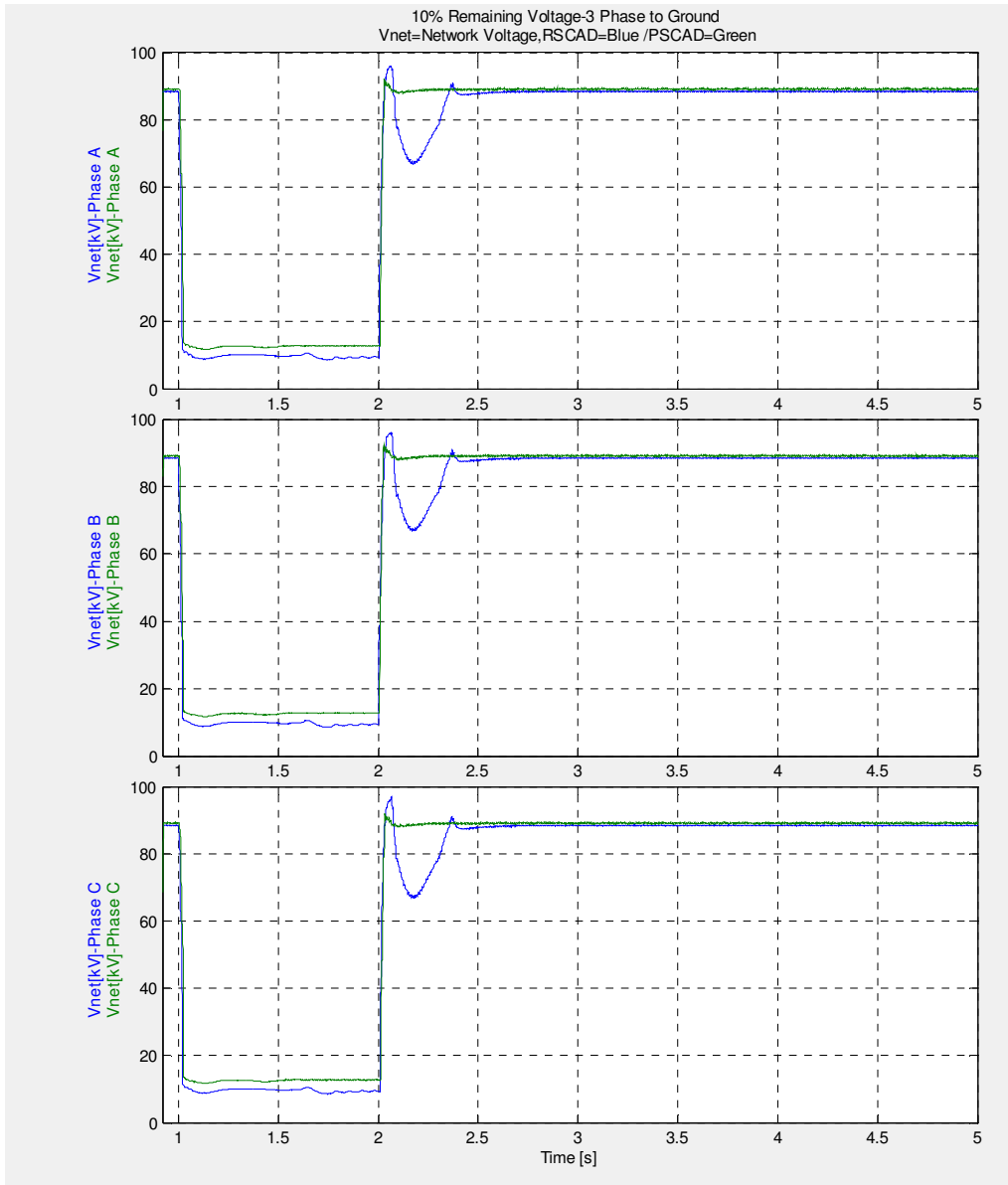


Figure 7.1-Network Voltages

As it is shown in figure 7.1 fault duration is 1 second and network voltage is reduced by 90% in a 3 phase to ground fault. (Voltage values are in RMS) fault is removed after 1 second. It is shown that after the fault is removed the RSCAD show different behavior for voltage plots.

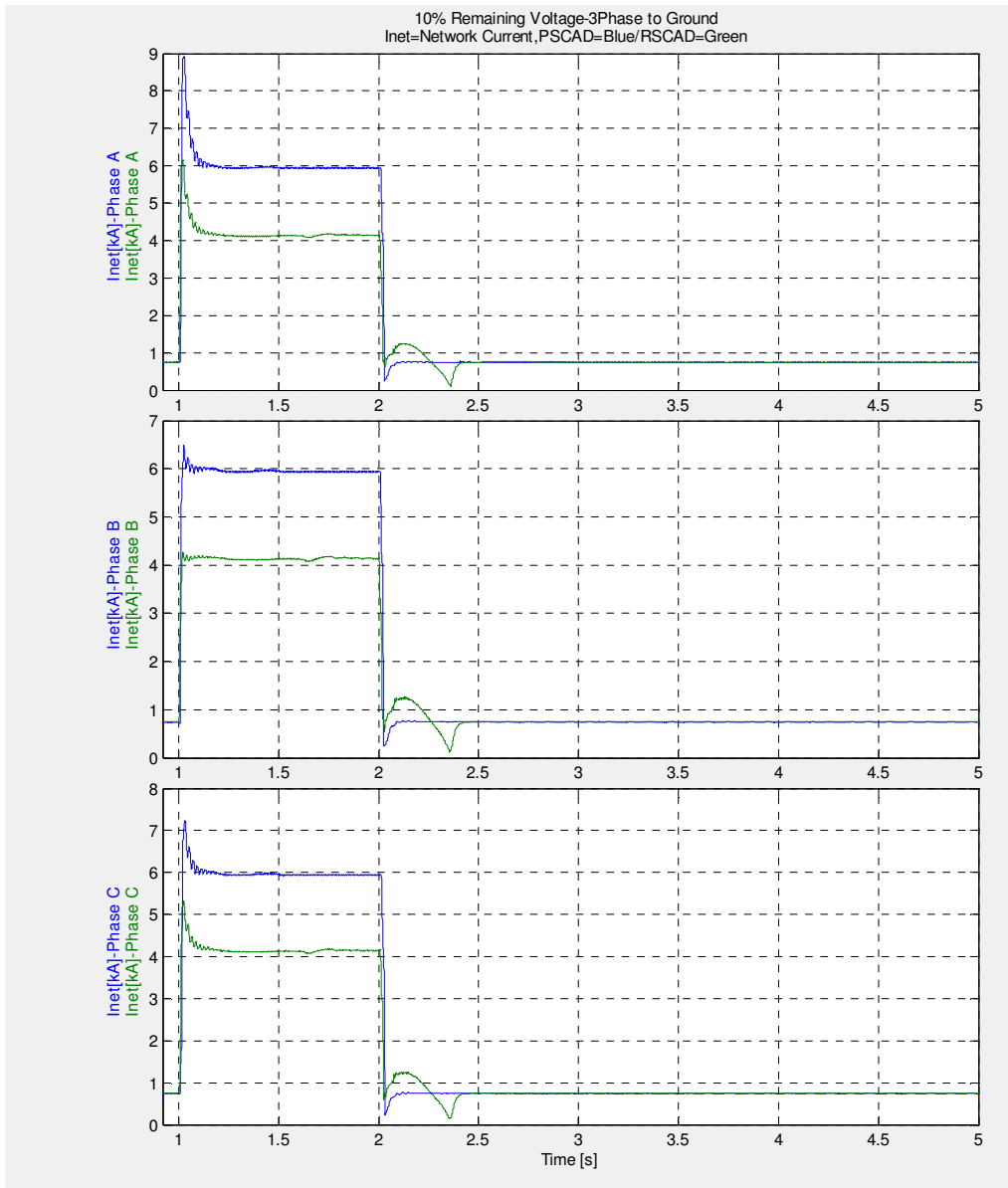


Figure 7.2-Network Currents

Figure 7.2 shows network currents are considerably increased because the voltage is reduced in network terminals to 10 % of nominal voltage, there is a difference of about 2 KA between fault current in PSCAD and RSCAD model it is also shown that network responses in PSCAD and RSCAD model are not similar.

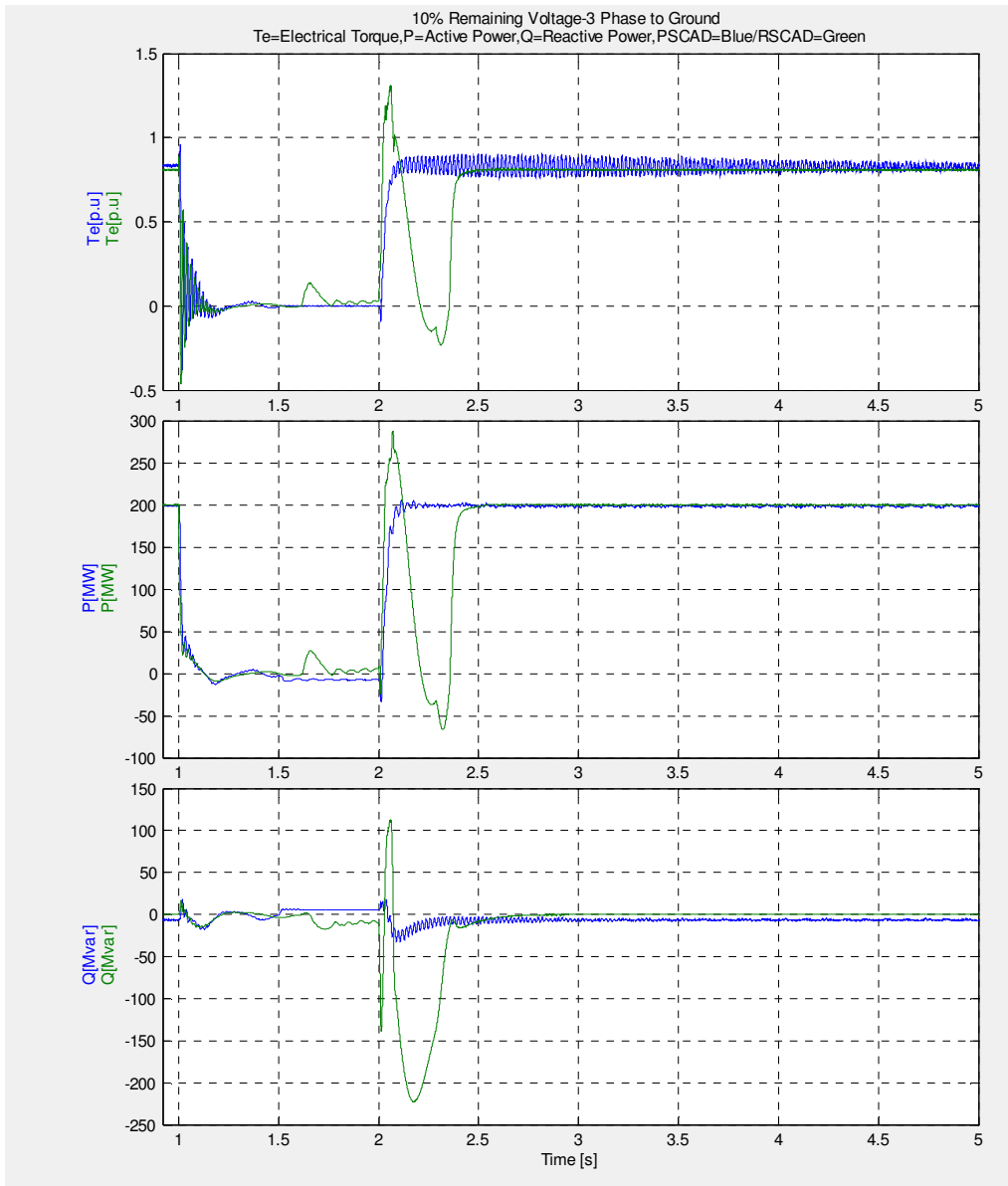


Figure 7.3-Torque, Active and Reactive power

As it is shown in figure 7.3, when a short circuit happens in the network consequently generator active power of P_e and electrical torque T_e will become almost zero. After clearing the fault both of them come back to the references value defined in the rotor side controller. Injected reactive power from rotor side controller to rotor is defined to be zero and controller tries to keep this value during the instability. Figure 7.3 shows that the current RSCAD and PSCAD models are not consistent after the fault is recovered.

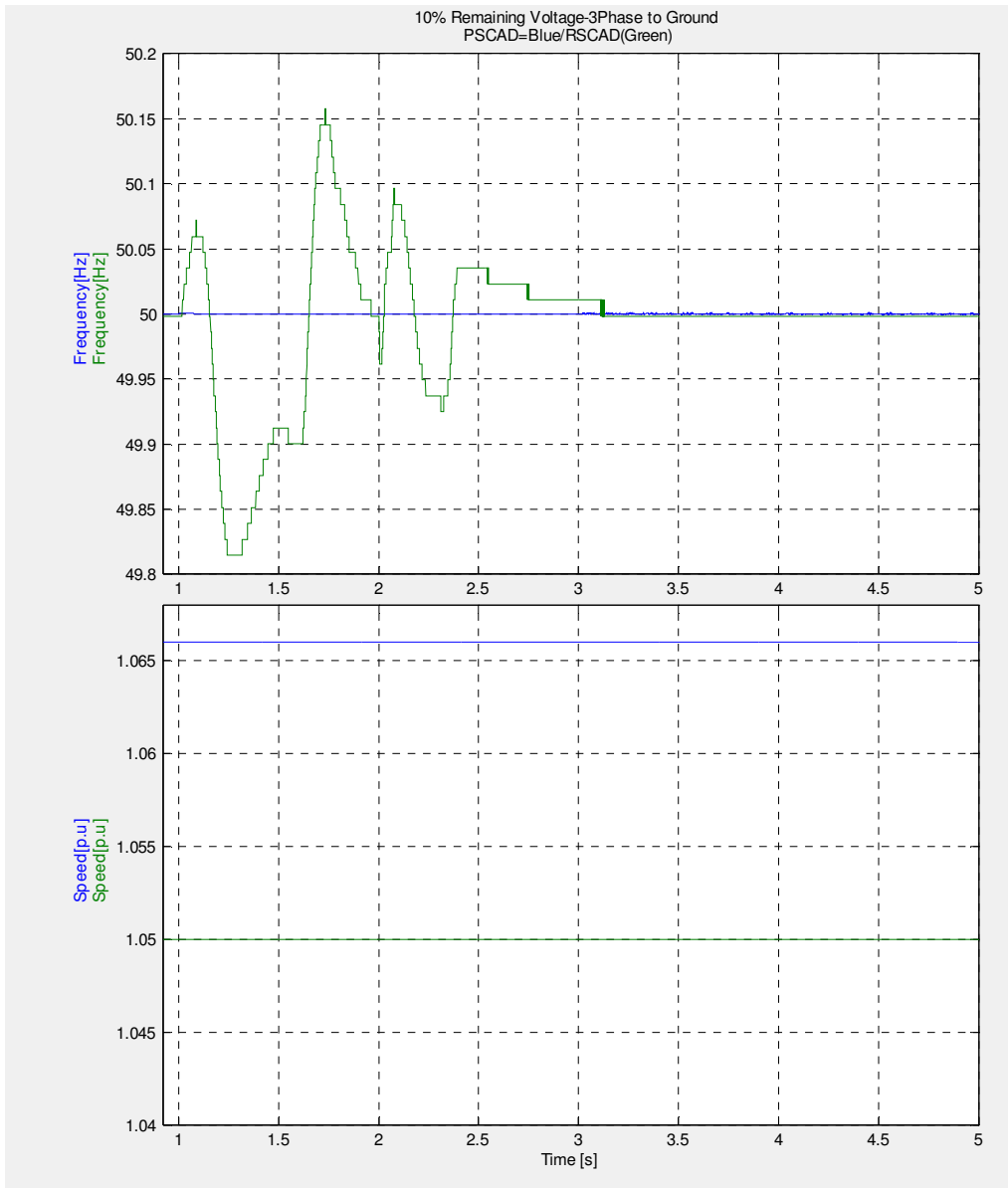


Figure 7.4-frequency and speed

In figure 7.4 it is seen that frequency variations in RSCAD are much higher than the PSCAD model which is almost constant at 50 Hz. Both models are working at fixed speed mode, and as the frequency is produced in the PLL block, consequently a PLL investigation in RSCAD is needed.

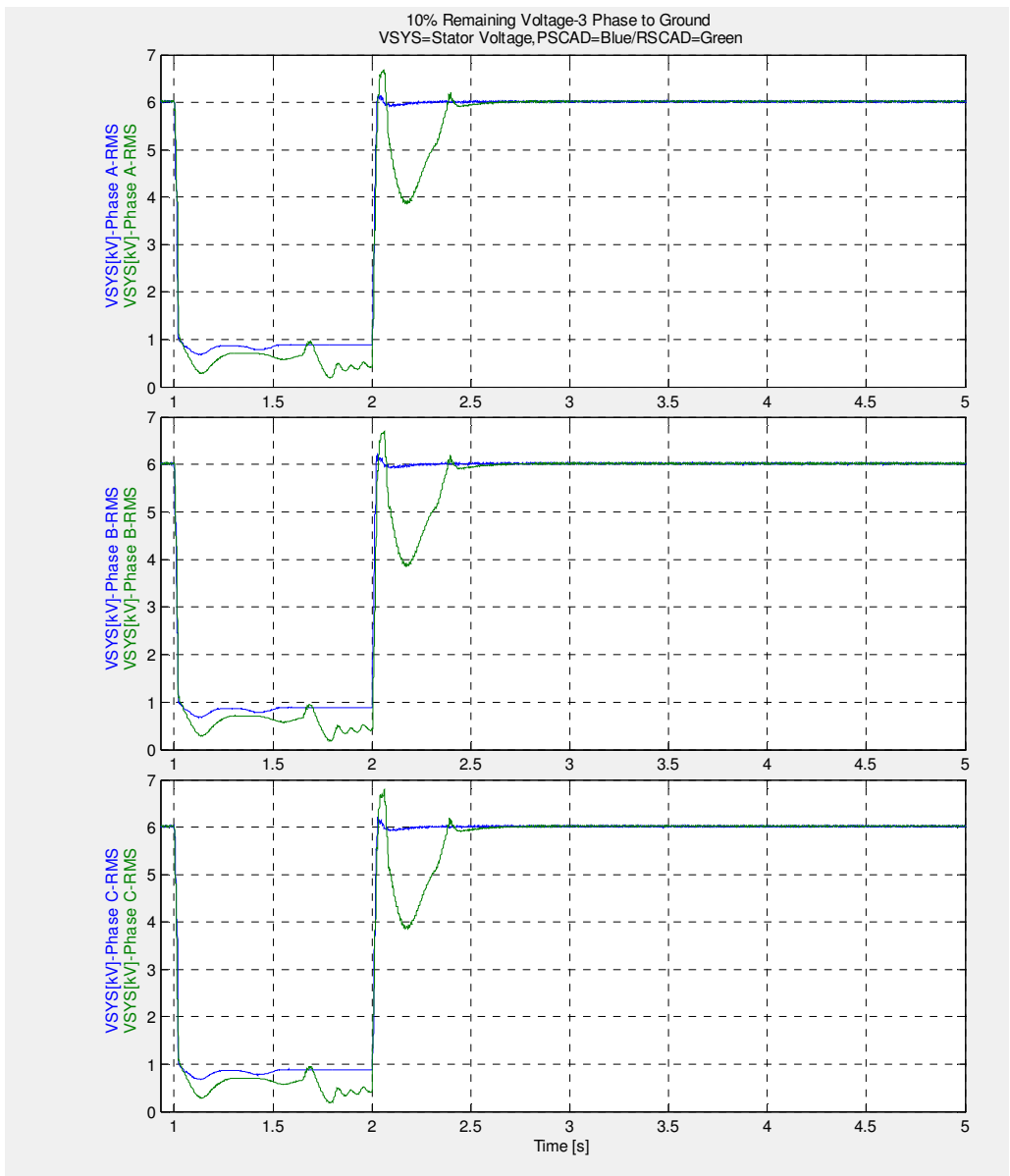


Figure 7.5-Stator voltage

Same as network voltage in figure 7.5 it is depicted that stator voltage is also reduced during the fault and again it is shown that after voltage recovery the behavior of models are different.

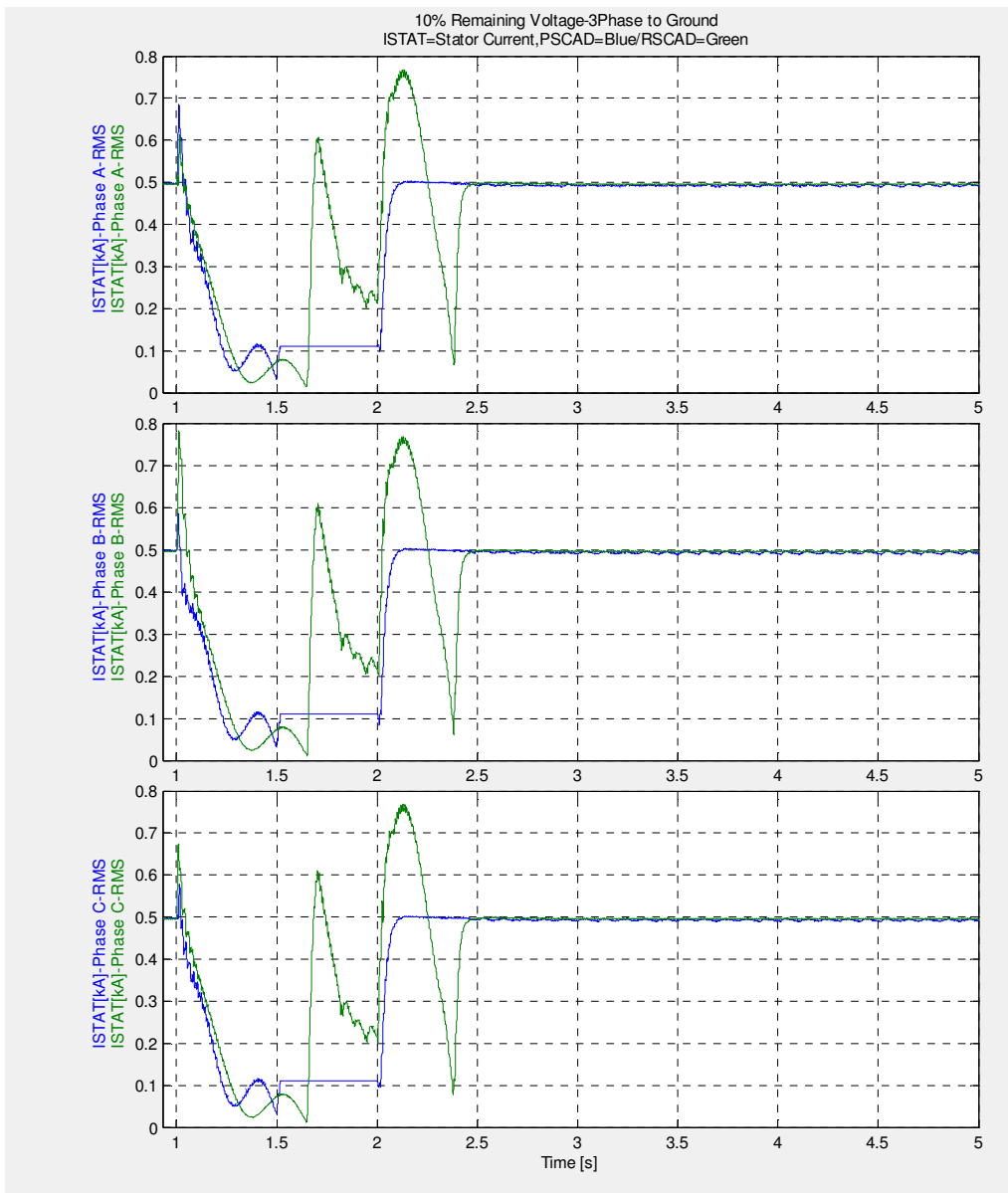


Figure 7.6-Stator current

In figure 7.6 it is depicted that stator current response is also different during fault and once the fault is removed. Stator current should increase during the fault as the voltage is decreased due to a short circuit in grid.

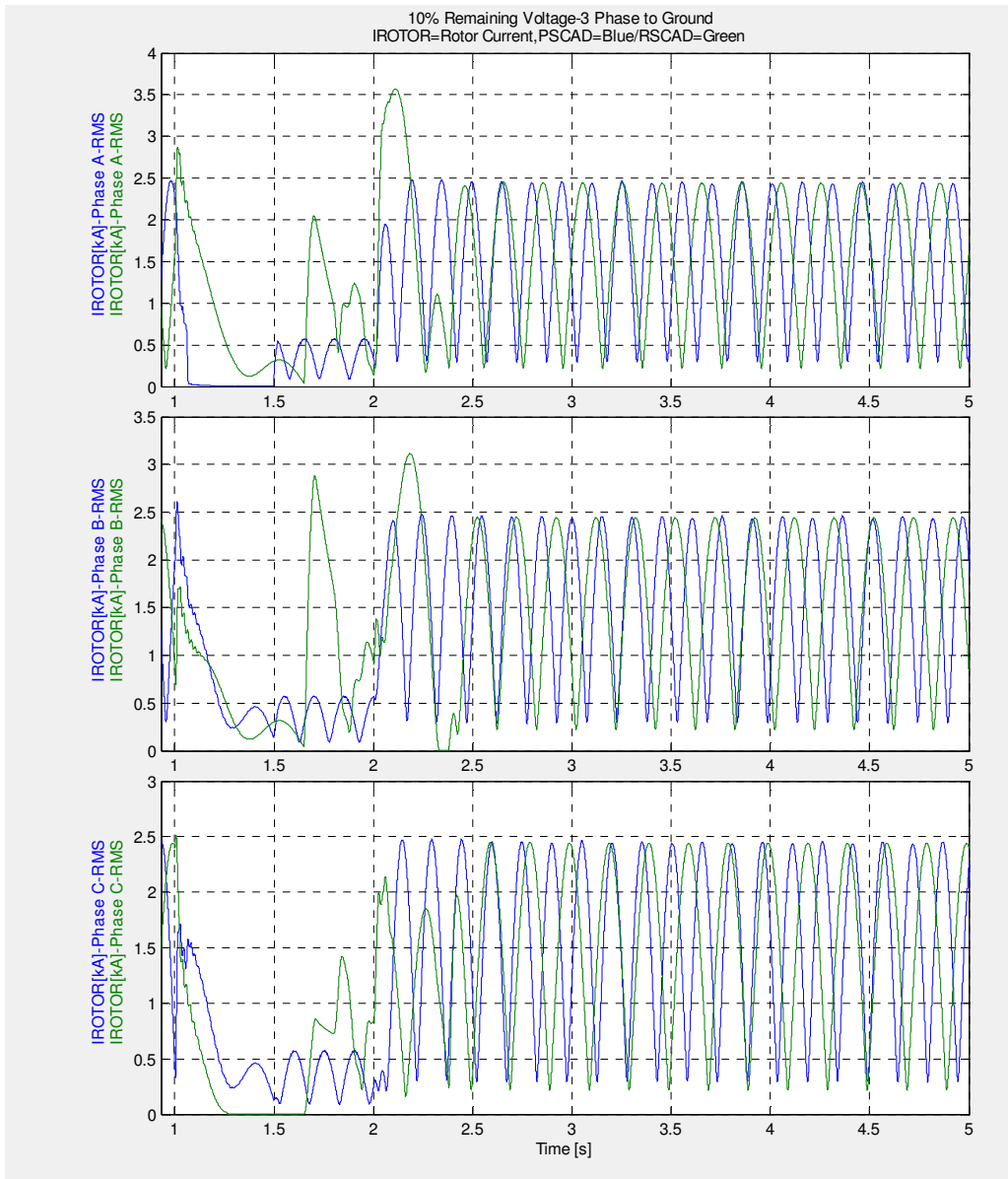


Figure 7.7-Rotor current

According to figure 7.7 rotor current plots are showing different behavior during fault.

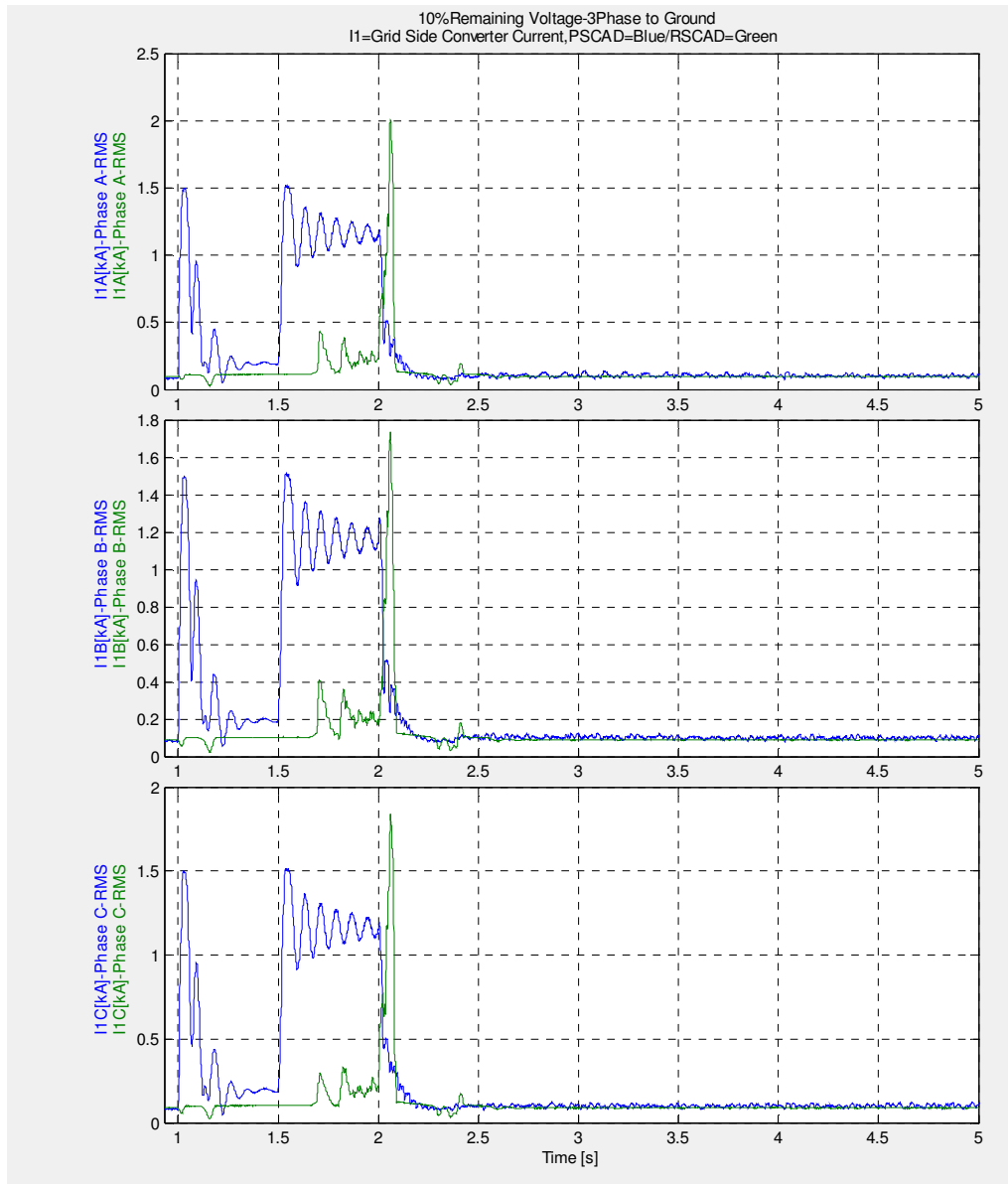


Figure 7.8-Grid side converter current

Grid side converter is loaded more with the increase of DC link voltage, which happens during the fault, and tries to keep the dc link voltage constant and around the rated value. Figure 7.8 should be compatible with figure 7.10, where DC link voltage variations are shown. In other words Grid side converter current should increase when DC link voltage in increasing or decreasing. It seems Grid side converter response in RSCAD is not compatible with the PSCAD model, and it doesn't respond to the first peak of dc link voltage, and also is not helping to reduce dc link voltage after 1.5 sec.

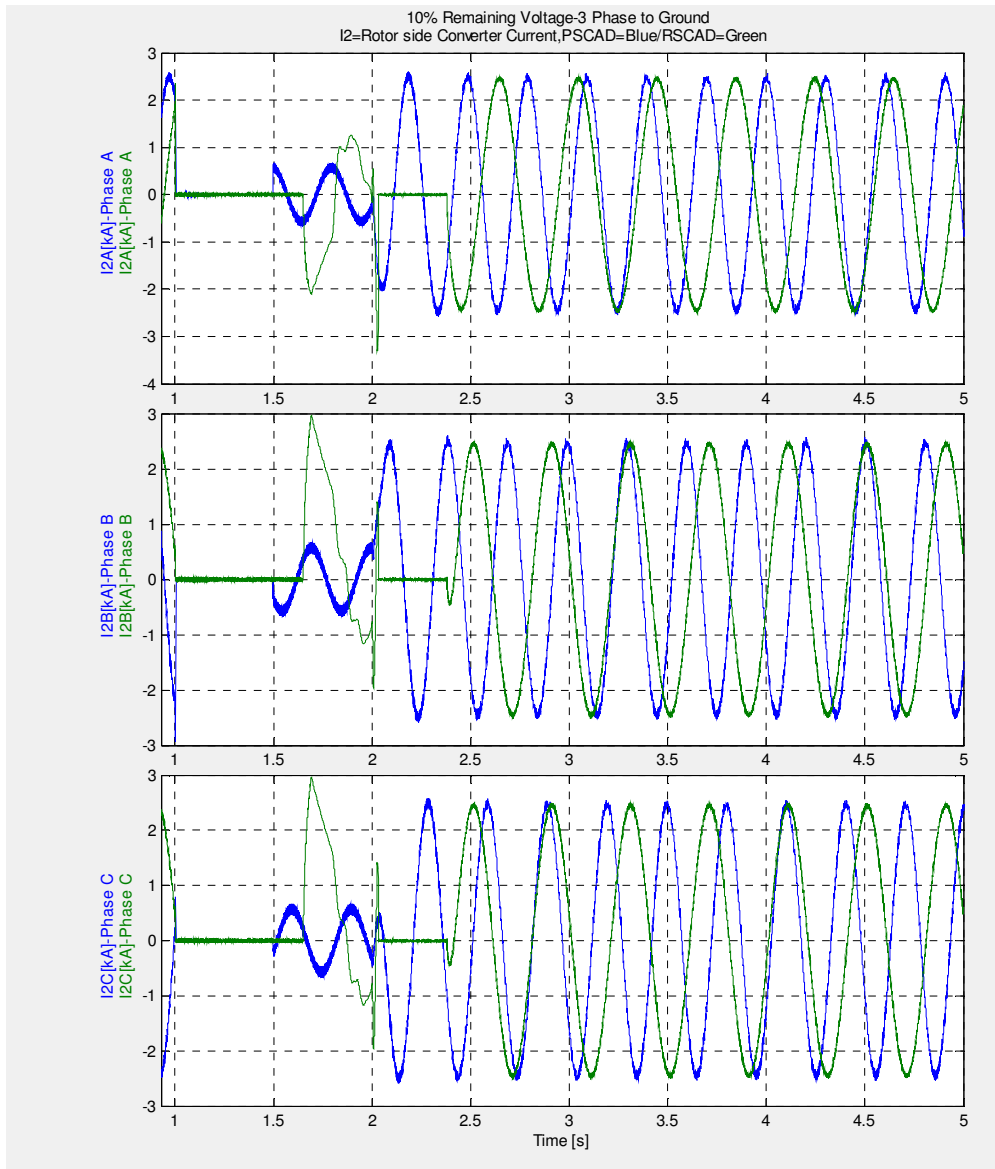


Figure 7.9-Rotor side converter current

Rotor side current has a frequency which is dependant to the slip; in synchronous speed rotor current will be a DC current. It is seen in figure 7.9 that when crowbar is activated rotor side converter current is bypassed by a short circuit in crowbar, but rotor current for example in phases B and C reaches to high value which is not desirable, and not consistent with PSCAD plot.

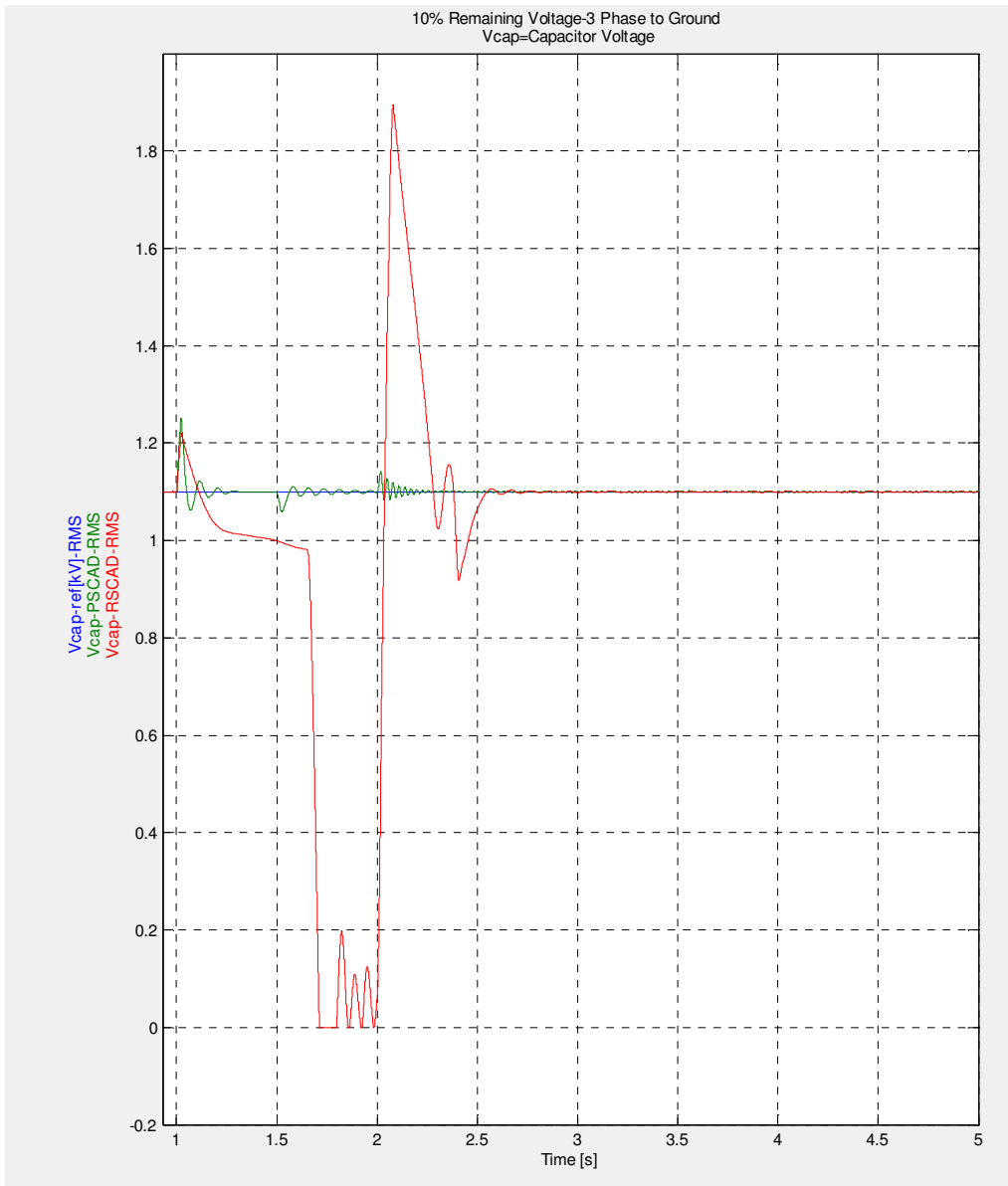


Figure 7.10-Dc- link voltage

As already mentioned during the fault there is an unbalance between the input and output active power in controller, and as at the output electrical power is almost zero due to the fault, dc-link voltage will increase quickly just after fault. As is shown in figure 7.10, it is depicted that the reference value of dc link voltage is 1.1 kV, and capacitor voltage exceeds this value in both RSCAD and PSCAD models for the first right after short circuit happens, but PSCAD grid side controller is able to control the dc link voltage during the fault but it seems the RSCAD grid side controller is not doing the task for reducing the voltage and that's why the crowbar is activated for RSCAD model twice. It is very clear that RSCAD model is behaving completely different comparing the dc link voltages, as it goes down to zero, meaning output power is more than input power in this case, which is not the case for PSCAD model, where voltage is more stable. There is a huge peak voltage in RSCAD when the fault is cleared which is not the case for

PSCAD model, which will activate crowbar twice, while PSCAD model only activate the crowbar only once according to figure 7.11 and 7.12. But still a small increase in voltage is expected even with crowbar activation which is related to the first peaks in rotor current.

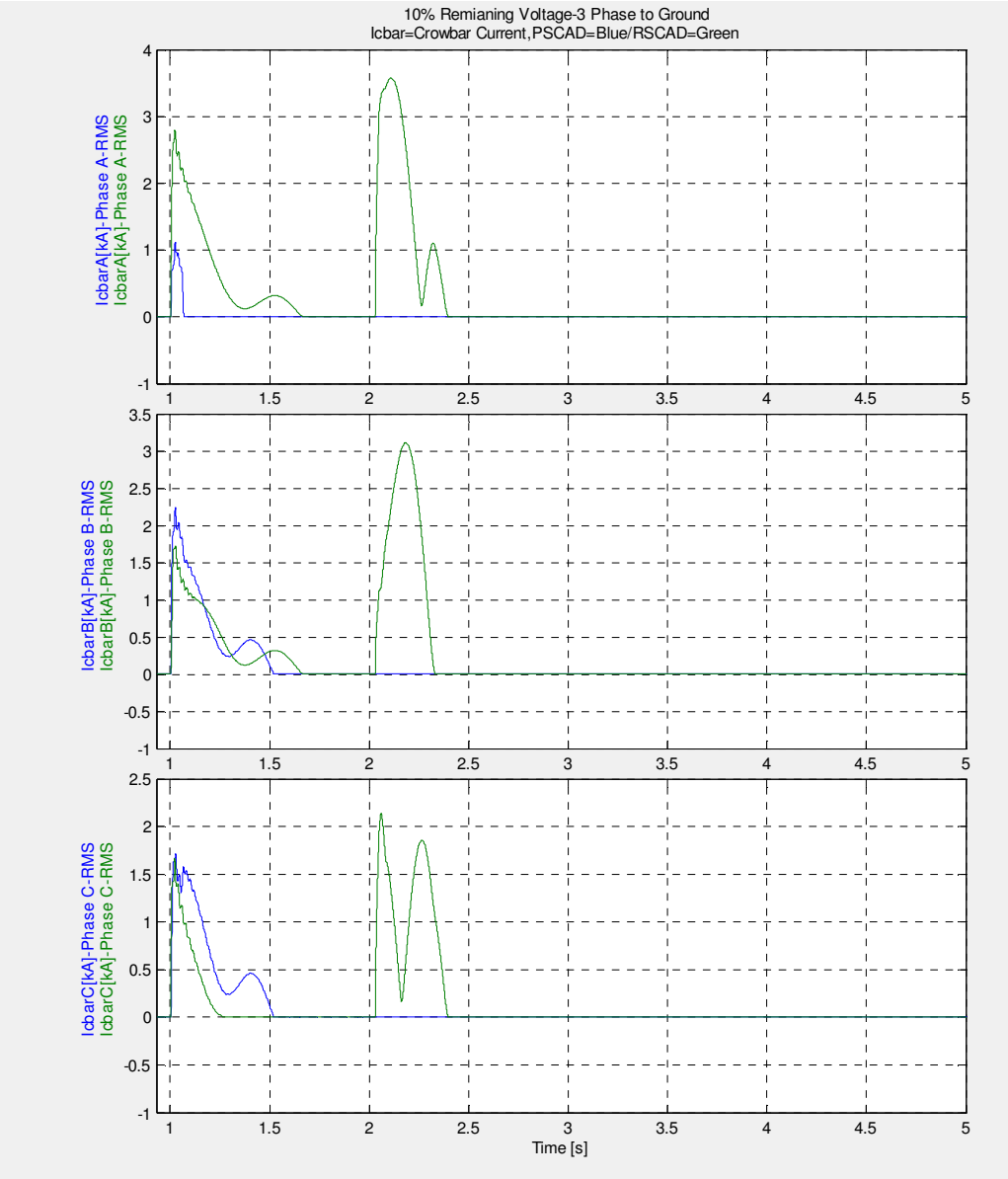


Figure 7.11-Crowbar current

It is shown in figure 7.11 that when the voltage in dc link exceeds the amount which is defined in crowbar the excessive rotor inrush current is passed through the crowbar instead of being injected to the controller, which is the purpose of using crowbar.

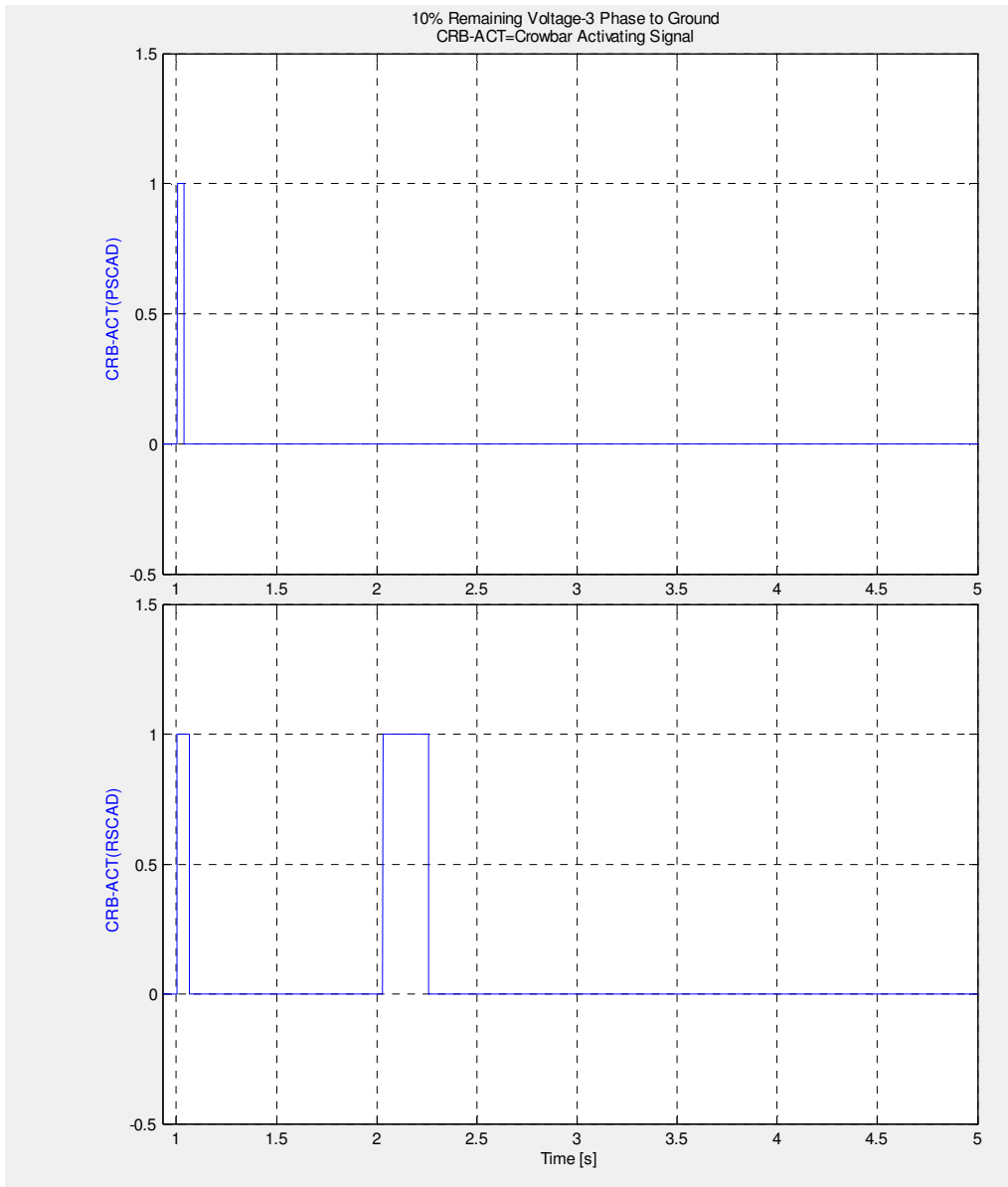


Figure 7.12-Crowbar Activation Signals

In figure 7.12 it is shown that crowbar is activated two times in RSCAD, and one time in PSCAD model.

7.2 200 MW DFIG, RSCAD Model Verification against PSCAD:

For modifying process, differences between RSCAD and PSCAD plots during normal and transient operation are studied. To show the effect of modification in this project as an example frequency plots for PLL are compared in section 7.2.1.

7.2.1 Modifying PLL in RSCAD

It was seen that before modification Grid frequency in RSCAD is changing from 49, 8 to almost 50, 2 Hz during the transient of fault, which in PSCAD model increases up to 50, 0006 Hz. As frequency is produced in PLL block the PLL block in RSCAD model is entirely investigated to find the problem and apply required corrections, and modifications. Figure 7.2.1 and 7.2.2 are showing frequency responses before and after modification in PLL, and as it is illustrated the frequency response is much less than before.

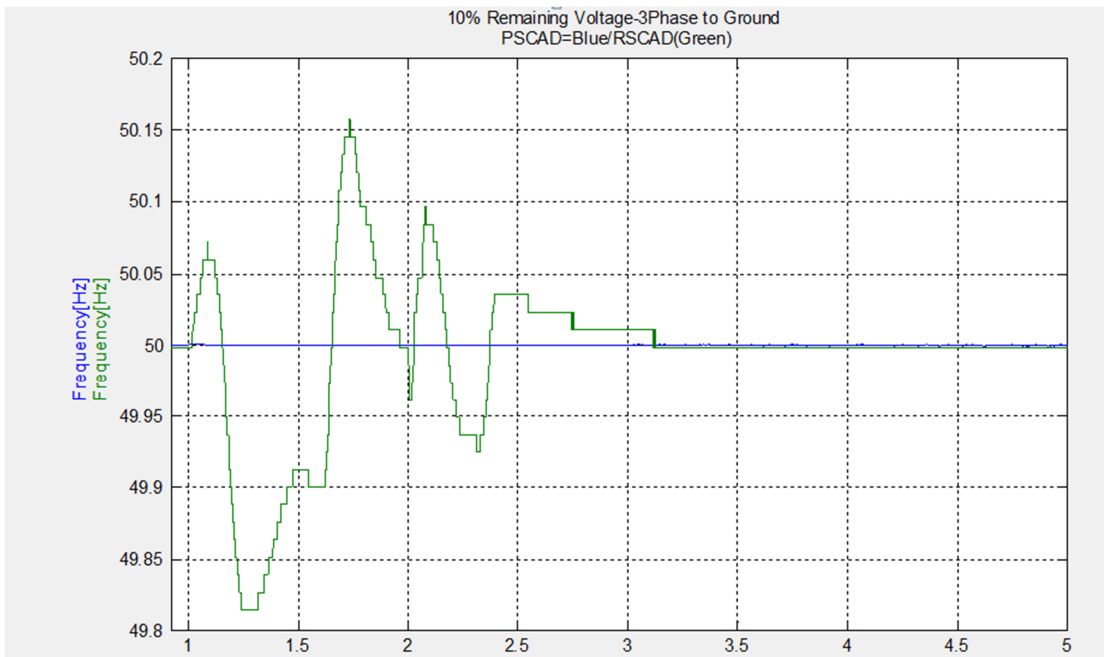


Figure7.2.1-Grid frequency Dynamic Performance in PLL in RSCAD model-Before PLL Modification

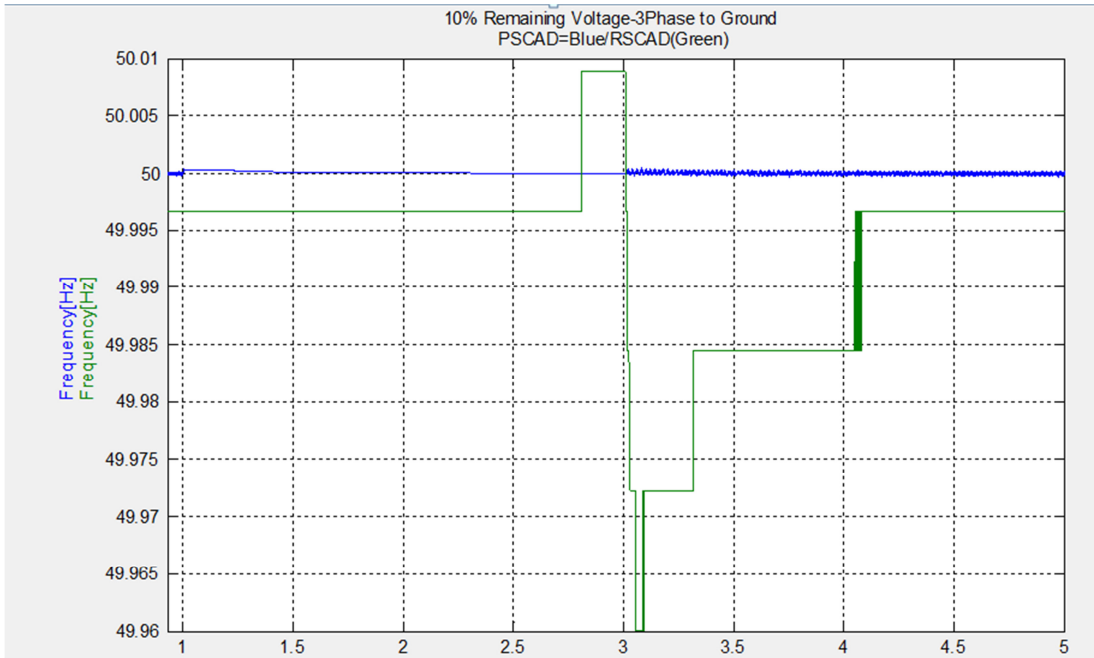


Figure7.2.2- Grid frequency Dynamic Performance in PLL in RSCAD model-After PLL Modification

The investigation was continued by working on Grid Side and Rotor Converter and crowbar block in RSCAD, the controller parameters are changed according to PSCAD , the controllers itself was updated, after all these modification the final plots are compared with PSCAD model in the next section 8.

8 Output from TS plot (AFTER MODIFICATION):

At this section models in PSCAD and RSCAD are verified against each other after modifying the RSCAD model according to the PSCAD model. The plots are investigated during a 3 phase to ground fault case with duration of 1 sec, and with 10% remaining voltage.

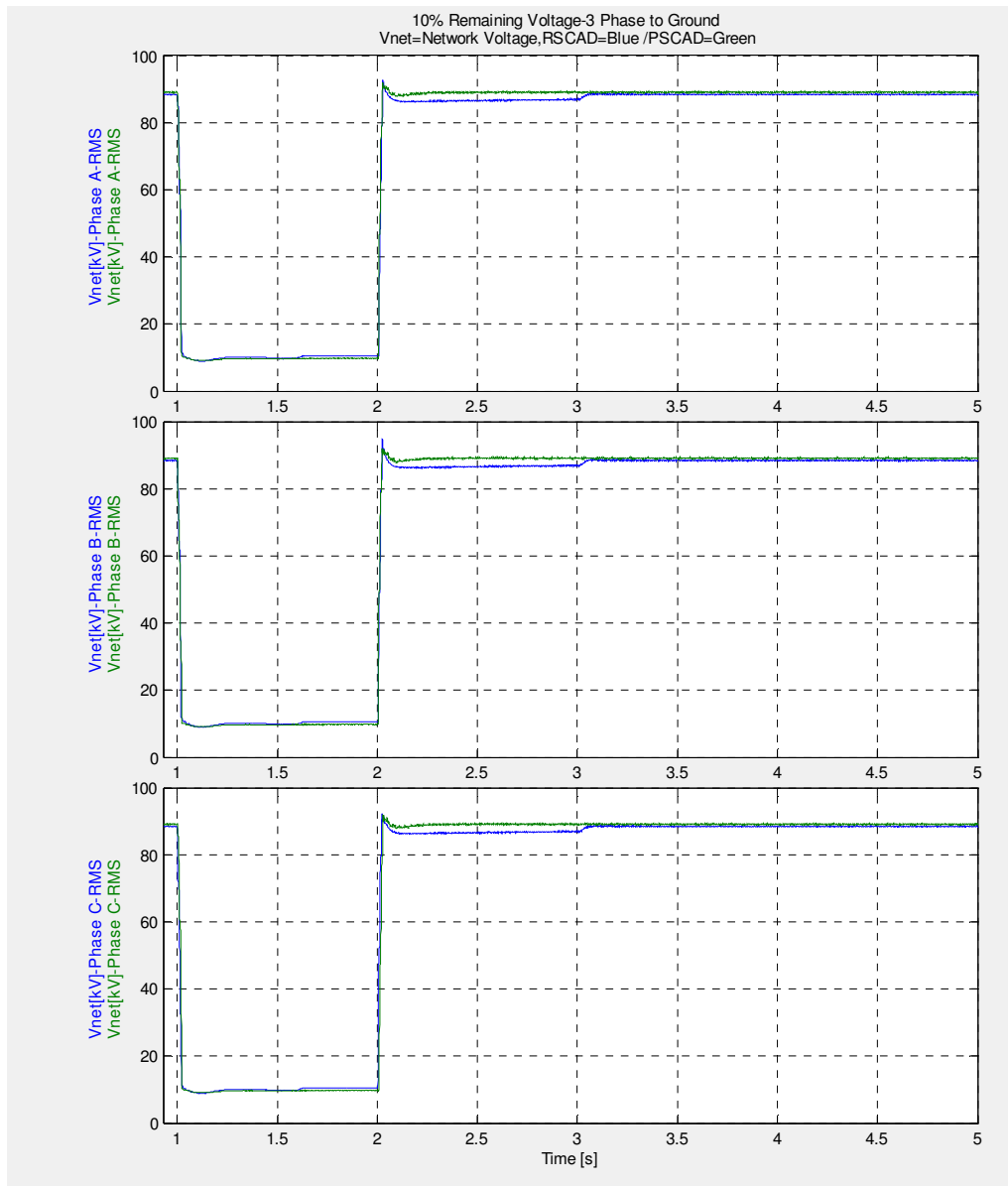


Figure8.1-Network voltages

The network disturbance is applied at time 1 s, and stator voltages in phases A, B and C are reduced to 10% remaining voltage. The fault is cleared at the time instant 2 s, as it is depicted in Fig8.1, after modification RSCAD plots are improved and more similar to PSCAD model.

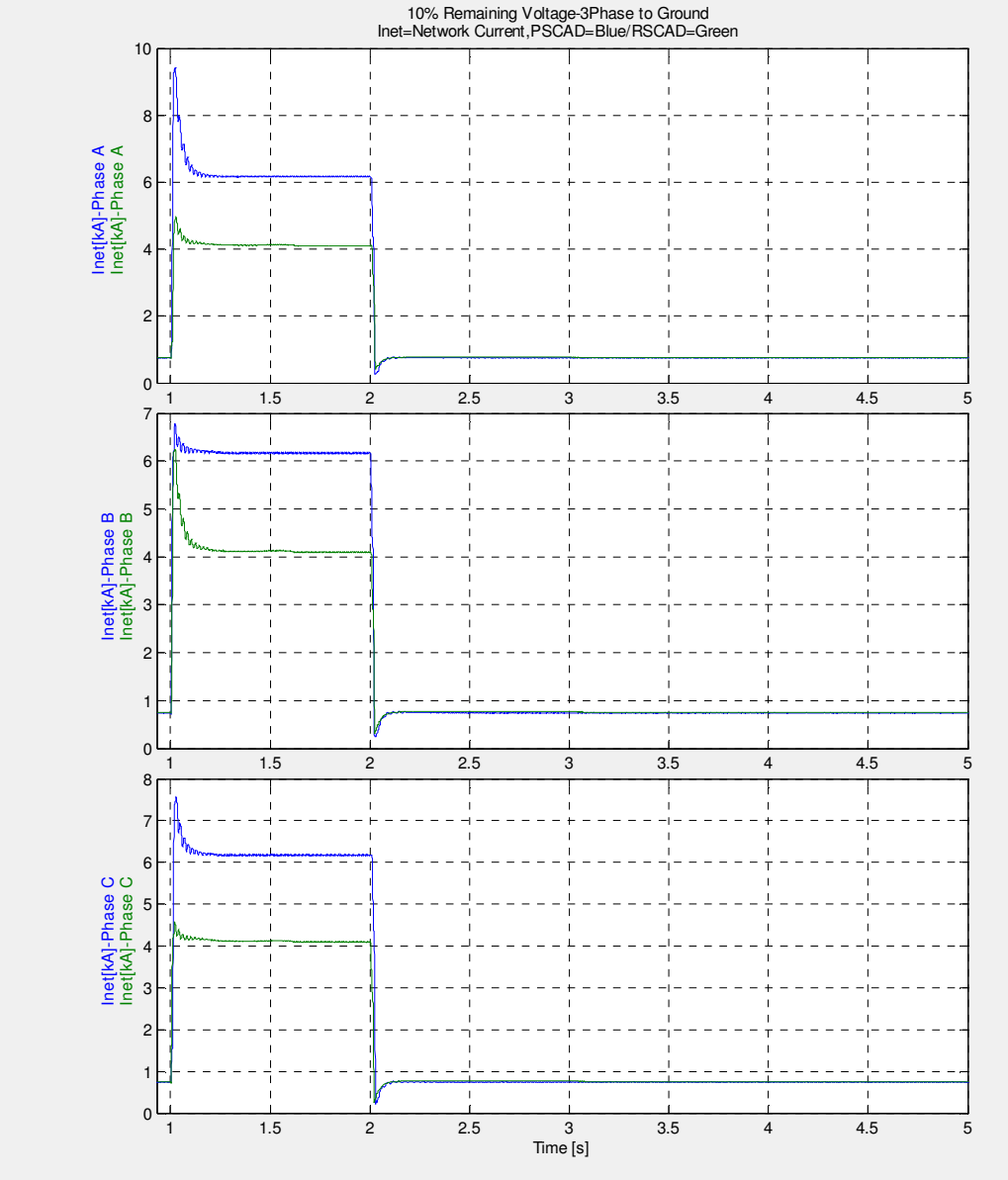


Figure8.2-Network Currents

Network current also increases due to the 3 phase fault as it is shown in figure8.2,and RSCAD plotts after clearing the fault are more consistent with PSCAD plotts,nevertheles still there is a difference between the fault current between two models.

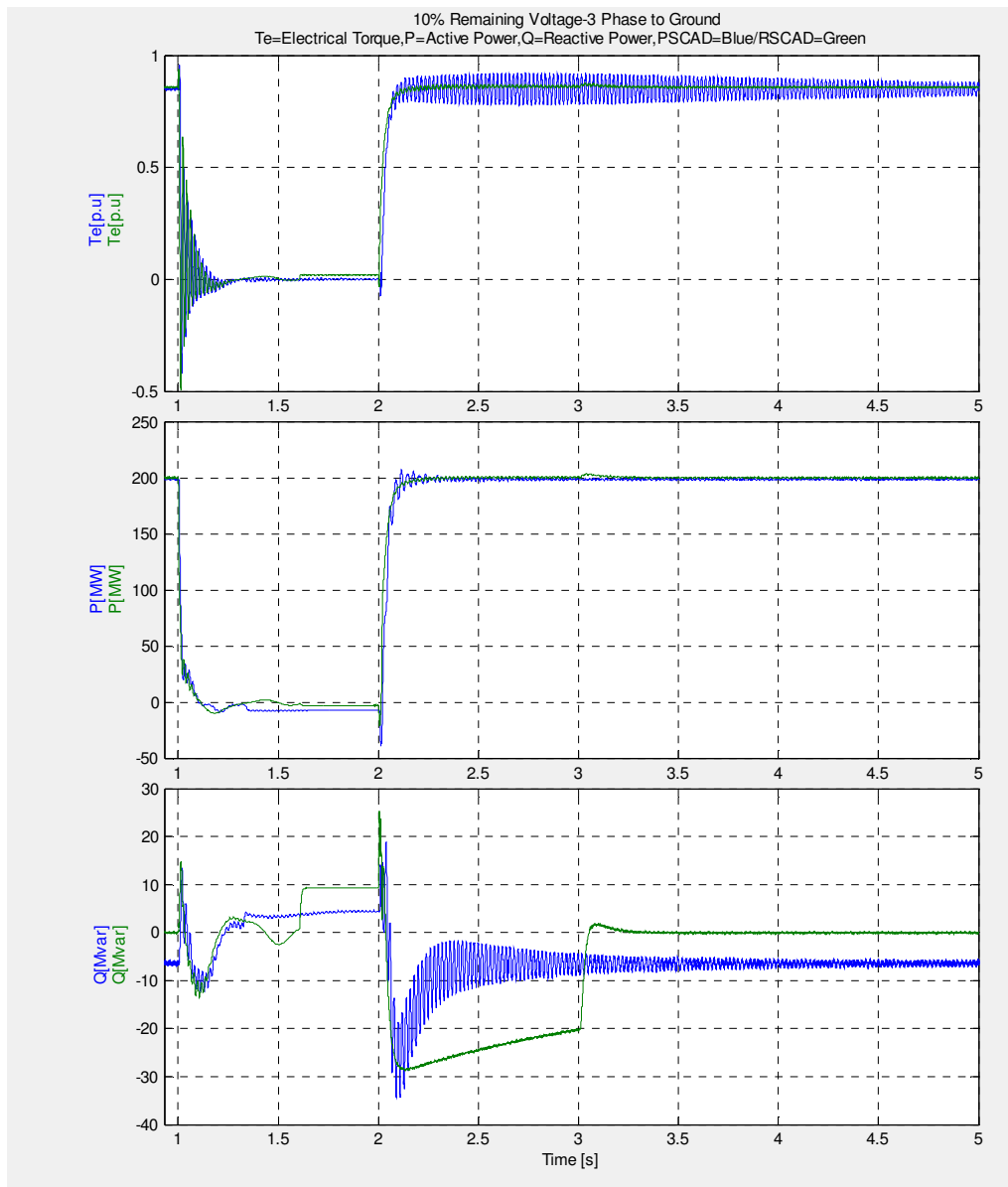


Figure8.3-Torque, Active and Reactive power

As it is shown in figure 8.3 when 3 phase short circuit fault happens generator T_e and P_e decreases which is expected. After the fault is removed in 2 sec it can be seen that the plots in PSCAD and RSCAD are very similar and more compatible. Consumed reactive power in PSCAD model is higher than RSCAD because the numbers of transformers in PSCAD and RSCAD model are basically different in the studied models. Although reactive power plot is not quite similar in two models but the results are more compatible rather than before.

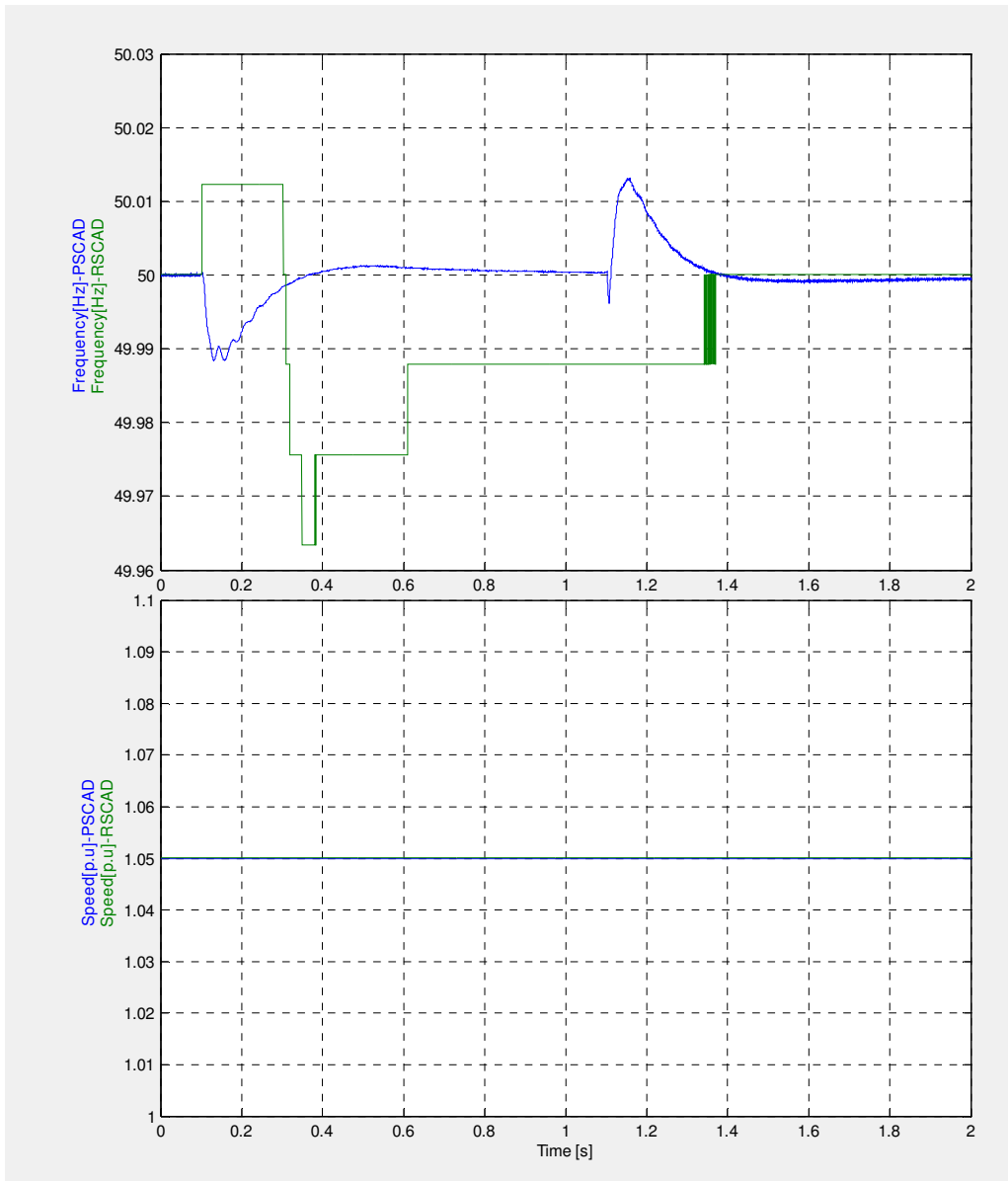


Figure8.4-Frequency and Speed

Frequency variation are improved to much extent as according to figure 8.4 the variations are limited within 50.01 Hz and 49.96 Hz, and PSCAD and RSCAD results are much closer now.

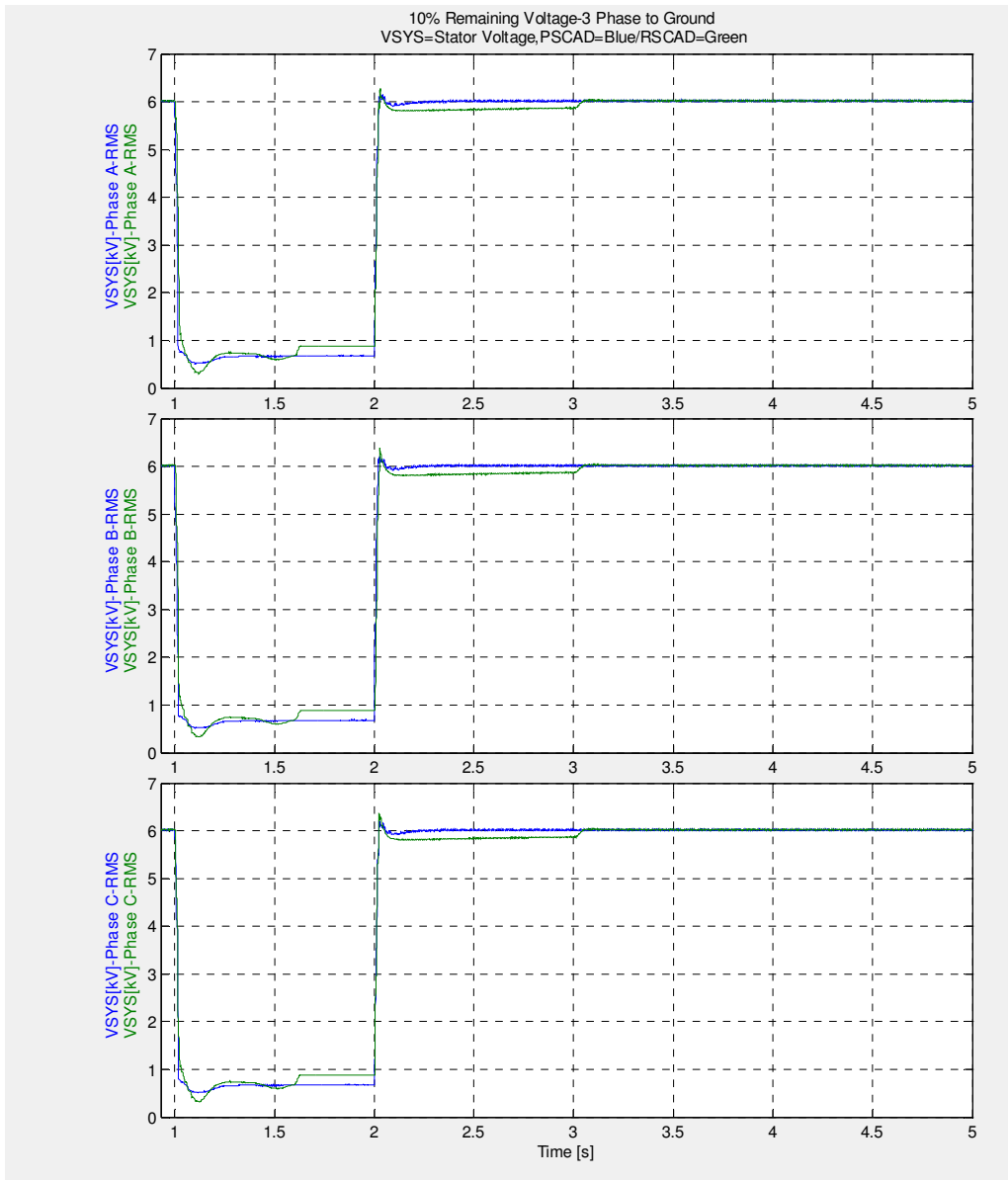


Figure 8.5-Stator Voltage

Figure 8.5 shows that stator voltage after fault is reduced to about 10% which is expected according to the fault type, comparing plot 7.5 and 8.5 it is seen that the stator voltages are more compatible after modification.

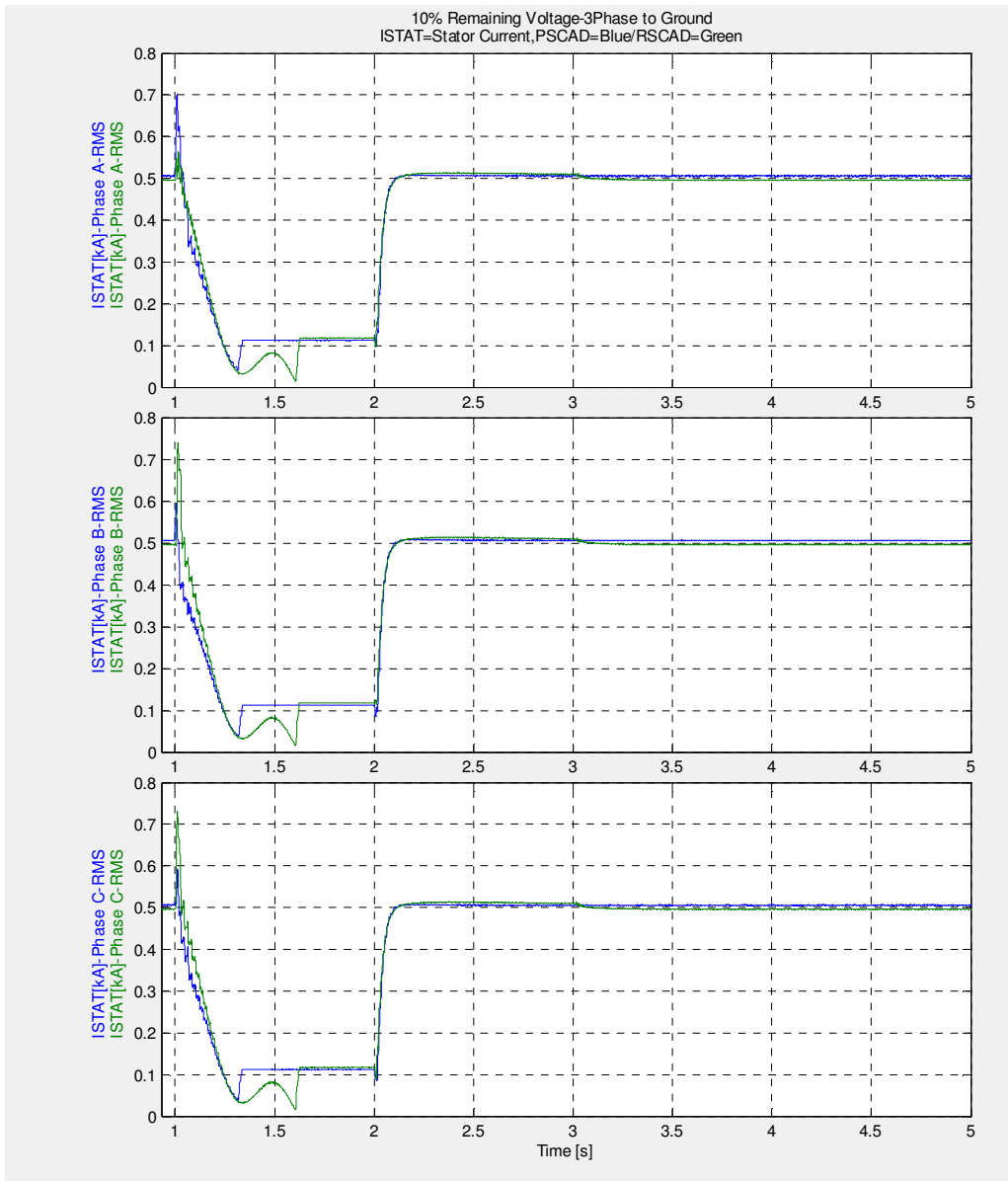


Figure8.6-Stator Current

According to fig.8.6 stator current increases for a very short time after the moment fault has happened and then drops quickly during the fault duration.

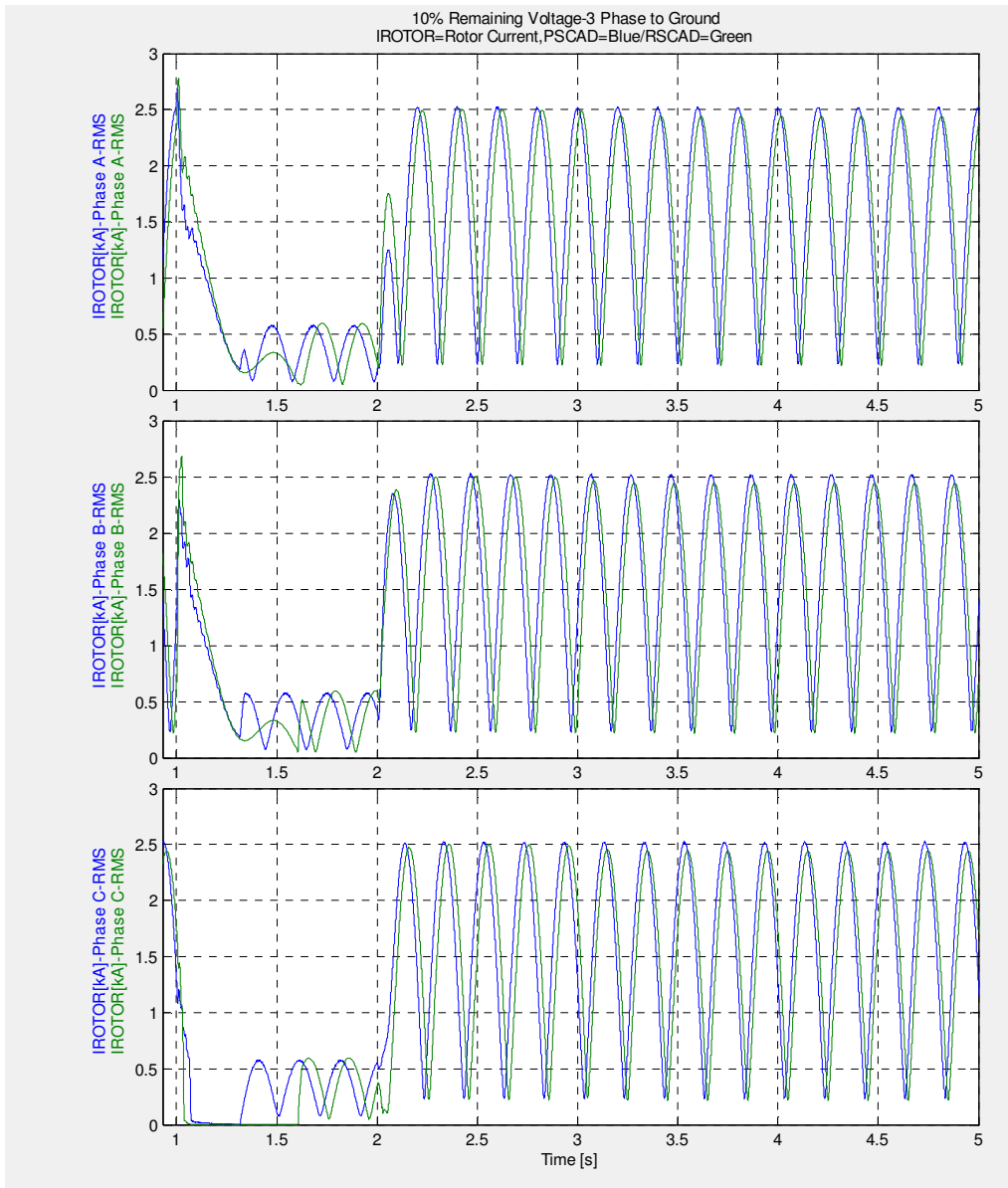


Figure8.7-Rotor Current

In figure 8.7 Similar to fig 8.6 rotor current grows once the fault has applied and reduces during the grid disturbance.

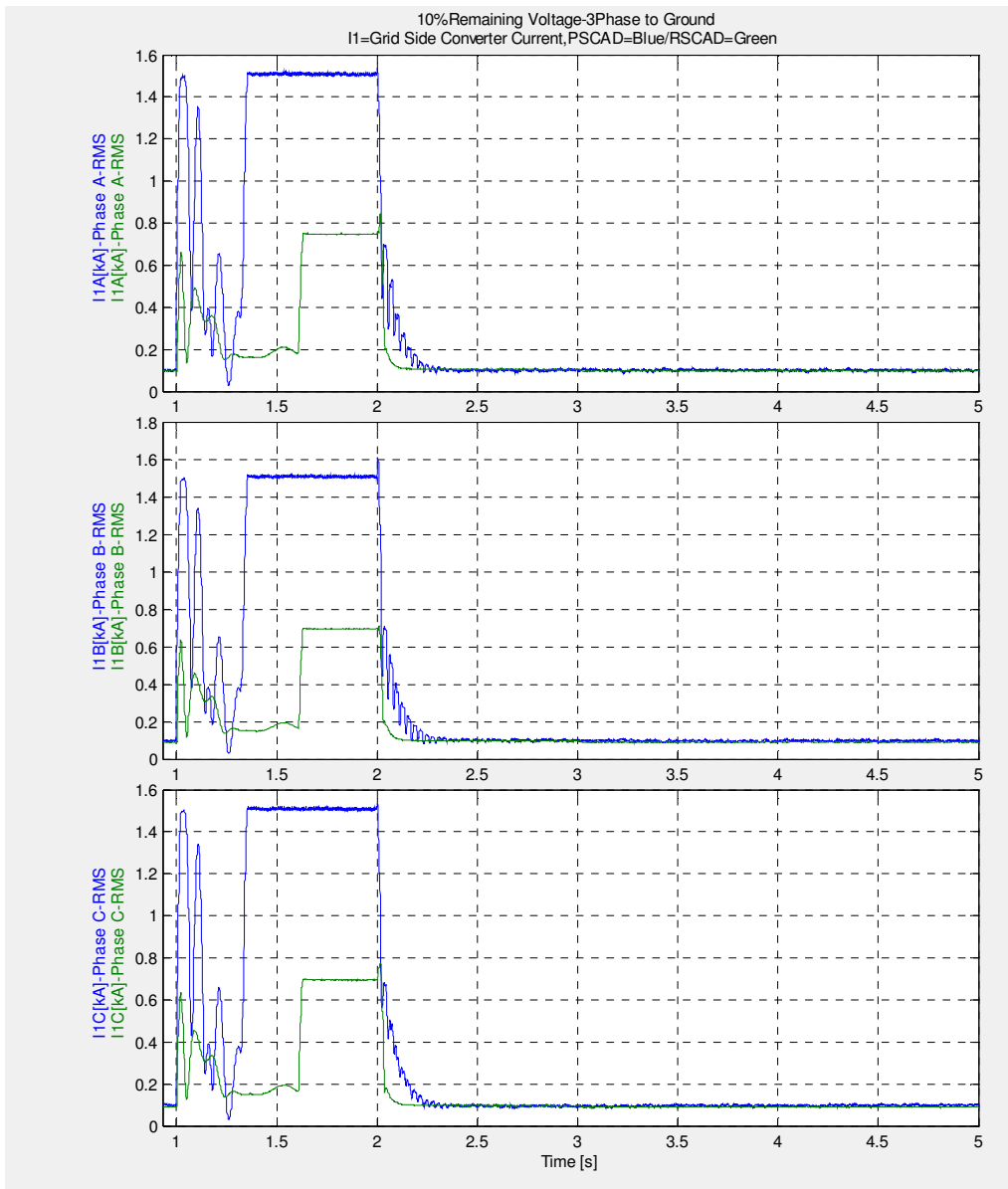


Figure 8.9-Grid side converter current

In figure 8.9 it is seen that both PSCAD and RSCAD models have oscillations in grid side controller current at the moment that fault has applied which can be related to the first peak of dc link voltage in figure 8.11 in RSCAD result when dc link voltage starts to decrease after about 1.6 sec grid side converter is raised again to compensate to dc link voltage drop. In PSCAD grid side controller tries to compensate dc link voltage reduction after around 1.3 sec.

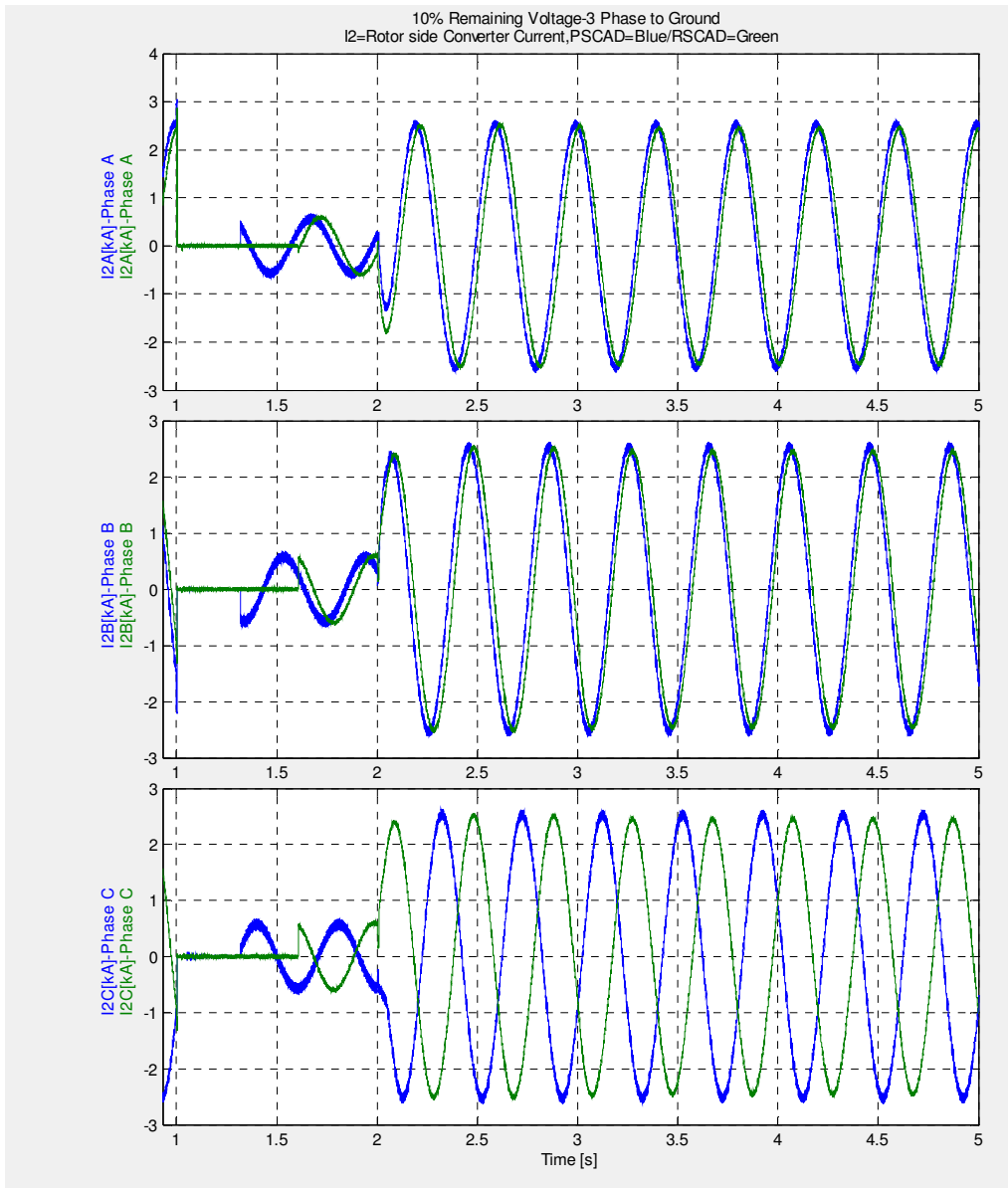


Figure 8.10-Rotor side converter current

It is seen that when crowbars are activated rotor side converter is protected from excessive rotor current.

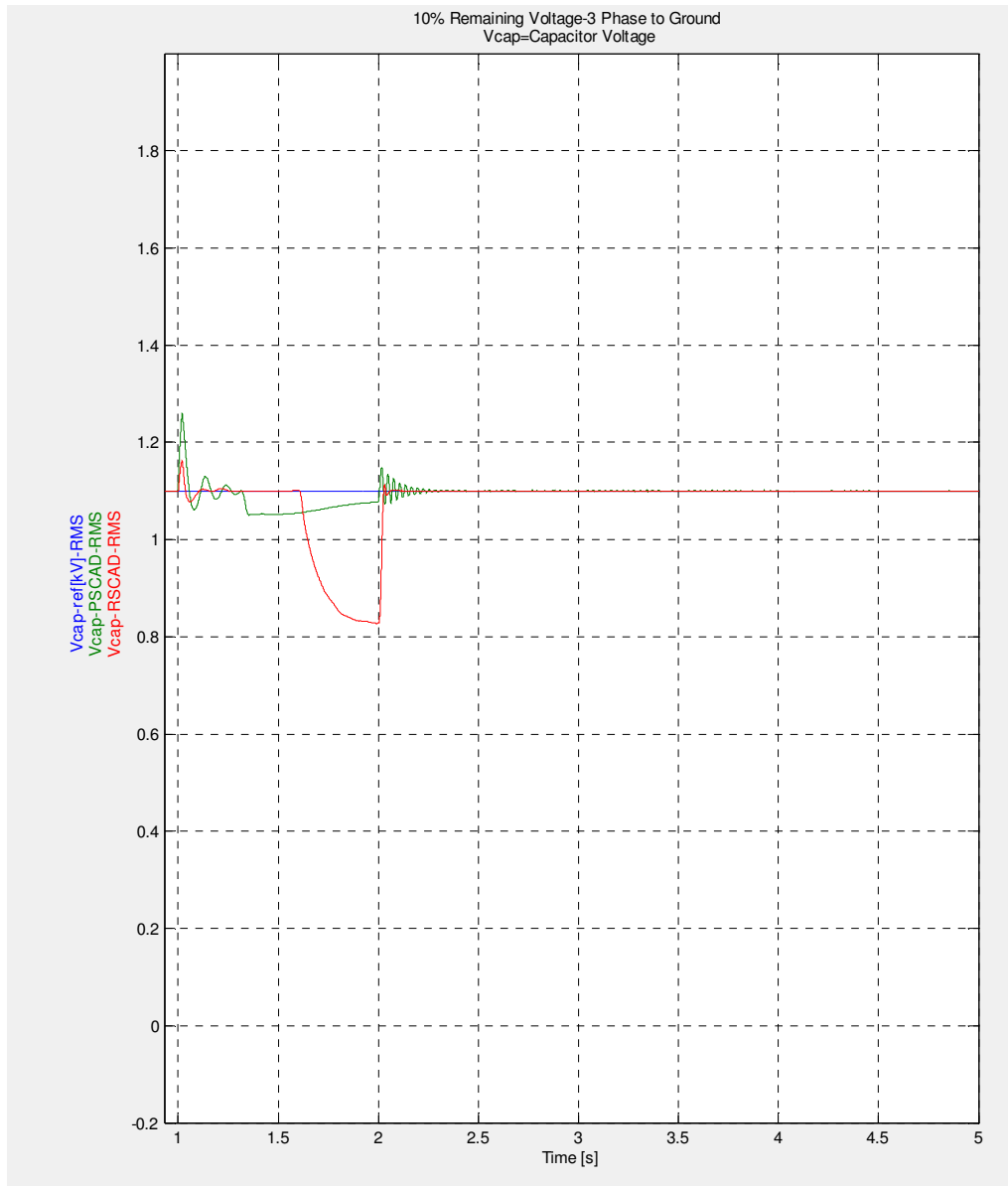


Figure 8.11-DC-link Voltage

In is shown in Figure 8.11 that dc-link voltage raises in both PSCAD and RSCAD models at the time instant 1 s and exceeds the crowbar activating limit value. The reason for the dc-link voltage increase in the beginning of the disturbance is the converters are not able to deal with the high inrush current coming from the rotor at a very short time. After modification RSCAD results for DC-link are more compatible to PSCAD results. It seems that still stator side converter in PSCAD has a better performance as DC-link voltage in RSCAD has more variations.

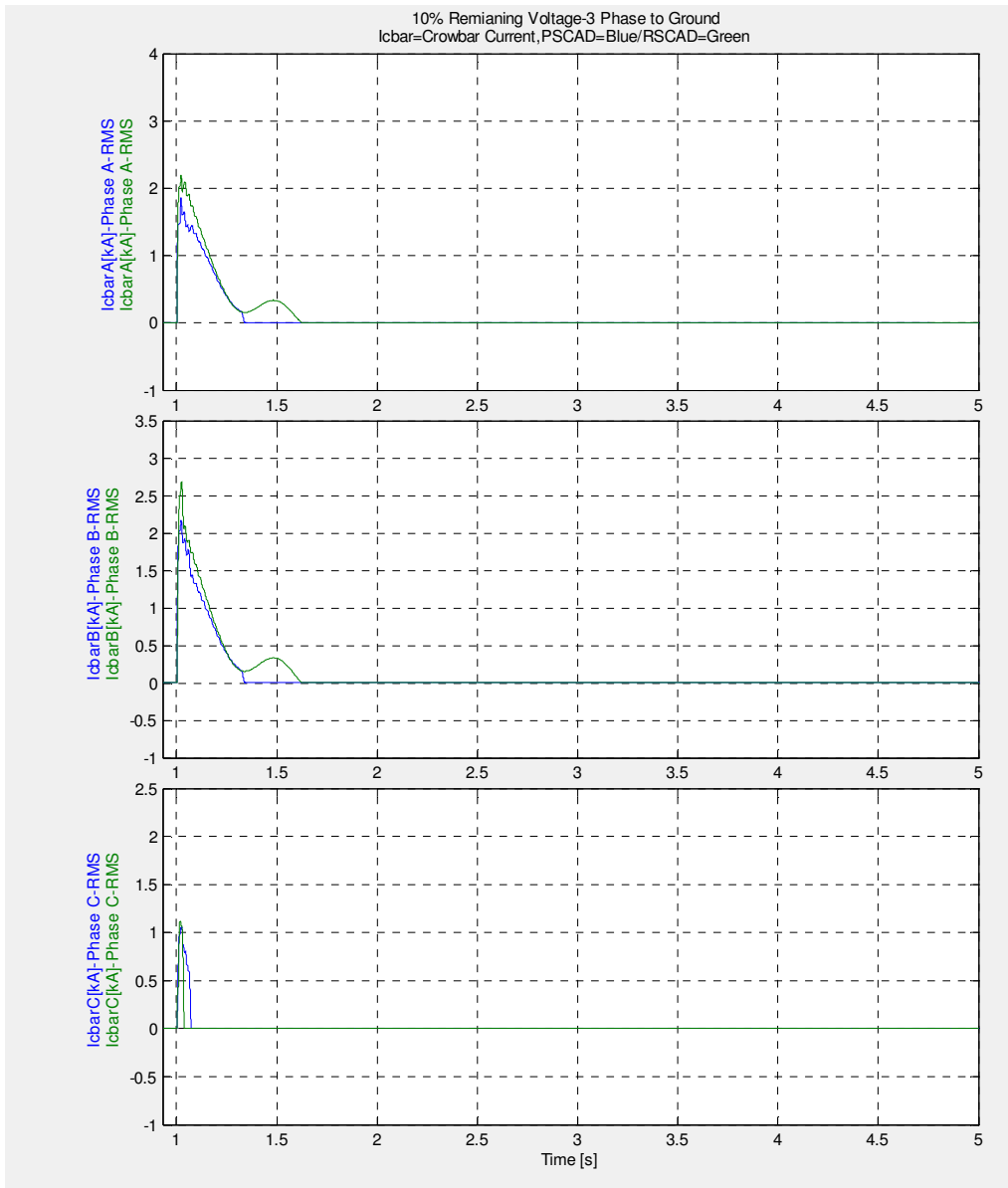


Figure 8.12-Crowbar currents

Looking at crowbar currents and crowbar activating signals in Figure 8.12 and 8.13 in both models it is obvious that crowbars are activated only once after disturbance which shows RSCAD model is more similar to PSCAD after modification.

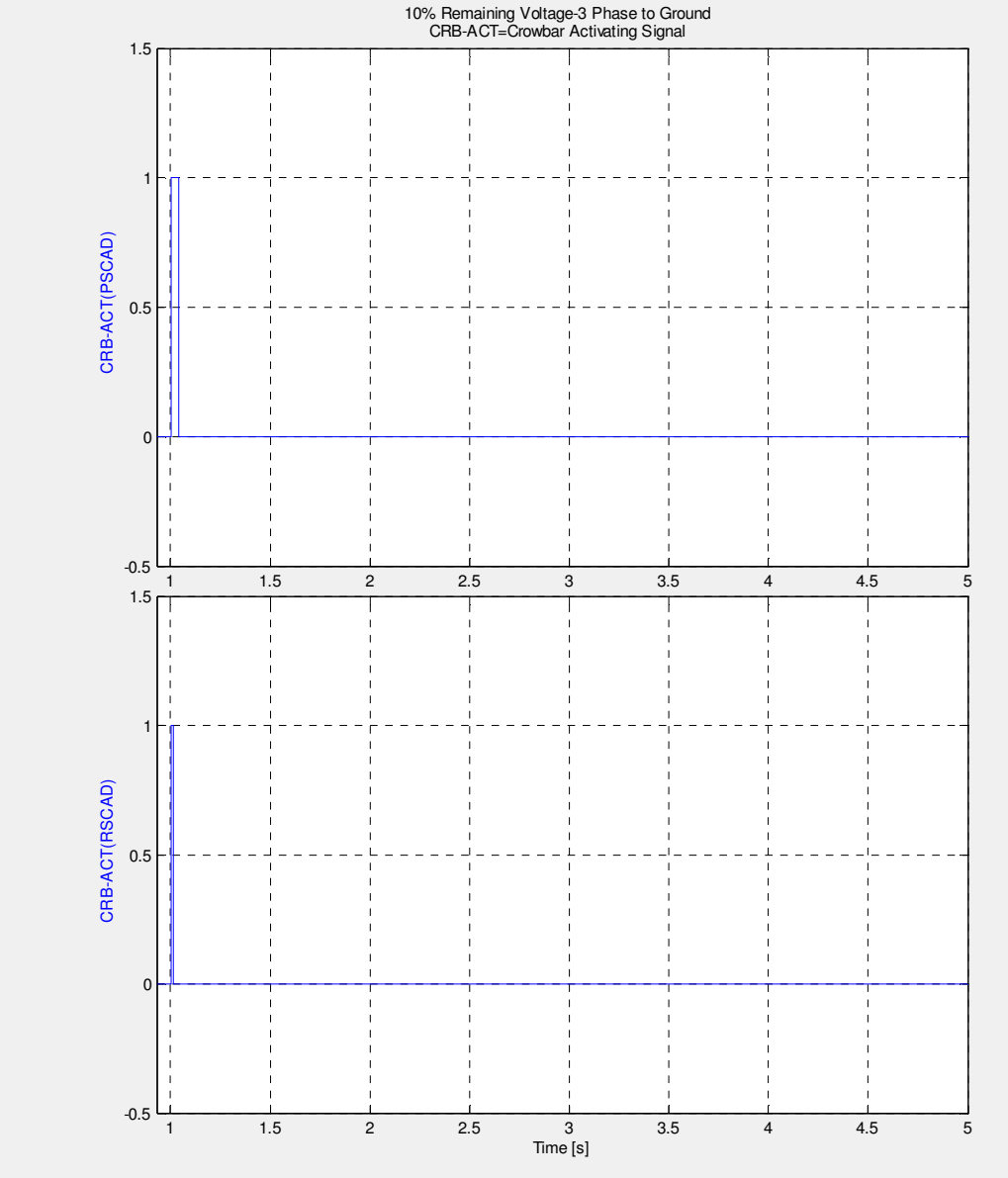


Figure 8.13-Crowbar Activating signal

8.1 CASE II: 80% Remaining Voltage 3ph – G

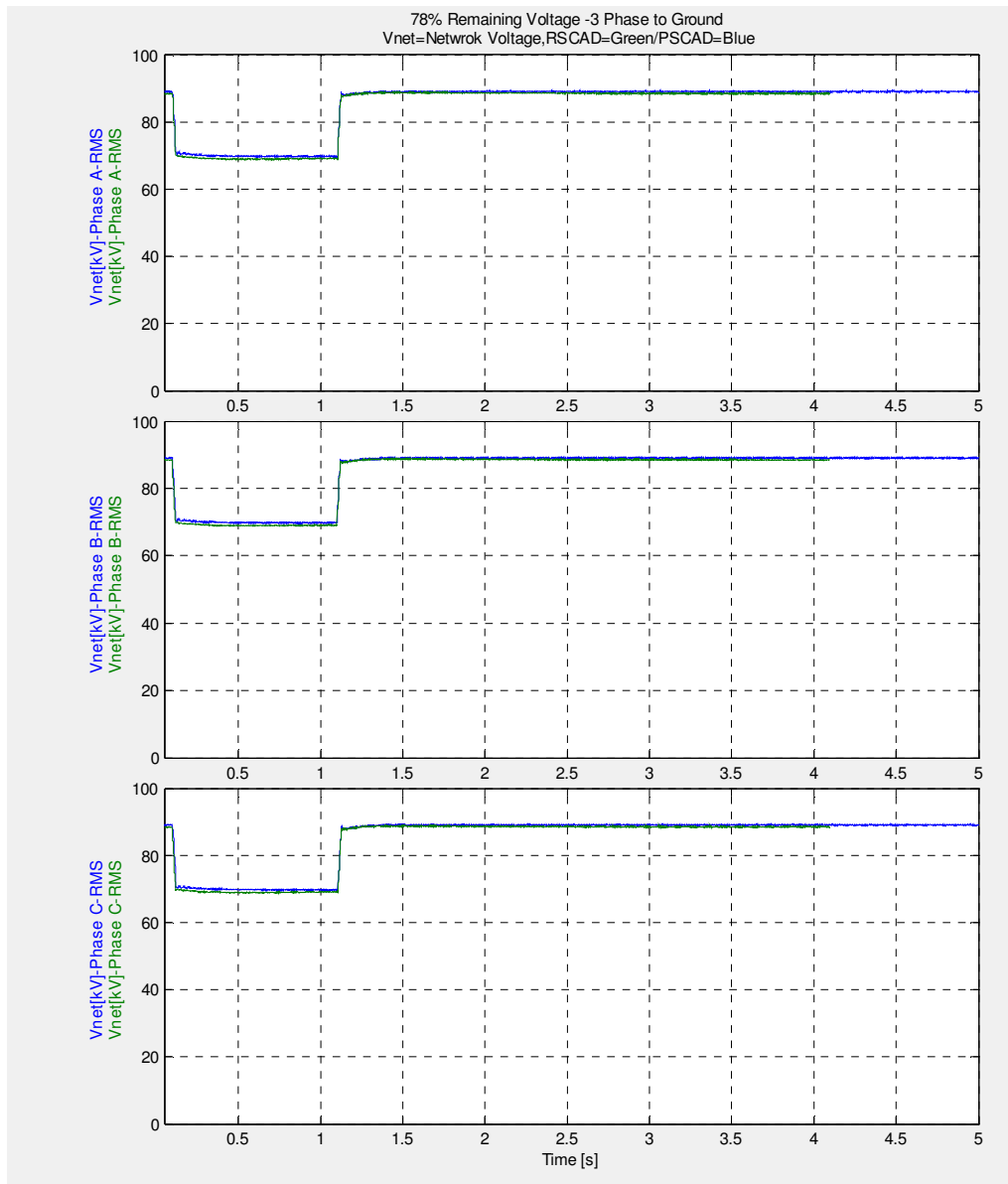


Figure 8.1-Network Voltages

At this case as in figure 8.1 is depicted fault is reducing the voltage by 20% this time, fault duration is still 1 sec.

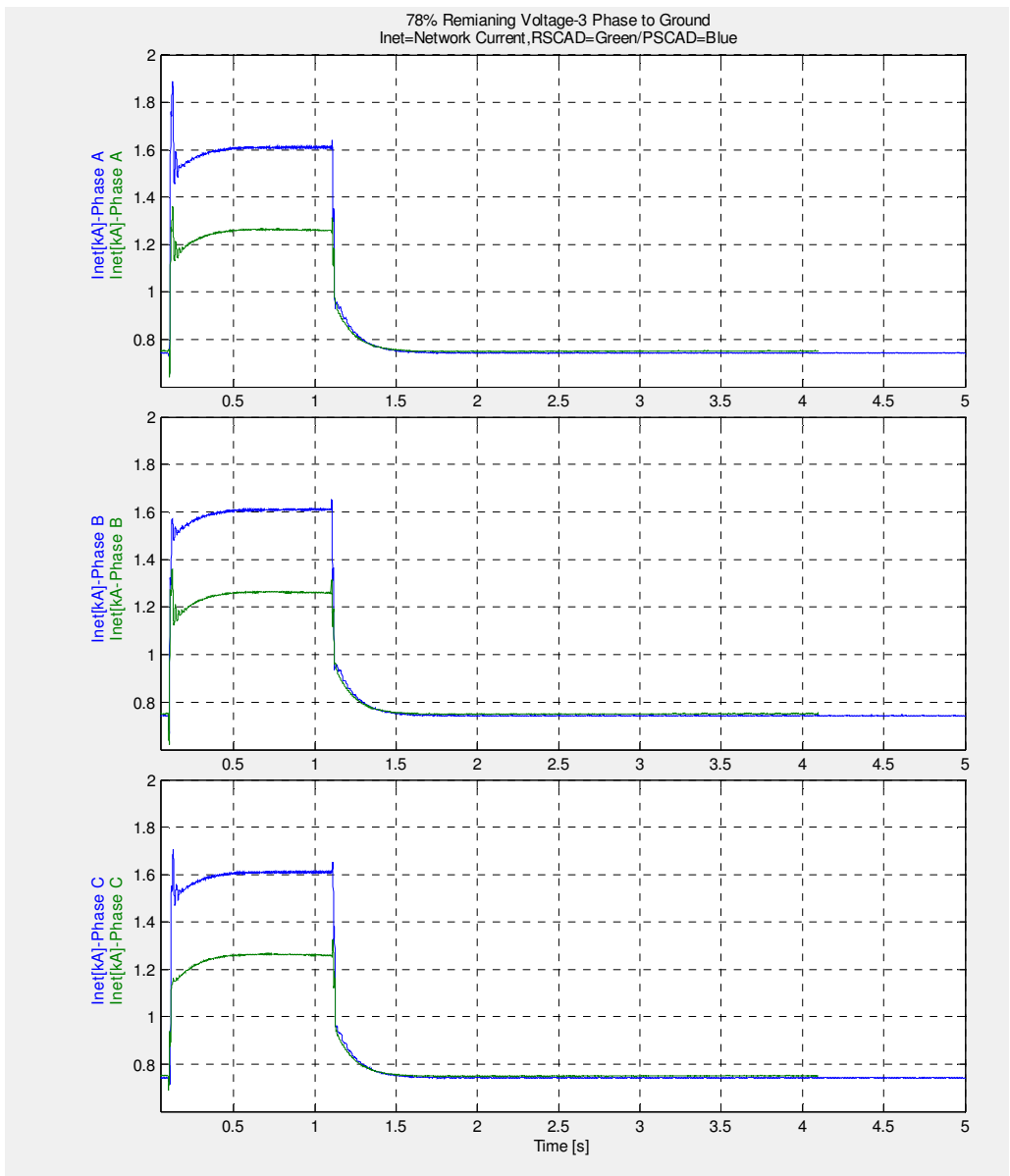


Figure 8.2-Network Currents

In figure 8.2 network current in both models increases same as the previous fault cases, but again there is a difference in current magnitude during the fault.

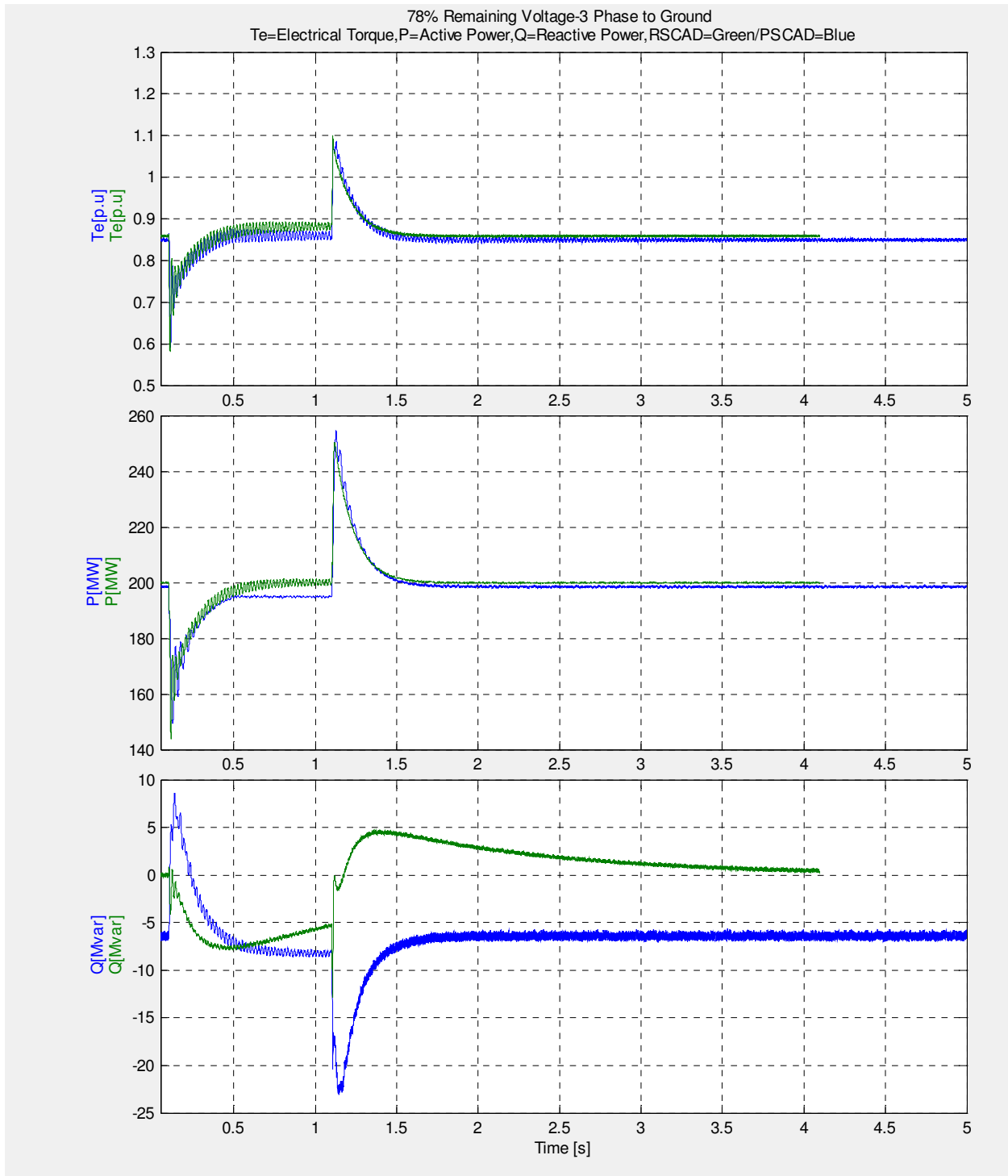


Figure 8.3-Torque, Active and Reactive power

Torque and active power comeback to the reference value in both PSCAD and RSCAD models. Reactive power in RSCAD is about zero during steady state and PSCAD model consume an amount of reactive power regarding that number of transformer in PSCAD model is more. Both models are adjusted to not have reactive power injection from rotor controller.

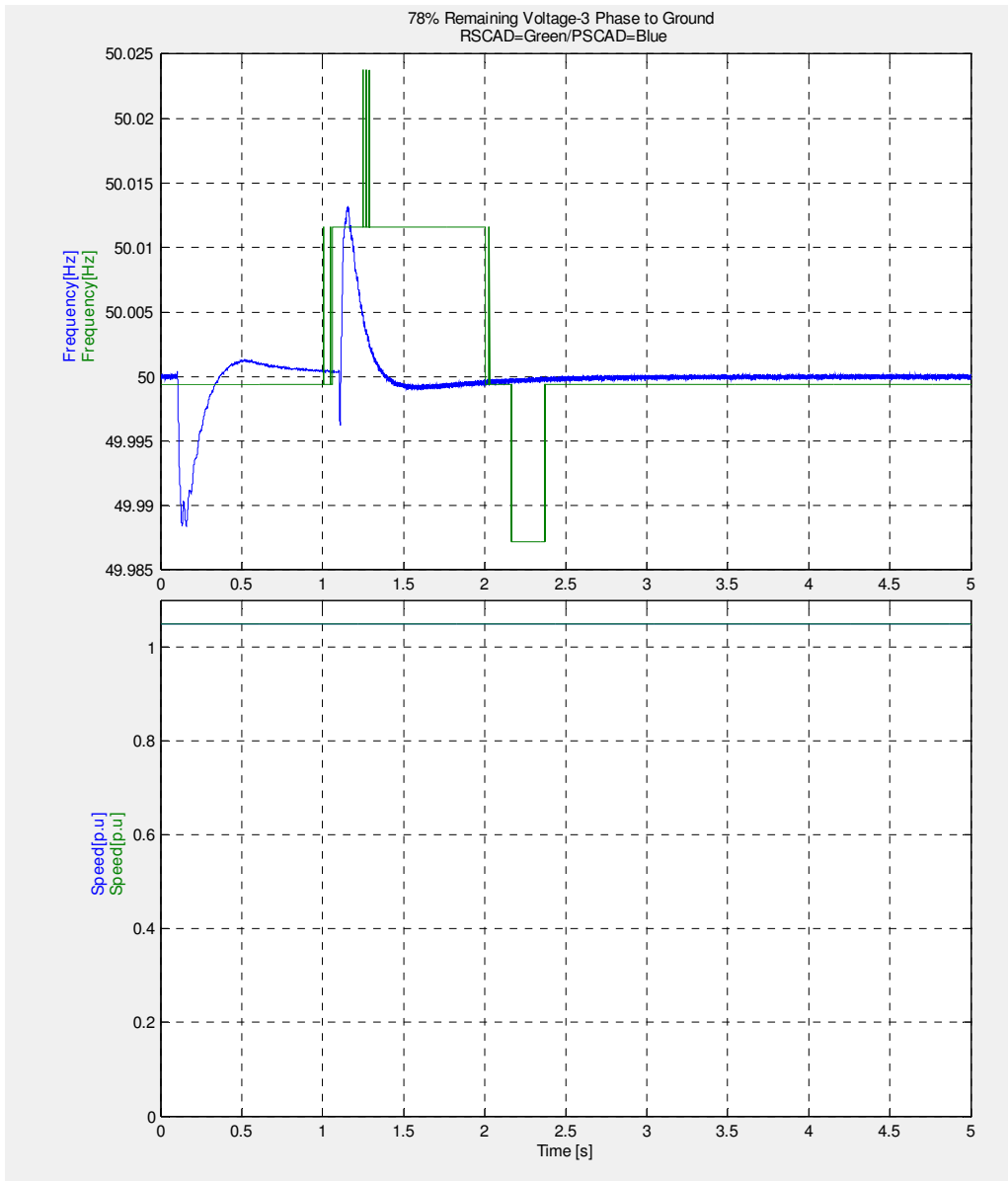


Figure 8.4-Frequency and speed

Frequency variations in both PSCAD and RSCAD models are shown in figure 8.4 and speed is defined fixed for DFIG.

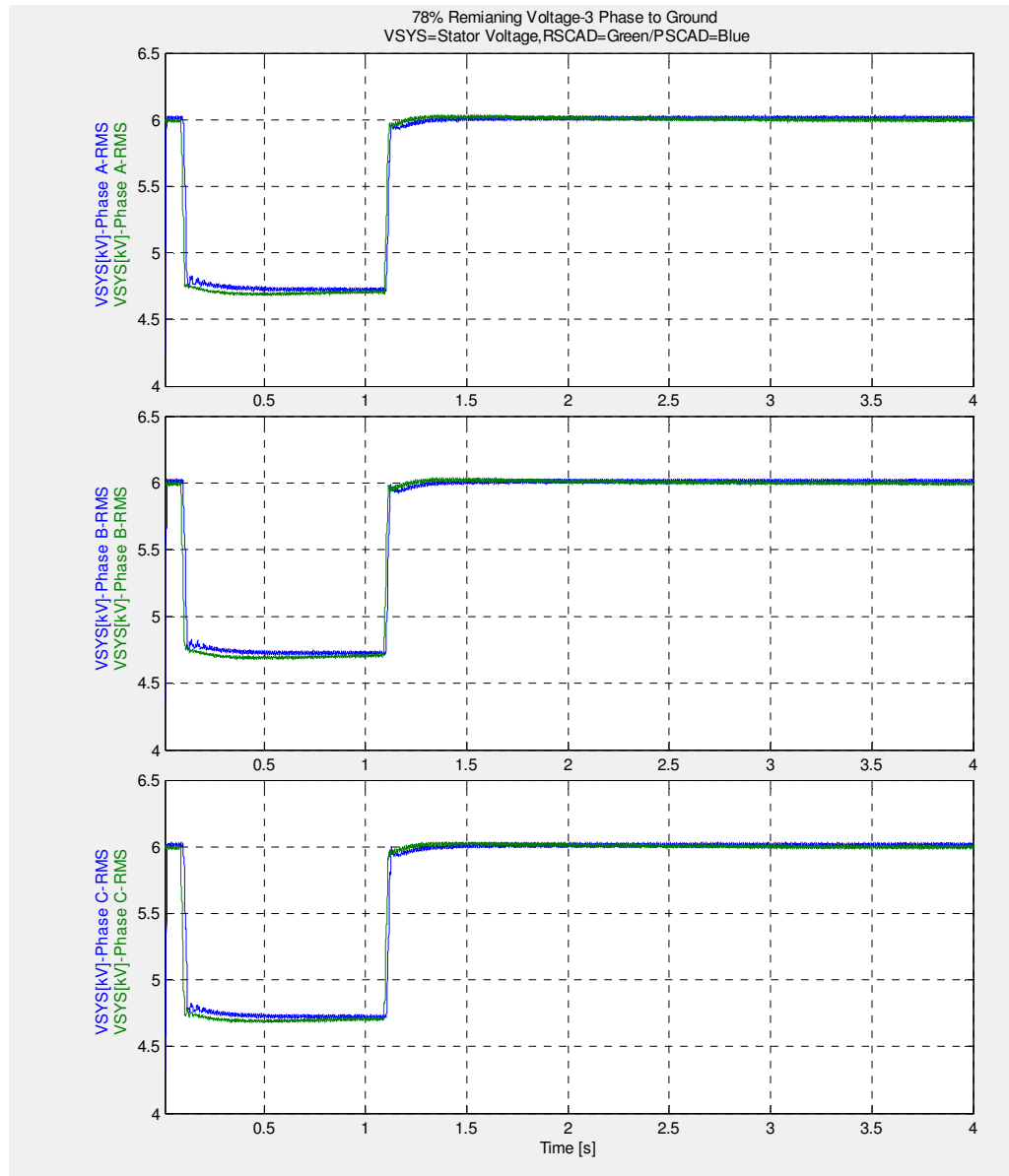


Figure 8.5-Stator Voltage

Stator voltage also decreases by about 20% in figure 8.5

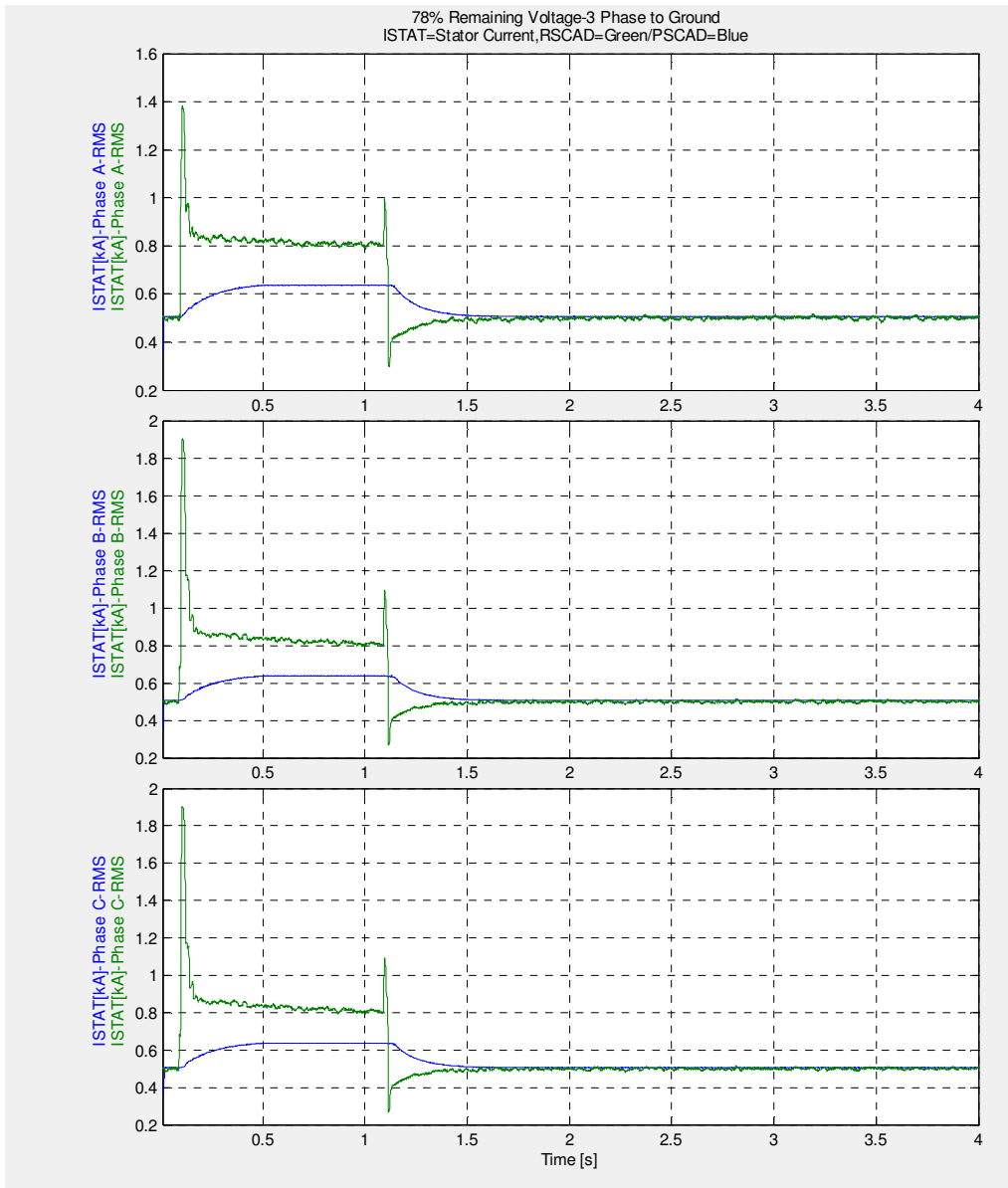


Figure 8.6-Stator Current

Unlike the previous fault cases which crowbar was activated, in 80% remaining voltage fault case crowbar is not triggered and in figure 8.6 it is seen that stator current also in both models has increases after the fault has applied which is quite different from the 90% remaining voltage fault case.

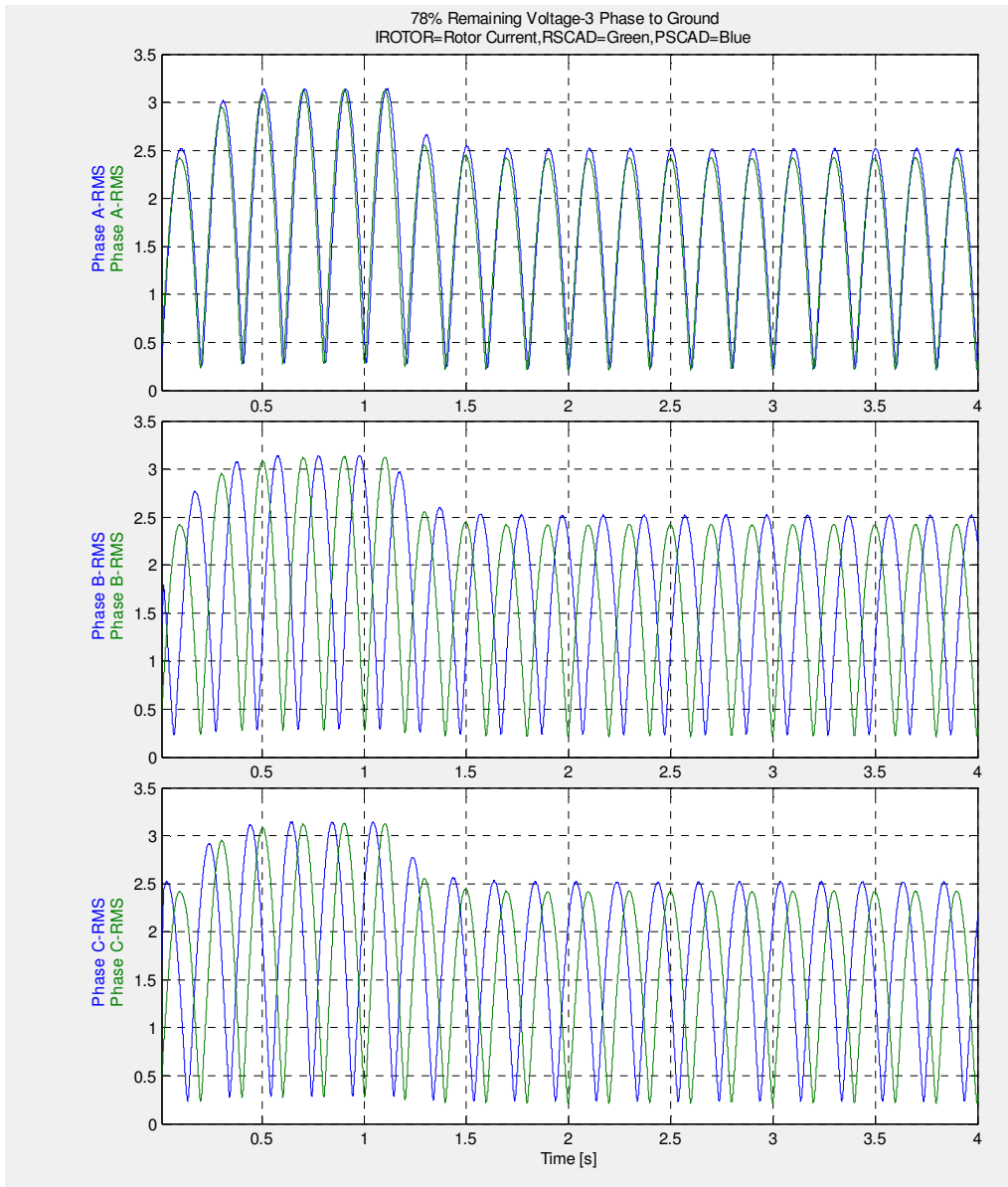


Figure 8.7-Rotor Current

It is very clear that also rotor current has increases after the fault, unlike the 90% remaining voltage fault case.

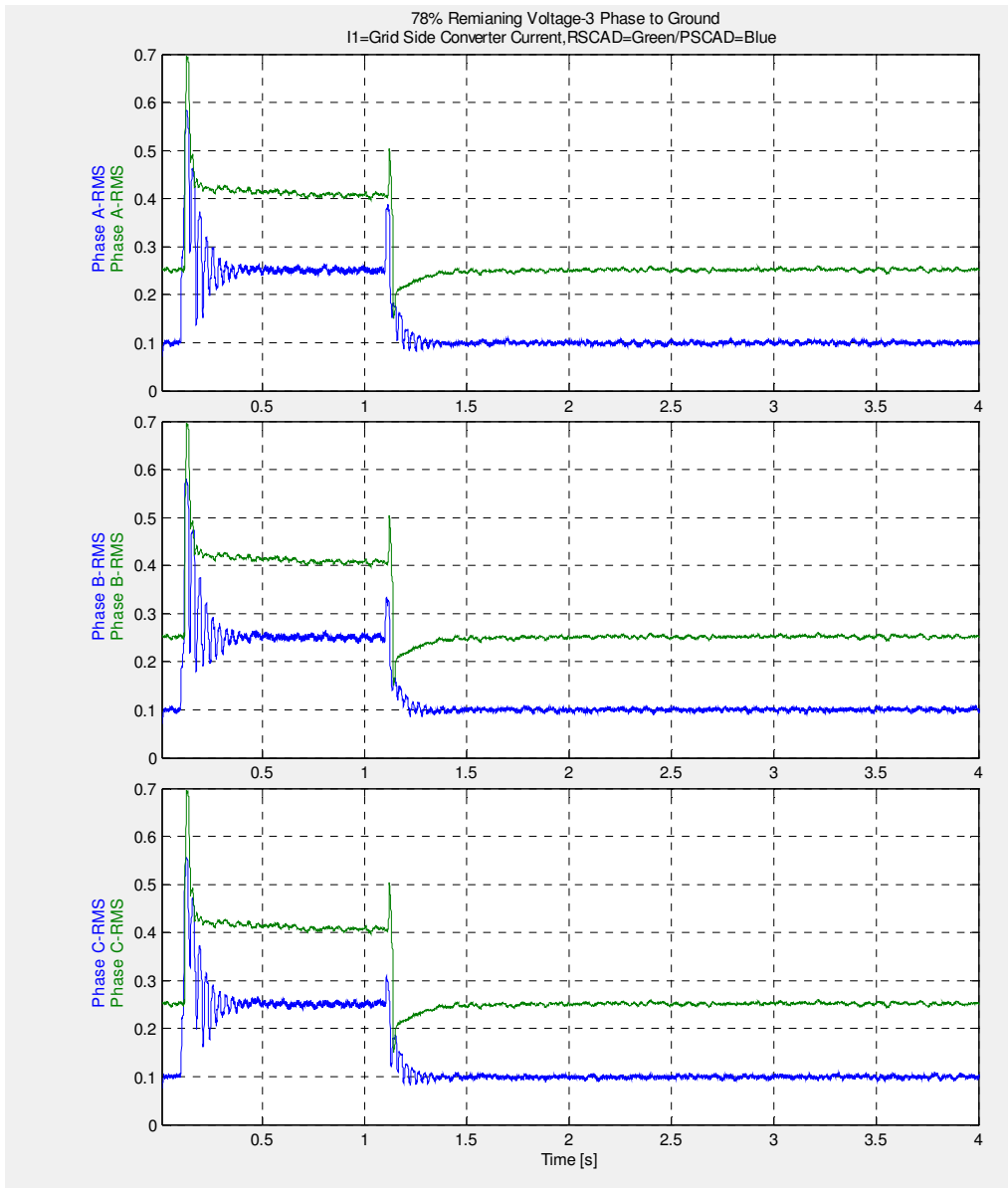


Figure 8.8-Grid side converter current

Grid side converter current in both models now has increase according to figure 8.8 from the beginning of fault event which is expected due to power imbalance between two sides, and these currents are different during fault.

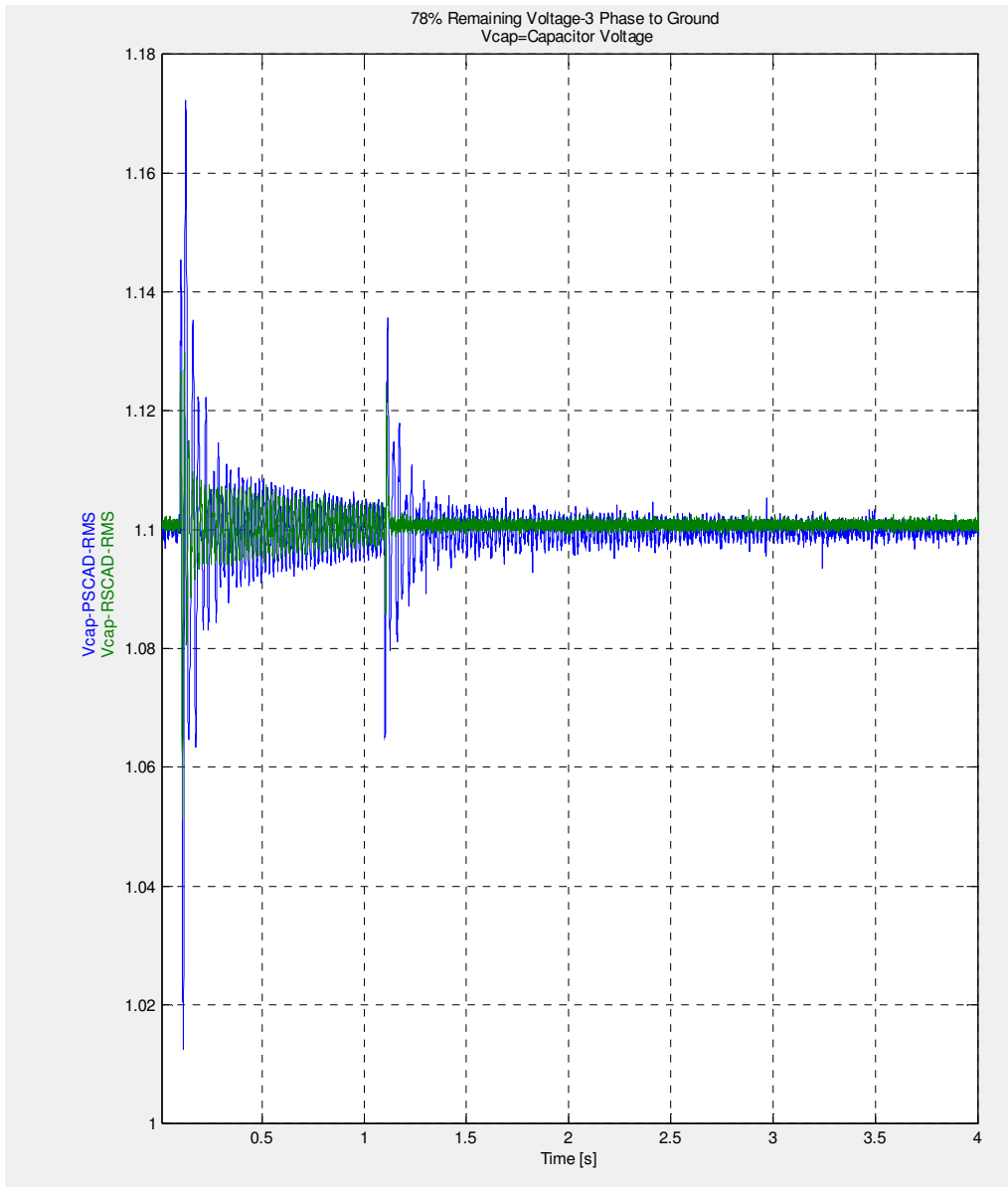


Figure 8.9-Dc-link voltage

According to figure 8.9 both voltages are less than the crowbar activation level, resulting that crowbar shouldn't be activated which is shown is confirmed by figures 8.10

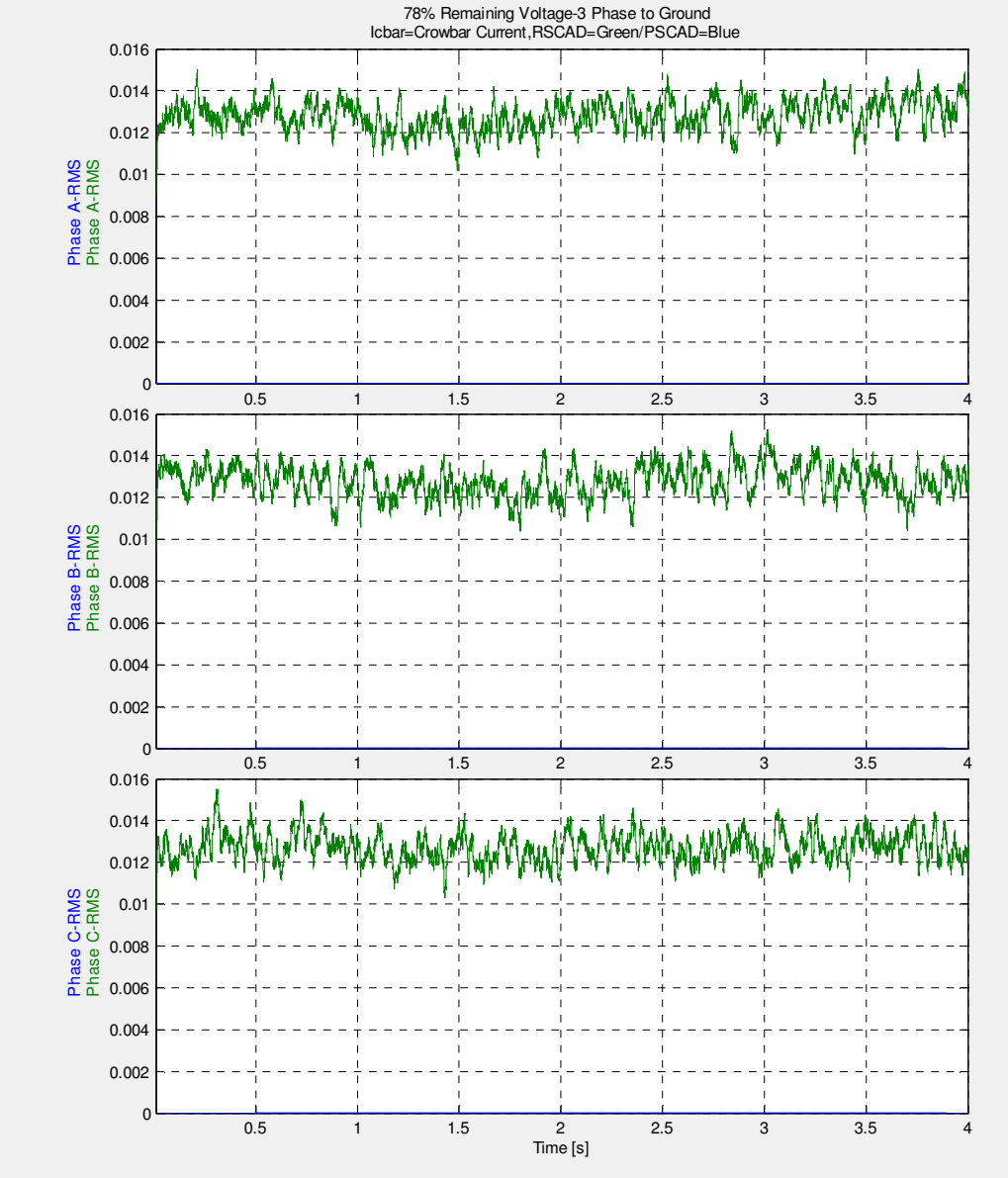


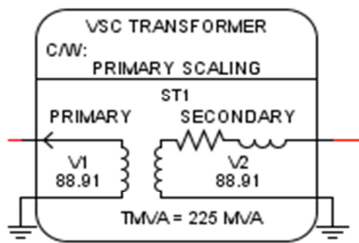
Figure 8.10-Crowbar current

Chapter 8

9 PART II- Scaling of DFIG in RSCAD and modifying the model against PSCAD

9.1 PART A: Investigations in Scaling transformer settings, Small time step blocks, and Infinite voltage source model

The purpose is to scale the DFIG model up to 800 MW to reduce the amount of the processors in RTDS, when a wind farm is going to be modeled. There is a component inside RSCAD which is scaling transformer. The problem is that by increasing the scaling level to about 600 MW in RSCAD the model becomes unstable. In spite of that the scaling method used in both PSCAD and RSCAD model is based on the same principle, this component in RSCAD model is investigated and tested to focus on any possible difference in PSCAD and RSCAD. The investigations about scaling feature are divided into part A and B.



rtds_vsc_SCL_TRF1					
ENABLE G/TAO D/A OUTPUT		SIGNAL NAMES FOR RUNTIME AND D/A			
SIGNAL MONITORING IN RT AND CC			ENABLE FACEPLATE D/A OUTPUT		
SCALING OF PRIMARY CRT AND EFFECT ON LARGE DT			SIGNAL OUTPUT OPTIONS		
CONFIGURATION			TRANSFORMER PARAMETERS		
Name	Description	Value	Unit	Min	Max
Name	Transformer name:	ST1			
prc12	If BRIDGE uses 2 proc, place on #:	1		1	2
tapch	Include Tap Changer on Primary:	No		0	0
enscl	Include Scaling of Influence on Primary:	Yes		0	0
suerr	-- If Include Scaling, suppress WARNING:	No		0	0
sdtcmp	Include RC damper parallel to Secondary winding:	No		0	0
<input type="button" value="Update"/> <input type="button" value="Cancel"/> <input type="button" value="Cancel All"/>					

Figure 9.1.1-Setting of Scaling Transformer

A three single phase transformer shown in figure 9.1.1 is used to for scaling. There are some parameters that can be adjusted in the component. The effect of having RC damper in secondary of scaling transformer is going to be investigated. It should be mentioned in PSCAD there is not a built in scaling transformer component like RSCAD.

1. **RC dampers:** RC dampers are activated or disabled in secondary of the scaling transformer.
 - RC damper application is to decrease the oscillations in stiff networks. The purpose is to see if this RC branch can help to remove the instability while the scaling level increases. This is something that does not exist in PSCAD model therefore the following cases are studied:
 - With RC branch set to default values
 - Without RC branch

It is noticed that there are some other differences between PSCAD and RSCAD model, that should be studied;

DFIG model in RSCAD is divided into two separate small time step blocks, which are connected via a fictitious transmission line, and this issue also should be studied.

2. **(GIS)Imaginary transmission line:** The effect of Transmission line between DFIG and voltage source block (GIS) need to be studied.
 - As it was discussed in RTDS simulation to it is desired to reduce the time step for more accuracy in small time step, consequently the scaling transformer and network model with fault branches are placed in another small time step block to reduce the small time step value. As it was mentioned before If there are different VSC subsystems in the model each sub system in small time step should be linked to the other small time sub systems via a cable or transmission line to keep the time step lower than 4 μ sec for entire system. This limitation does not exist in PSCAD model, and consequently there is not any imaginary transmission line in PSCAD model as a result the effect of having GIS or not having GIS on the scaling level should be studied.

Regarding that the used infinite voltage source in RSCAD is a signal generator, and this is different from PSCAD model, this part of model also should be investigated.

3. **-Voltage source modeling**
 - Voltage source model in PSCAD is a 3- phase voltage source model, but in RSCAD a fixed frequency ramp generator and a 3-phase wave generator is used. To study this difference between used components two case are investigated:
 - With Ramp function
 - With voltage source model

Results of these investigations are compared in different cases, and the cases will be simulated to highlight any link between the instability in RSCAD and these issues.

In following plots:

PG=200 MW DFIG active power (MW)

SL1=scaling level

P1 and Q1=scaled power (MW, MVAR)

E_d =stator voltage magnitude (p.u)

9.2 Model with GIS and Ramp Function -Without RC Values

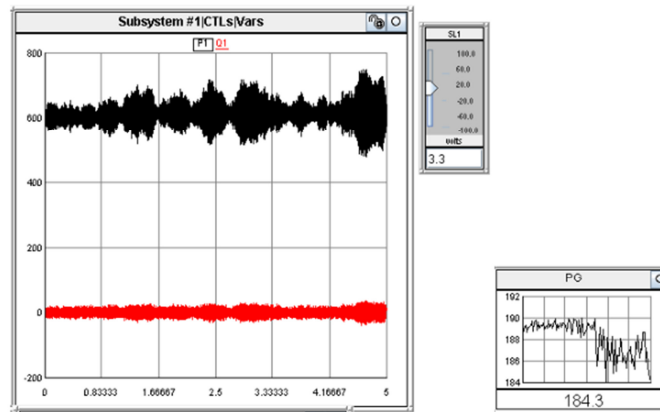


Figure 9.2.1- Scaled Power

It is seen in figure 9.2.1 that the slider value (SL1) can increase up to 3.3, and after that model becomes unstable. The amount of the oscillations in P1 is also noticeable in 600 MW, and the power at the DFIG terminal (PG) also has a drop. Also the voltage at the stator (E_d) is also decreasing according to figure 9.2.2.

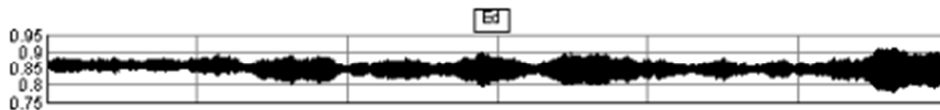


Figure 9.2.2- Stator Voltage magnitude in p.u

9.3 Model with GIS and Ramp Function-With RC Values

RC damper is activated now in the second case to see the difference. Default values are (R=100 Ω , C=1 μ F)

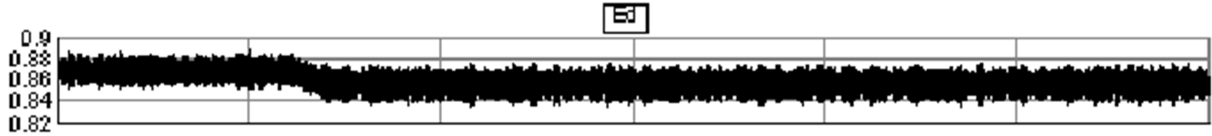


Figure 9.3.2- Stator Voltage magnitude in p.u

One influence of the RC damper in this case is reducing the oscillations of the power. It is shown that the power at the stator is slightly higher compared to case 9.2. The stator voltage is also slightly higher according to figure 9.3.2. It is observed that the slider value can be sent to 4.2 in figure 9.3.3, and system will not become unstable.

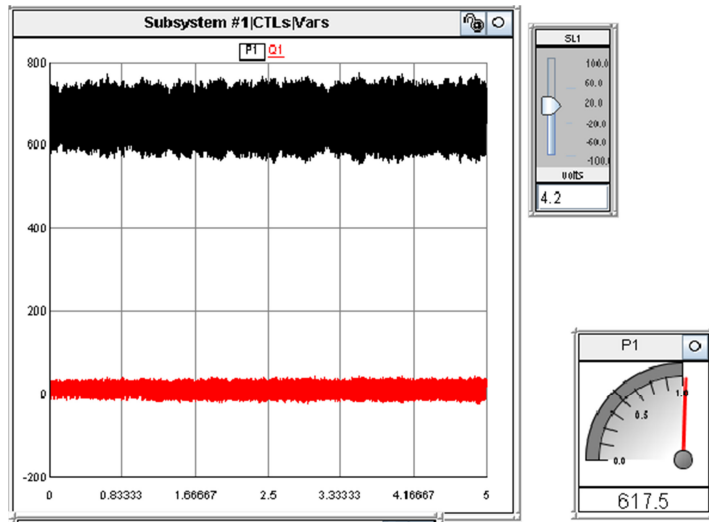


Figure 9.3.3 -Maximum Possible Scaling Level

9.4 No GIS-Ramp Function-No RC Values

In this case the GIS is removed to eliminate the tline from RSCAD and RC values are not considered and the scaling transformer is placed inside the DFIG model and make the model more similar to the PSCAD model, This increases the time steps, which may influence the results.

At this case scaling can be increased up to 3.7, which is shown in figure 9.4.1.

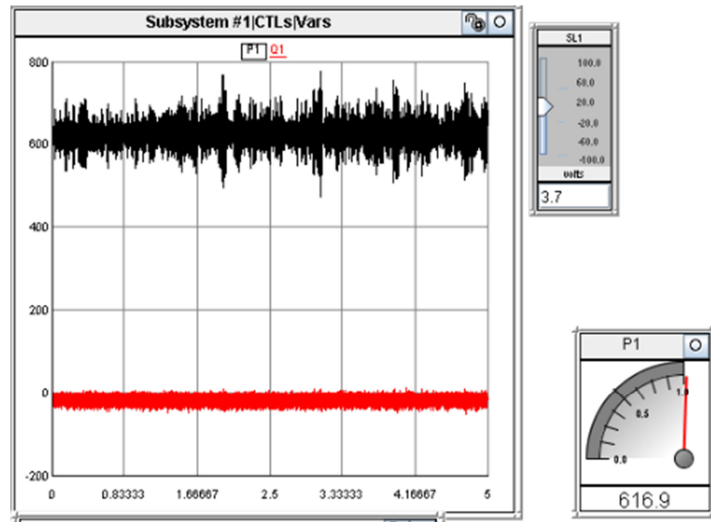


Figure 9.4.1- Scaled Power

9.5 No GIS-Ramp Function- RC Values

In this case the slider can be increased up to 4.3 in figure 9.5.1;

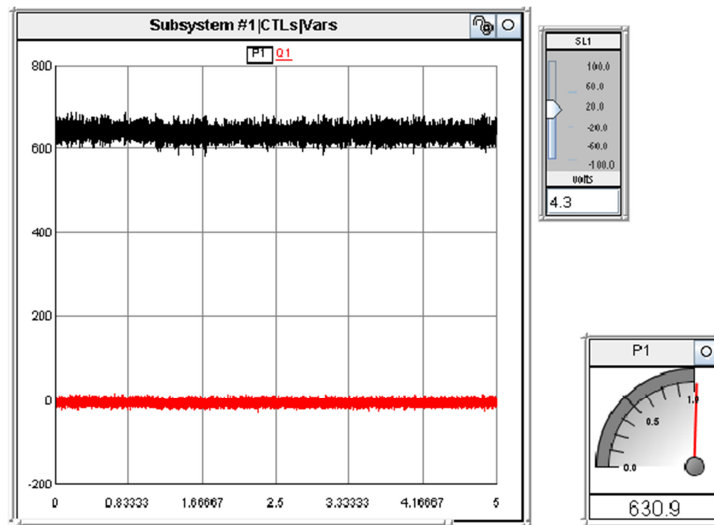


Figure 9.5.1- Scaled Power

9.6 No GIS –No Ramp Function - No RC Values

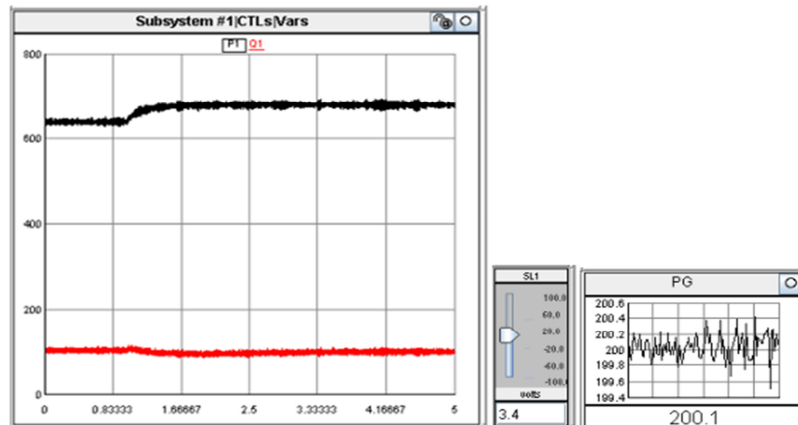


Figure 9.6.1- Scaled Power

Power at the stator of DFIG is higher than the model with ramp function according to figure 9.6.1.

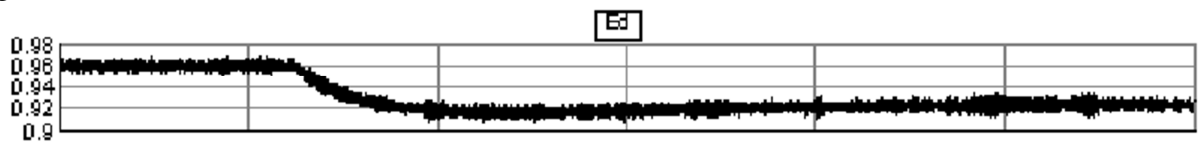


Figure 9.6.2-Stator Voltage magnitude in p.u

The slider value can be sent to 3.8 at the maximum possible point.

9.7 No GIS-No Ramp Function - RC Values

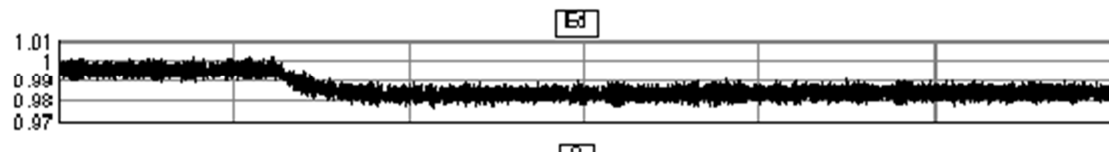


Figure 9.7.2-Stator Voltage magnitude in p.u

The slider value can be sent to SL=3.5 at the maximum and generator can produce 700MW according to figure 9.7.3.

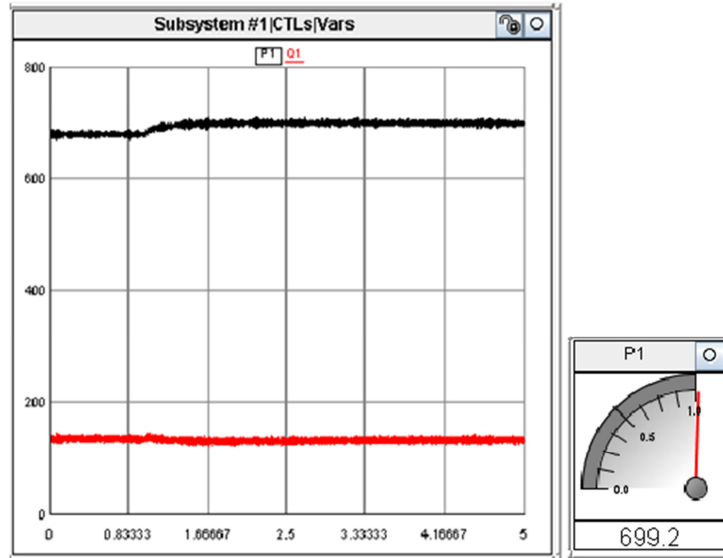


Figure 9. 7.3- Scaled Power

Conclusion:

It is seen that removing both GIS and Ramp function does not solve the scaling transformer problem. But removing the GIS and ramp function and using the large time step infinite voltage source is giving the most accurate results compared to the other cases. Changing the RC damper is helping to reduce the oscillations, and might not be a useful method for improving the scaling transformer performance from the stability point of view. In the best case which is the last case turbine can produce 700 MW, and if the slider is sent to the higher values the system starts to become unstable. According to above investigations it was seen that neither RC damper settings nor number of small time step blocks and infinite voltage source model are not affecting stability of the model.

9.8 PART B: Investigations in interfacing of Scaling Transformer

There is a limitation in the maximum amount of scaling in interface transformer in small time step which is 120 and power can't be regulated up to 800 MW, which is our purpose for this project, and consequently using a 5MW DFIG same as PSCAD model can't create 800 MW even by using scaling transformer. Also it is shown that 5MW model in both large and a small time step network has oscillation problems, which make it impractical for creating 800 MW DFIG model. Using 5MW model is creating oscillations in P1 and Q1 in this case; in figure 9.8.1 it is shown that making the network stronger and also changing the RC damper values can't reduce these noises.

$$4.95 < P_G < 5.05 \text{ But } 4.7 < P1 < 5.3$$

This oscillation increases linearly from 6%, and when we increase the scaling value for example to 120 to create 600 MW the amount of oscillation will be about 100MW peak to peak. So using the 5W case will not be a good idea as the produced P1 and Q1 will be much noisy and not appealing.

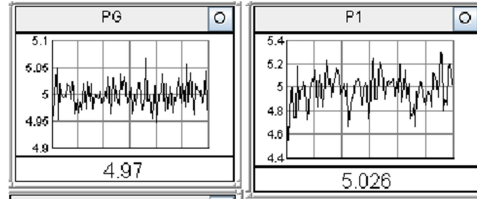


Figure 9.8.1-Power Oscillations in 5 MW DFIG

If instead of using 5MW a 200 MW model is used these oscillations will be much less and about 1% as it is shown in figure 9.8.2:

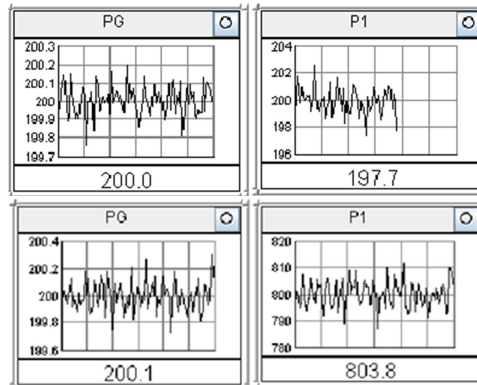


Figure 9.8.2-Power Oscillations in 200 MW DFIG

As a result it is preferred to use 200 MW model for this study .As a result I only have put the following cases including 5 MW connected to large dt, that can be regulated up to 800 MW.

Case 1: 200 MW DFIG connected to large dt

Case 2: 200 MW DFIG connected to small dt

Case 3: 5 MW DFIG connected to large dt. (Similar to PSCAD)

For case 3, DFIG parameters and 3 winding transformer voltage levels are same as PSCAD. After running the models with the given network parameters it was seen that none of these cases can be scaled up to 800 MW even the case that is same as PSCAD model and they become unstable when the scaling level increases.

After that studies were continued by using 230 kV network for all of the cases (to represent a stronger network). It was verified that all of the cases could successfully be scaled up to 800MW using a network with higher voltage level. Also if the network inductance value is decreased by 30% or more then, all again all the models will have no problem with scaling function and can produce 800 MW.

Case 4: This case is investigating a sample RTDS model that has its own controller and parameters and quite different from this project. This model has 1.6 MW DFIG in large dt, and finally only scaling transformer is added to this model and then connected to the network similar to cases 1, 2 and 3. It was shown that this model also can't produce more than 400 MW with 154 kV network, on the other hand it could be scaled up to 500 and create more than 800 MW if this model is connected to a stronger network. These results can confirm that this instability problem in scaling can't be related to the studied model and its controllers and parameters, but the focus should be on the network and interface point instead.

9.9 Possible Causes for Instability

9.9.1 Stiffness of Network

According to small time step document main system parameters affect the stability of interfacing. Basically scaling transformer is a current injection to the secondary side of scaling transformer, and then system bus should be able to accept this current injection without creating an excessive change in voltage. When an injection occurs and the bus is too stiff, the voltage on the main system can become noisy. One possibility is that the subjected network at the project is too stiff for interfacing or is current stiff. **If the high frequency impedance of the main system side is too high then the bus may be too stiff and the interface may be unstable.** This point can show the importance of having stronger networks for interfacing purposes. It seems that network parameters like impedance and voltage have direct impact on the interface instability, and our network seems is much stiff for interfacing in RSCAD, this also should be considered that this model is working with the same network and controllers in PSCAD! [18]

9.9.2 Time Delays in Interfacing Loop

Another problem, which might create the instability, is the introduced time delay in interfacing loop, and this is explained in interfacing to analogue simulator document section 2.2.3, in RTDS documents and proposes a voltage divider to explain the effect of this time delay in figure 9.9.2.1. [18]

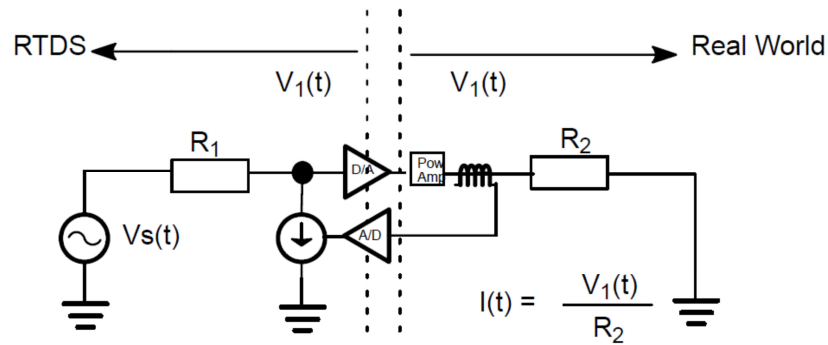


Figure 9.9.2.1-Interface between Scaling Component and Network

$$\frac{V_1(Z)}{V_s(Z)} = \frac{R_2}{R_2 + R_1 Z^{-1}}$$

Equation 9-1

R_2 =The equivalent impedance of DFIG side

R_1 =The equivalent impedance of the network side

And this expression is stable only if $R_1 < R_2$

When the scaling factor increases the injected current from secondary side (DFIG side) increases, which means the value of R_2 is reducing slowly, and reducing stability margin of interface. Consequently it is expected that adding parallel impedance in the network side or adding series impedance on the DFIG side should increase the stability margin due to this issue.

This equation also tells that if there is a weak network, which means R_1 is too high then it means the risk of instability is more, which can make $R_1 > R_2$. Different configuration for parallel impedance were tried in DFIG side, and in the most of the cases the system was still unstable for powers up to 800 MW, and finally it was seen that there was only one configuration with certain values of R and C, that could make the model stable for 800 MW. The R and C values in the branch, which could make the model stable, were quite a few.

Comparing Impedances Z_1 and Z_2 :

In the following figures the impedance of DFIG side Z_2 in both 200 MW DFIG and RTDS model are compared with the network impedance Z_1 before and after adding the RC damper branch;

Before adding RC damper branch:

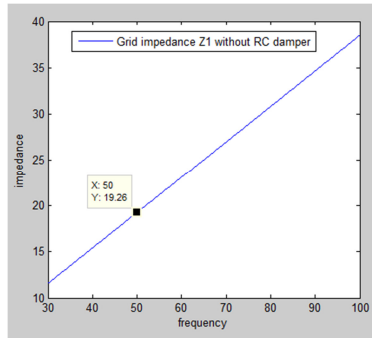


Figure 9.9.2.2-Network Impedance Z_1

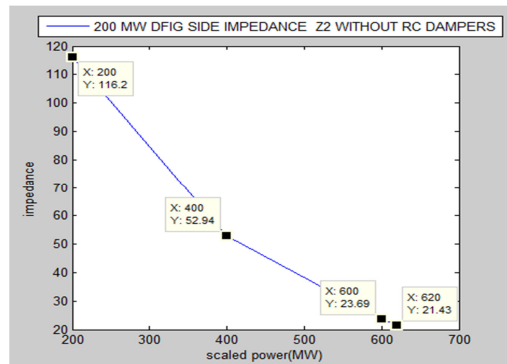


Figure 9.9.2.3-DFIG Impedance Z_2 for 200MW Model

200 MW case: As it is shown, when the scaling is set to 3.1 (620MW) in 50 Hz, $Z_1 = 19.26\Omega$ where $Z_2 = 21.43\Omega$ and this is quite close to instability limit mentioned earlier in time delay instability condition.

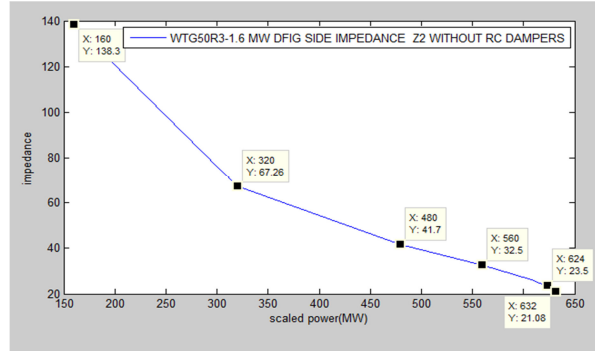


Figure 9.9.2.4-DFIG Impedance Z_2 for 1.6 MW Model

WTG50R3 1.6 MW case: similarly, when the scaling is set to 395 (632MW) in 50 Hz, $Z_1 = 19.26\Omega$ where $Z_2 = 21.08\Omega$ and this is again quite close to instability limit mentioned earlier in time delay instability condition.

After adding RC damper branch:

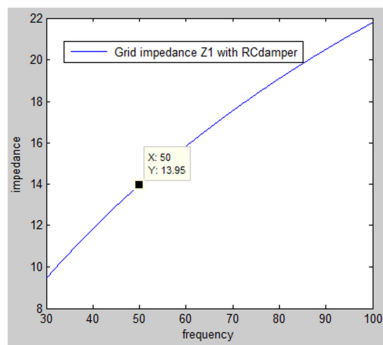


Figure 9.9.2.4-Netwrok Impedance Z_1

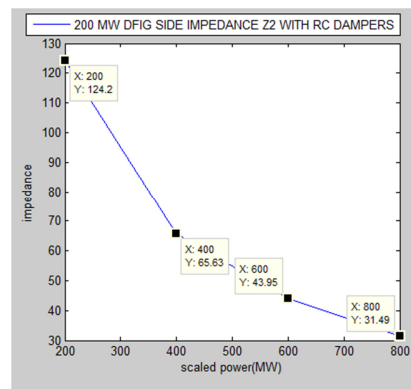


Figure 9.9.2.5-DFIG Impedance Z_2 for 200MW Model

200 MW case: According to the shown plots now when the scaling is set to 4 (800MW), $Z_1 = 13.95\Omega$ in 50 Hz where $Z_2 = 31.49\Omega$ and this is giving more stability margins during scaling.

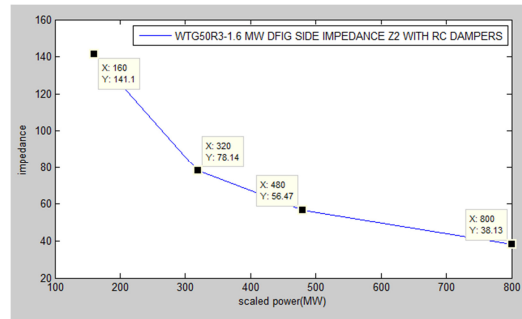


Figure 9.9.2.6-DFIG Impedance Z_2 for 1.6 MW Model

WTG50R3 1.6 MW case: similarly when the scaling is set to 500 (800MW) in 50 Hz, $Z_1 = 19.26\Omega$ where $Z_2 = 38.13\Omega$ and using RC damper is providing more stability margin for scaling.

It should be mentioned that in weak network connections if the scale factor is higher than 3 the stator side voltage starts to decrease, which can also affect the value of impedance Z_2 , and make it even smaller, This is not the case, when we put the external RC branch with certain values, and it seems it is making the network stronger, and keeping the voltage at stator, which resulting to higher DFIG side impedance.

To evaluate how network parameters are affecting the stability in RSCAD following cases are investigated,

- **L_p (Parallel inductance):** By changing L_p value from 0.06128 H to 0.04128 H in figure 9.9.2.7 the model can be scaled up to 800 MW. By having higher inductance value the stator voltage is kept constant during the scaling, which was not the case when the original values that were used. It is also seen that the resistance values is not affecting the instability.
- **Voltage level:** By increasing the network voltage level from 154 Kv to 230 Kv also all the models can produce up to 800 MW properly and the plots are good.
- **RC branch:** Adding external RC branch in parallel to network with certain values for R and C also can make the mode stable for scaling.

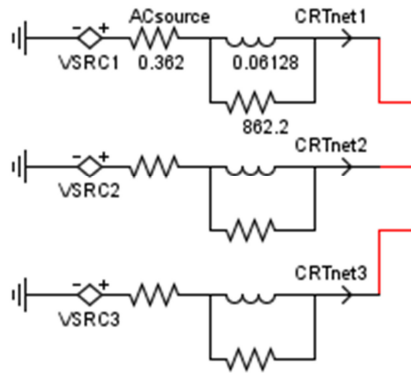


Figure 9.9.2.7-Network Parameters

9.10 Plots for 800 MW DFIG Verified against PSCAD

Verification of 800 MW DFIG against PSCAD model is same as 200 MW discussed in section 8, due to this similarity only produced power after scaling and in figures 9.10.1.1 and 9.10.1.2 are shown in figure. It is seen that by using the built RC branch the model becomes stable.

9.10.1 Normal Operation

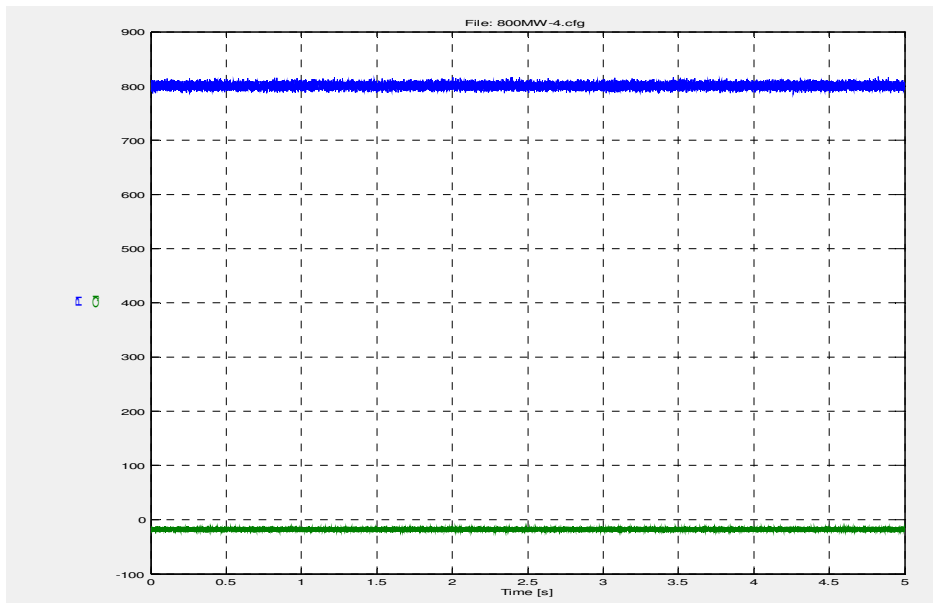


Figure 9.10.1.1-Normal Operation Active and Reactive Power (MW)

9.10.2 CASE I: 10% Remaining Voltage 3ph-G

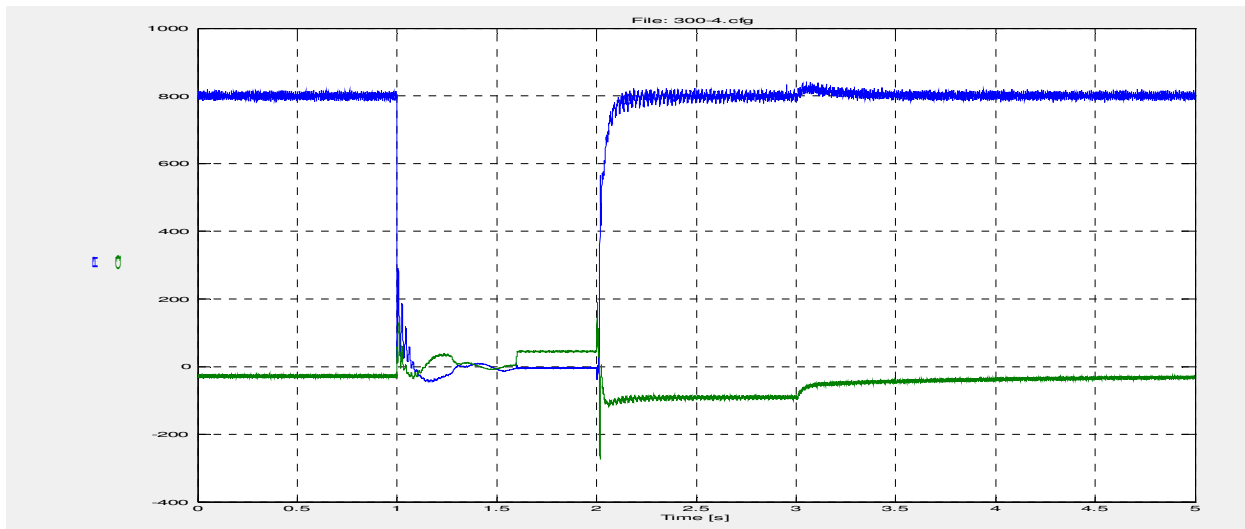


Figure 9.10.1.2-Normal Operation Active and Reactive Power (MW)

Chapter 9

10 Conclusion and future work

10.1 Conclusion

For first part of the project dealt with verification of 200 MW DFIG model in RSCAD against the PSCAD model, after modifying the controller in RSCAD the behavior of the model is improved, and most of the results are more compatible to PSCAD model, but still there are some differences between models specially for frequency, network and grid side converter currents during the fault. DC voltage response is improved compared to before but still DC voltage change in RSCAD is not completely same. Except these differences other plots were showing a high degree of similarity between models. RSCAD is an online simulation tool with its own limitations and with a different calculation method and it seems having exactly same results is not something practical.

For part two of the project, which was about studies on scaled model in RSCAD there are some possible reasons for instability in RSCAD model, which mainly are related to network impedance and inherent interface time delays in RSCAD.

10.2 Future Work

This work could remark the problems in RSCAD model to much extent, and it seems that by having further investigations it is possible to improve RSCAD model behavior for verification purposes. This is not still so clear why a RC branch with only certain values for R and C can solve the mode instability, and this issue needs more thinking.

At this work wind speed for both models were considered as a fix value, but this also would be very interesting to analyze the RSCAD model behavior against the PSCAD model for variable wind speed operation.

For part two the results with proposed explanations are sent to RTDS Company and this work can continue after having more information from the manufacturer and designer of the simulator. It is also an interesting subject to find out why only one RC branch with certain values can make the model stable for scaling.

References

[1] Control of a Double-Fed Induction Generator for Wind-Power Plants

W. Hofmann A. Thieme

[2] Doubly Fed Induction Generator Systems for Variable Speed Wind Turbine

Rui Melício¹, V.M.F. Mendes²

[3] PSCAD/EMTDC based simulation of double fed induction generator for wind turbines

Farhad Shahnai¹, Mohammad B.B. Sharifian²

[4] Thesis for the degree of doctor of philosophy Dynamic models of wind turbines

Abram Perdanad

[5] Scientific work for sustainable power production and transportation

Farhad Shafiei

[6] Control of Double Fed Induction Generator for Wind Conversion System

Driss Saidani, Othman Hasnaoui and Rachid Dhifaoui

Research Unit: Electrical Machines and Power Systems (RME), INSAT Tunisia

[7]ABB online

[8]Chalmers lecture electric drive I

[9]Chalmers lecture electric drive II

[10]Doubly fed induction generator (DFIG) using back to back PWM converters and its application to variable speed wind energy generation

R.Pena,J.C.Clare,G.M.Asher.IEE proc.power Appl.,Vol.143,No.3,May 1996

[11]Vector Controlled Doubly Fed Induction Generator for Wind Applications

Dr. Ani Gole, Dept. of Electrical and Computer Eng., University of Manitoba.

[12]Novel Phase-Locked Loop Using Adaptive Notch Filter

Lin Xu¹, Yang Han^{1, 2}, Li-Dan Zhou¹, Gang Yao¹, Mansoor¹, Chen Chen¹, Junmin Pan¹

[13] Enhanced Frequency-Adaptive Phase-Locked Loop for Distributed Power Generation System Applications

S. Eren, M. Karimi-Ghartemani, and A. Bakhshai

[14] Wind turbine driven doubly fed induction generator sample model

[15] Small time step presentation by RTDS

[16]Input-Admittance Calculation and Shaping for Controlled Voltage-Source Converters

Lennart Harnefors, Member, IEEE, Massimo Bongiorno, Student Member, IEEE, and Stefan Lundberg, Member, IEEE

[17]Dynamic Behavior of DFIG-Based Wind Turbines during Grid Faults

I. Erlich*, H. Wrede**, and C. Feltes* * University of Duisburg-Essen, 47057 Duisburg, Germany ** SEG GmbH & Co. KG, 47906 Kempen, Germany

[18] RTDS Manual